E-ISSN: 2147-1959

MIRT

Molecular Imaging and Radionuclide Therapy

February 2024 Volume 33 Issue 1 www.tsnm.org

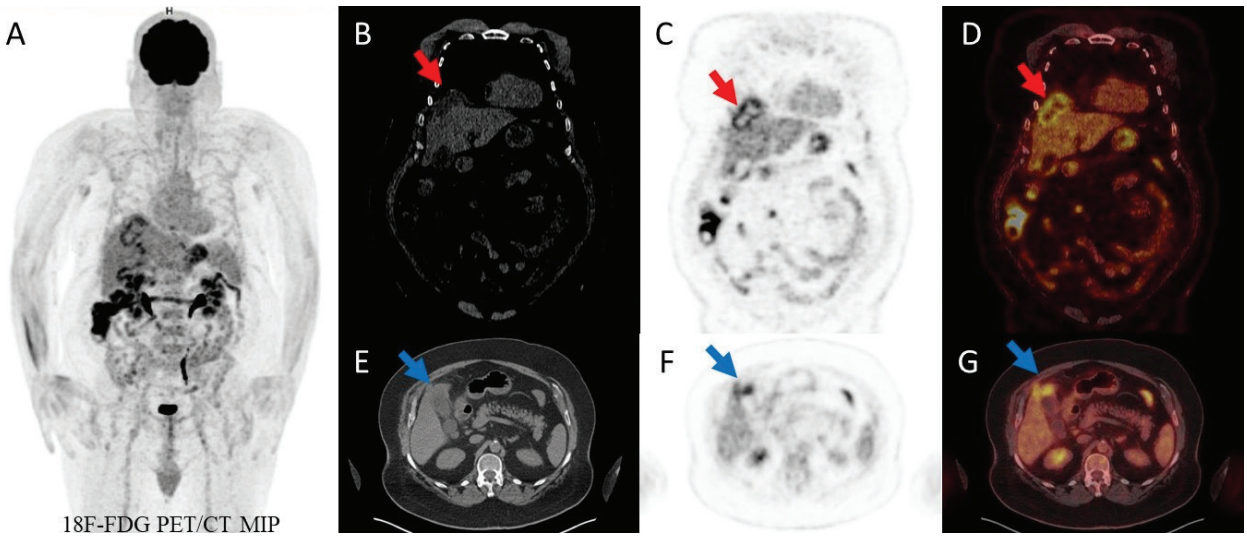

"Official Journal of the Turkish Society of Nuclear Medicine"

galenos yayınevi

TURKISH SOCIETY OF NUCLEAR MEDICINE 1975

MIRT

Molecular Imaging and Radionuclide Therapy

MIRT

Molecular Imaging and Radionuclide Therapy

Turkish Society of Nuclear Medicine
Cinnah Caddesi Pilot Sokak No: 10/12 Çankaya 06650 Ankara, Türkiye **Phone:** +90 312 441 00 45 **Fax:** +90 312 441 12 95 **Web:** www.tsnm.org **E-mail:** dernekmerkezi@tsnm.org
"Formerly Turkish Journal of Nuclear Medicine"

Reviewing the articles' conformity to the publishing standards of the Journal, typesetting, reviewing and editing the manuscripts and abstracts in English, creating links to source data, and publishing process are realized by Galenos.

Publisher Contact
Address: Molla Gürani Mah. Kaçamak Sk. No: 21/1 34093 İstanbul, Türkiye
Phone: +90 (530) 177 30 97 / +90 539 307 32 03
E-mail: info@galenos.com.tr/yayin@galenos.com.tr
Web: www.galenos.com.tr
Publisher Certificate Number: 14521

Online Publication Date: February 2024
ISSN: 2146-1414 **E-ISSN:** 2147-1959
International scientific journal published quarterly.

MIRT

Molecular Imaging and Radionuclide Therapy

Please refer to the journal's webpage **(https://mirt.tsnmjournals.org/)** for "Aims and Scope", "Instructions to Authors" and "Ethical Policy".

The editorial and publication process of Molecular Imaging and Radionuclide Therapy are shaped in accordance with the guidelines of ICMJE, WAME, CSE, COPE, EASE, and NISO. The journal is in conformity with the Principles of Transparency and Best Practice in Scholarly Publishing.

Molecular Imaging and Radionuclide Therapy is indexed in **Pubmed, Pubmed Central (PMC), Emerging Sources Citation Index (ESCI), TUBITAK-ULAKBIM, Scopus, Gale/Cengage Learning, EBSCO databases, ProQuest Health & Medical Complete, CINAHL, Embase, J-Gate, IdealOnline, Türkiye Atıf Dizini-Turkiye Citation Index, Turk Medline, Hinari, GOALI, ARDI, OARE, AGORA** and **CNKI**.

The journal is published electronically.

Owner: Murat Fani Bozkurt on Behalf of Turkish Society of Nuclear Medicine

Responsible Manager: Murat Fani Bozkurt

MIRT
Molecular Imaging and Radionuclide Therapy

CONTENTS

Original Articles

Interesting Images

MIRT
Molecular Imaging and Radionuclide Therapy

CONTENTS

Original Article
Mol Imaging Radionucl Ther 2024;33:1-10 DOI:10.4274/mirt.galenos.2023.26122

Role of ^{18}F-FCH PET/CT in Detecting Recurrences of Prostate Cancer After Curative Treatments

Küratif Tedavilerden Sonra Prostat Kanseri Nükslerinin Tespitinde ^{18}F-FCH PET/BT'nin Rolü

Corinna Altini[1], Artor Niccoli Asabella[2], Francesco Tramacere[3], Angela Sardaro[4], Antonio Rosario Pisani[1], Alessandra Castelluccia[3], Dino Rubini[1], Cristina Ferrari[1]

[1]*University of Bari Aldo Moro, School of Interdisciplinary of Medicine, Department of Nuclear Medicine, Bari, Italy*
[2]*A. Perrino Hospital, Clinic of Nuclear Medicine, Brindisi, Italy*
[3]*A. Perrino Hospital, Clinic of Radiotherapy, Brindisi, Italy*
[4]*University of Bari Aldo Moro, School of Interdisciplinary of Medicine, Department of Radiology and Radiation Oncology, Bari, Italy*

Abstract

Objectives: To evaluate the role of ^{18}F-fluorocholine (^{18}F-FCH) positron emission tomography/computed tomography (PET/CT) in prostate cancer (PC) patients with biochemical recurrence who were submitted to different curative treatments.

Methods: Seventy-five patients with PC who underwent ^{18}F-FCH PET/CT for biochemical recurrence were retrospectively analyzed to distinguish patients who were submitted only to prostatectomy (PR group), only to radiotherapy (RT) on prostate with curative intent (RT group), and to both (PR + RT group). Correlations between ^{18}F-FCH PET/CT and outcome and between prostate-specific antigen (PSA) values and sites and the number of metastases were analyzed. The performance of ^{18}F-FCH PET/CT in relation to the PSA value and of maximum standardized uptake value (SUV_{max}) value in relation to patient outcome were assessed by receiver operating characteristic (ROC) curves.

Results: ^{18}F-FCH PET/CT relapses mostly involved lymph nodes, bones, and prostate bed. K-cohen test showed moderate agreement with the outcome in the whole population and in the PR group, whereas in the RT group it was perfect and in PR + RT fair. A statistically significant difference in PSA values was observed in the presence of lymph node metastases and with multiple metastases. ROC curves showed PSA cut-off values of 1.96 ng/dL, 1.95, 1.81, and 2.96, respectively, in the whole population, PR, RT and PR + RT group. SUV_{max} cut-off values of 3.75, 3.45, and 4.7 were described in the whole population, PR group, and PR + RT group.

Conclusion: The study confirms that ^{18}F-FCH PET/CT is still valid in PC patients with suspected biochemical recurrence. Therefore, we can affirm that it still makes sense to perform it both with high PSA values and with lower values when prostate-specific membrane antigen tracers are not available.

Keywords: ^{18}F-FCH PET/CT, prostate cancer, biochemical recurrences, radical prostatectomy, curative radiotherapy

Öz

Amaç: Farklı küratif tedavilere yönlendirilmiş olan biyokimyasal nükslü prostat kanseri (PK) olan hastalarda ^{18}F-florkolin (^{18}F-FCH) pozitron emisyon tomografisi/bilgisayarlı tomografinin (PET/BT) rolünü değerlendirmektir.

Yöntem: Biyokimyasal nüks için ^{18}F-FCH PET/BT uygulanan 75 PK'li hasta, yalnızca prostatektomi (PR grubu) uygulanan, yalnızca küratif amaçlı prostat radyoterapisi (RT) uygulanan (RT grubu) ve her ikisi birden uygulanan hastalar (PR + RT grubu) olmak üzere üç gruba ayrılarak retrospektif

Address for Correspondence: Corinna Altini MD, University of Bari Aldo Moro, School of Interdisciplinary of Medicine, Department of Nuclear Medicine, Bari, Italy
Phone: +39 0805592913 **E-mail:** corinna.altini@hotmail.it ORCID ID: orcid.org/0000-0002-8949-2405
Received: 14.07.2023 **Accepted:** 25.09.2023

olarak analiz edildi. ^{18}F-FCH PET/BT ile sonlanım arasındaki korelasyon ve prostat spesifik antijen (PSA) değerleri ile metastaz bölgeleri ve sayısı arasındaki korelasyon analiz edildi. ^{18}F-FCH PET/BT'nin PSA değerine göre performansı ve SUV_{maks} değerinin hasta sonlanımına göre performansı alıcı işletim karakteristik (ROC) eğrileri ile değerlendirildi.

Bulgular: ^{18}F-FCH PET/BT relapsları çoğunlukla lenf nodlarını, kemikleri ve prostat yatağını tutuyordu. K-cohen testi tüm popülasyonda ve PR grubunda sonlanımla orta derecede uyum gösterirken, RT grubunda mükemmel ve PR + RT grubunda iyi uyum gösterdi. Lenf nodu metastazı varlığında ve çoklu metastaz varlığında PSA değerlerinde istatistiksel olarak anlamlı farklılık gözlendi. ROC eğrileri tüm popülasyonda, PR, RT ve PR + RT gruplarında sırasıyla 1,96 ng/dL, 1,95, 1,81 ve 2,96 PSA kesme değerlerini gösterdi. Tüm popülasyonda, PR grubunda ve PR + RT grubunda SUV_{maks} kesme değerleri 3,75, 3,45 ve 4,7 olarak gösterildi.

Sonuç: Çalışma, biyokimyasal nüks şüphesi olan PK'li hastalarda ^{18}F-FCH PET/BT'nin hala geçerli olduğunu doğrulamaktadır. ^{18}F-FCH PET/BT'nin kullanımının hem yüksek PSA değerlerinin varlığında hem de prostat spesifik membran antijeni izleyicileri mevcut olmadığında daha düşük PSA değerlerinin varlığında hala anlamlı olduğu doğrulanmıştır.

Anahtar kelimeler: ^{18}F-FCH PET/BT, prostat kanseri, biyokimyasal nüksler, radikal prostatektomi, küratif radyoterapi

Introduction

Prostate cancer (PC) is the most frequent cancer in men and the third leading cause of death in developed countries. Multiple treatment options are available depending on several factors, both patient- and disease-related. Curative treatment options include surgery and radiation therapy. In addition, in the modalities of surgical and radiation therapy, the technique options vary. Because of the various aspects that can influence the therapeutic choice, an unequivocal estimate of the possibility of recurrence cannot be performed (1).

In patients with PC, recurrences after radical treatment can occur in 20-50% of patients after radical prostatectomy (PR) and in 30-40% of patients after radiotherapy (RT) (2).

Detection and localization of all recurrences is important for selecting the appropriate treatment. After curative treatments, the state of the disease is monitored by prostate-specific antigen (PSA) setting. When PSA levels increase, there is a need to confirm the suspicion of recurrence and to assess whether the disease is localized or metastatic (1).

Imaging methods are needed to detect and localize recurrences, and to conventional methods, nuclear medicine offers numerous possibilities for restaging PC patients. Today, with technological progress, numerous radiopharmaceuticals have demonstrated high diagnostic performance in PC patient management. However, their distribution is not feasible in all nuclear medicine operative units in western countries and even less in the remaining ones.

Among all positron emission tomography/computed tomography (PET/CT) whole body techniques, the use of ^{18}F-fluorocholine (^{18}F-FCH) until the last decade was celebrated as the most important and most innovative radiopharmaceutical for the evaluation of PC patients (3).

^{18}F-FCH is a substrate for phosphatidylcholine synthesis, a cell membrane component with increased biosynthesis in tumor tissues; the upregulation of choline kinase activity induced by cancer results in higher choline uptake by neoplastic cells. Several studies have investigated the role of ^{18}F-FCH PET/CT in the management of PC, and the evaluation of recurrence after radical treatment has emerged as the main clinical application (1,2).

Currently, ^{18}F-FCH PET/CT is in the background compared to the new radiopharmaceutical, but all advantages such as easier production, long half-life, and easy supply are still valid (1,3).

On the basis of these statements, the aim of this study was to analyze the state of the art in our territorial reality with the aim of evaluating the role of ^{18}F-FCH PET/CT in the detection of relapses in patients with localized PC treated with PR and/or RT.

Materials and Methods

Seventy-five patients with a diagnosis of PC (adenocarcinoma) who underwent ^{18}F-FCH PET/CT for the biological suspicion of PC relapse from October 2020 to November 2021 were included in the study. A retrospective observational analysis was performed, and the institutional review board did not require ethical committee approval for the review of patient files. All patients provided written informed consent to the use of their data for clinical research in an anonymous form.

Fourty-one/75 patients were previously submitted only to PR (PR group), 13/75 were submitted only to RT on the prostate with curative intent (RT group), and 21/75 patients were submitted to both procedures with curative intent (PR + RT group).

The inclusion criteria consisted of: histologically proven PC, treatment with curative intent (PR and/or RT), and

biochemical recurrence as defined by the guidelines of the European Association of Urology (4).

Patients with distant metastases at diagnosis or with non-diagnostic scans were excluded. The mean age of the patients was 71 years (range 42-87 years old) and the mean Gleason score at diagnosis was 7 (range 5-9). The mean time between treatment and ^{18}F-FCH PET/CT was 6 years (range 1-16 years), and the mean PSA level at the time of ^{18}F-FCH PET/CT was 5.85 ng/mL (range 0.02-79 ng/mL, median 1.97 ng/mL).

^{18}F-FCH PET/CT

^{18}F-FCH PET/CT preparations consisted of a 6-h fast. A dose of approximately 3-4 MBq/kg body weight (range 240-390 MBq/kg) of ^{18}F-FCH PET/CT was intravenously administered. All scans were obtained using a hybrid PET/CT scanner (Discovery 710, GE, General Electrics, Milwaukee, WI, USA). After 5 min post-injection, early ^{18}F-FCH PET/CT images of the pelvis were acquired targeting the prostate area, followed by a whole-body image acquisition after 60 min, from the skull base to the proximal third of the femurs (5-6 bed positions). A 3D acquisition mode PET scan was performed for the same longitudinal coverage (2.5 min per bed position). The PET data were reconstructed over a 128 matrix with a pixel size of 4.75 mm and a slice thickness of 2 mm. The following co-registered CT parameters were used: pitch 0.98, gantry rotation speed of 0.5 s/rot, 120 kV, and modulated tube current of 140 mA. CT images were used for image fusion and anatomical localization and for attenuation correction of emission data.

Image Analysis

Image analysis was performed using a dedicated workstation (AW Server 4.7, General Electrics, Milwaukee, WI, USA). ^{18}F-FCH PET/CT scans were independently evaluated by two nuclear medicine physicians with at least 5 years of experience in image reading and who were aware of clinical data. In the event of disagreement, a third nuclear medicine physician's opinion was reached.

Maximum intensity projection, PET, CT, and PET/CT fused images in different planes (axial, sagittal, and coronal) were visualized simultaneously to correctly interpret the scans. Examinations were considered positive in the presence of focal areas of detectable increased tracer uptake, visually more intense than the background, not correlating with physiological tracer uptake and inflammatory articular processes, with or without any underlying lesion identified on the co-registered CT (5). The semiquantitative parameter maximum standardized uptake value (SUV_{max}) was collected in all visualized lesions.

Validation of Results and Outcomes

All patients were followed for at least 1 year after ^{18}F-FCH PET/CT, and data on outcome were collected. The final response regarding the presence of relapses was obtained from the results of surgical procedures performed and/or clinical instrumental follow-up.

Statistical Analysis

Analyses were performed in the entire population and in the 3 subgroups (PR, RT and PR + RT). Quantitative variables are expressed as mean standard deviation (SD). Categorical variables are presented with absolute and relative frequencies.

Chi-square and Kruskal-Wallis tests were applied to establish if the groups were comparable. The K-cohen test was applied for correlation between ^{18}F-FCH PET/CT results and outcome. The Mann-Whitney U test was used to compare the differences between continuous non-normally distributed variables such as PSA values and sites and the number of metastases detected at ^{18}F-FCH PET/CT and patient outcome. The performance of ^{18}F-FCH PET/CT in relation to the PSA value was assessed using the receiving operating characteristic (ROC) curve generated by plotting sensitivity versus specificity. The performance of the SUV_{max} value in relation to the patient outcome was also assessed using the ROC curve; a cut-off value was also identified. Statistical significance was assumed for p-values 0.05. All statistical analyses were performed using SPSS statistical software, version 25 (IBM Corporation, Armonk, NY, USA).

Results

The comparison performed for the main clinical variables among the total population and the groups showed that there were no statistically significant differences; therefore, the groups were comparable even if numerically different (Table 1).

Lesions Distribution

^{18}F-FCH PET/CT was positive in 46/75 (61.3%) patients and negative in 29/75 (38.7%) patients. On the 46 positive ^{18}F-FCH PET/CT, 6/46 (13%) showed only local recurrences, 24/46 (52.2%) showed lymph node involvement, 7/46 (15.2%) showed bone metastases, 1/46 (2.2%) showed both local and lymphatic involvement, 5/46 (10.9%) showed lymphatic and bone involvement, and 3/46 (6.5%) patients showed both bones and other distant metastases in the lung.

Considering the 41 patients in the PR group, ^{18}F-FCH PET/CT was positive in 24/41 (58.5%) patients, whereas it was negative in 17/41 (41.5%) patients. On the 24

Table 1. Characteristics of the whole population					
	Total (n=75)	**PR (n=41)**	**RT (n=13)**	**PR + RT (n=21)**	**p-value**
Age					
Mean ± SD Median (range)	71±7.20 70 (42-87)	71±7.78 71 (42-87)	71±7.10 70 (62-83)	70±6.28 70 (47-79)	0.600*
Gleason score, n (%)					
<8 ≥8	47 (63%) 28 (37%)	28 (68%) 13 (32%)	9 (69%) 4 (31%)	10 (48%) 11 (52%)	0.243**
PSA, ng/mL					
Mean ± SD Median (range)	5.74±12.71 1.94 (0.02-79)	4.84±12.93 1.43 (0.02-79)	4.25±3.66 2.56 (0.20-10.70)	8.41±15.66 2.50 (0.20-54.20)	0.132*

*Kruskal-Wallis test; **Chi-square test, SD: Standard deviation, PR: Prostatectomy, RT: Radiotherapy, PSA: Prostate-specific antigen

positive ^{18}F-FCH PET/CT, 5/24 (20.8%) showed only local recurrences, 11/24 (45.7%) showed only nodal lymph node involvement, 1/24 (4.2%) showed only bone metastases; 2/24 (8.4%) showed both local and lymphatic involvement, 4/24 (16.7%) showed lymphatic and bone involvement, and 1/24 (4.2%) patient showed local, node, and bone metastases (Figure 1).

Considering the 13 patients in the RT group, ^{18}F-FCH PET/CT was positive in 10/13 (77%) patients, while it was negative in 3/13 (23%) patients. On the 10 positive ^{18}F-FCH PET/CT images, 3/10 (30%) showed nodal lymph node involvement, 5/10 (50%) bone metastases (Figure 2), 1/10 (10%) showed both local and bone involvement, and 1/10 (10%) showed both bones and lung metastases.

Considering the 21 patients in the PR + RT group, ^{18}F-FCH PET/CT was positive in 12/21 (57.2%) patients, whereas it was negative in 9/21 (42.8%) patients. On the 12 positive ^{18}F-FCH PET/CT images, 1/12 (8.3%) showed only local recurrences, 9/12 (75.1%) showed nodal lymph node involvement, 1/12 (8.3%) bone metastases, and 1/12 (8.3%) patient showed both bones and distant metastases in the lung.

The distribution of relapses in ^{18}F-FCH PET/CT in all patients and as a function of the treatment performed is shown in Figure 3.

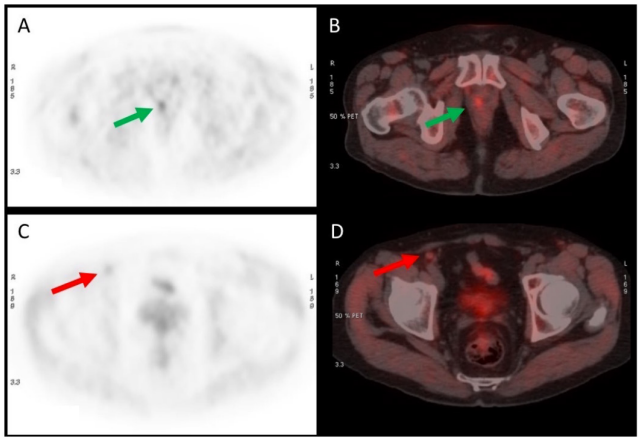

Figure 1. Seventy-eight years old man submitted 13 years before to PR for PC Gleason 7. He performed ^{18}F-FCH PET/CT because of PSA levels of 6.03 ng/dL. Axial PET (A) and fused images (B) showed local relapse (green arrows, SUV_{max}: 3.2) and (C, D) involvement of the right iliac lymphnode (SUV_{max}: 2.0, red arrows)
PR: Prostatectomy, PC: Prostate cancer, PET/CT: Positron emission tomography/computed tomography, PSA: Prostate-specific antigen, SUV_{max}: Maximum standardized uptake value, ^{18}F-FCH: ^{18}F-fluorocholine

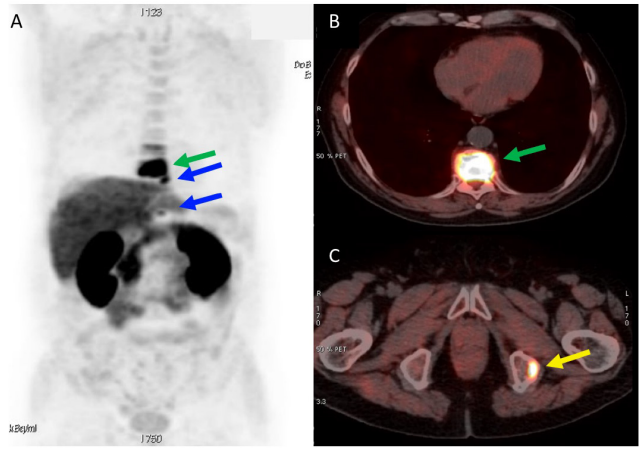

Figure 2. Sixty-four years old man submitted 6 years before to RT for PC Gleason 7. He performed ^{18}F-FCH PET/CT because of PSA levels of 2.56 ng/dL. MIP (A) and fused images (B, C) showed multiple bone lesions such as in D10 vertebra (SUV_{max}: 23.5, green arrow), D9 and D12 vertebrae (blue arrows) and left ischium (SUV_{max}: 20.1, yellow arrow)
RT: Radiotherapy, PC: Prostate cancer, PET/CT: Positron emission tomography/computed tomography, PSA: Prostate-specific antigen, MIP: Maximum intensity projection, SUV_{max}: Maximum standardized uptake value, ^{18}F-FCH: ^{18}F-fluorocholine

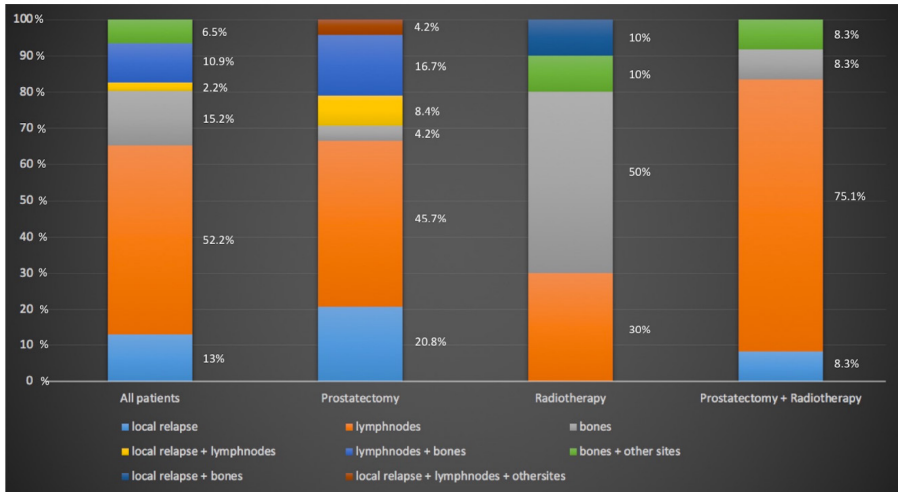

Figure 3. Distribution of relapses in [18]F-FCH PET/CT in all patients and as a function of the treatment performed
PET/CT: Positron emission tomography/computed tomography, [18]F-FCH: [18]F-fluorocholine

Outcome

At the follow-up, 50/75 (66.7%) patients were involved by relapses and/or metastases of PC; in the PR group, 25/41 (61%) patients, in the RT group, 10/13 (77%) patients and in PR + RT group 15/21 (71.4%) patients. Results concerning the agreement between [18]F-FCH PET/CT and the outcome are reported in Table 2.

PSA Level Evaluation

Considering the total population, mean PSA values were 9.34 ng/mL (range 0.36-79) in patients with positive concordance, 1.60 ng/dL (range 0.17-5.35) in patients with [18]F-FCH PET/CT positivity not confirmed at the follow-up, 1.20 (range 0.02-3.20) in patients concordant in excluding the disease, and 1.63 (range 0.92-2.50) in patients for whom relapses were not detected at [18]F-FCH PET/CT. The Mann-Whitney U test showed PSA levels higher in patients with positive [18]F-FCH PET/CT with difference statistical significant (p<0.0001) also in lymph nodes (p=0.002) and bone evaluation (p=0.007) and in patients with equal or more than 3 lesions (p<0.0001) regardless of the site.

In the PR group, mean PSA values were 8.50 ng/mL (range 0.36-79.00) in patients with positive concordance, 1.65 ng/mL (range 0.17-5.35) in patients with [18]F-FCH PET/CT positivity not confirmed at follow-up, 1.09 ng/mL (range 0.02-3.20) in patients concordant in excluding the disease, and 1.70 ng/mL (range 0.92-2.40) in patients for whom relapses were not detected at [18]F-FCH PET/CT. The Mann-Whitney U test showed PSA levels higher in patients with positive [18]F-FCH PET/CT with difference statistically significant (p=0.03) also in lymph nodes (p=0.021) and bone evaluation (p=0.038) and in patients with equal or more than 3 lesions (p=0.040) regardless of the site.

Table 2. [18]F-FCH PET/CT and outcome agreement

	Positive concordant	Negative concordant	Discordant ([18]F-FCH PET/CT positivity not confirmed)	Discordant (relapses not detected at [18]F-FCH PET/CT)	
Total (n=75)	40 (53.4%)	19 (25.3%)	6 (8%)	10 (13.3%)	K=0.538 (95% CI: 0.341-0.736) Moderate
PR (n=41)	20 (48.8%)	12 (29.3%)	4 (9.7%)	5 (12.2%)	K=0.544 (95% CI: 0.282-0.806) Moderate
RT (n=13)	10 (77%)	3 (23%)	-	-	Perfect
PR + RT (n=21)	10 (47.7%)	4 (19%)	2 (9.5%)	5 (23.8%)	K=0.290 (95% CI: -0.111-0.690) Fair

PR: Prostatectomy, RT: Radiotherapy, PET/CT: Positron emission tomography/computed tomography, [18]F-FCH: [18]F-fluorocholine, CI: Confidence interval

In the RT group, mean PSA values were 5.26 ng/mL (range 0.84-10.70) in patients with positive concordance and 0.89 ng/mL (range 0.2-1.33) in patients with concordance after excluding the disease. The Mann-Whitney U test showed that PSA levels were higher in patients with positive [18]F-FCH PET/CT with difference statistical significant (p=0.028) regardless of the sites and number of lesions.

In the PR + RT group, mean PSA values were 15.74 ng/mL (range 1.18-54.20) in patients with positive concordance, 1.47 ng/mL (range 0.90-2.04) in patients with [18]F-FCH PET/CT positivity not confirmed at follow- up, 1.96 ng/mL (range 0.20-2.92) in patients with concordance in excluding the disease, and 1.54 ng/mL (range 1.04-2.50) in patients for whom relapses were not detected at [18]F-FCH PET/CT. The Mann-Whitney U test showed PSA levels higher in patients with positive [18]F-FCH PET/CT with difference statistically significant (p=0.028) also in lymph nodes (p=0.016) and in patients with equal or more than 3 lesions (p=0.020) regardless of the site.

ROC curves elaborated to identify the optimal cut-off for predicting [18]F-FCH PET/CT positivity in all the groups analyzed are reported in Figure 4, while their results are reported in Table 3.

SUV_{max} Analysis

The mean SUV_{max} values in the [18]F-FCH PET/CT-positive patients were as follows: in the whole population, 7.8 (range 1.6-27.1); in the PR group, 6.8 (range 3.2-16.4); in the RT group, 9.2 (range 5.2-13.2); and in the PR + RT group, 6.0 (range 2.0-9.7).

ROC curves elaborated to identify the optimal cut-off of SUV_{max} in predicting the presence of the disease at the outcome are reported in Figure 5, while their results are reported in Table 4.

Discussion

Considerable progress has been made in the field of radical treatments for locally advanced PC, and currently, there are numerous choices that allow customizing the therapy on the basis of the characteristics of the disease and the patient's needs.

Radical surgical procedures have diversified, such as RT, for which technological advances have made it possible to create increasingly sophisticated protocols. Advances in external beam RT delivery techniques, such as intensity modulated RT and volumetric arc RT, allow delivery of the maximum dose to the target volume while sparing surrounding healthy tissue, optimizing response to treatment, and reducing genitourinary and intestinal

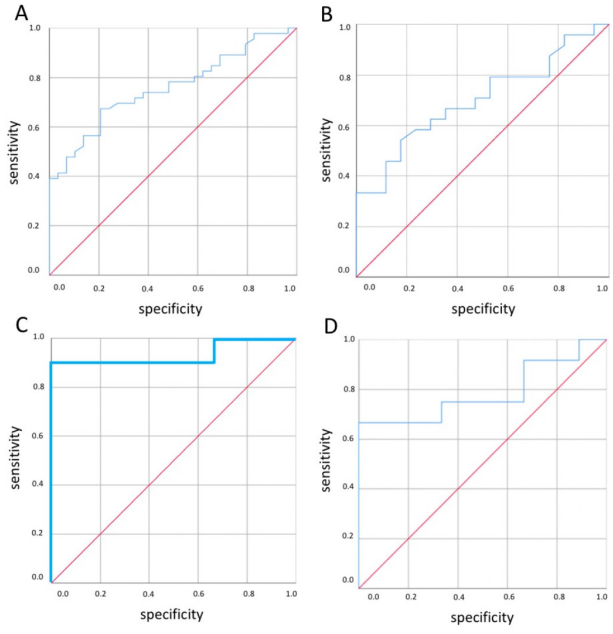

Figure 4. ROC analysis of PSA values optimal cut-off of for predicting [18]F-FCH PET/CT positivity; A: total population; B: patients submitted only to PR; C: patients submitted only to RT; D: patients submitted to PR + RT ROC: Receiver operating characteristic, PET/CT: Positron emission tomography/computed tomography, PSA: Prostate-specific antigen, PR: Prostatectomy, RT: Radiotherapy, [18]F-FCH: [18]F-fluorocholine

Table 3. Results about PSA levels in predicting [18]F-FCH PET/CT positivity

	Cut-off	Sensitivity	Specificity	
Total (n=75)	1,965 ng/mL	67.4%	79.3%	AUC =0.757 95% CI 0.651-0.864
PR (n=41)	1.95 ng/mL	54.2%	82.4%	AUC =0.701 95% CI 0.542-0.860
RT (n=13)	1.81 ng/mL	90%	100%	AUC =0.933 95% CI 0.789- 1.000
PR + RT (n=21)	2.96 ng/mL	66.7%	100%	AUC =0.787 95% CI 0.585- 0.990

PR: Prostatectomy, RT: Radiotherapy, PSA: Prostate-specific antigen, PET/CT: Positron emission tomography/computed tomography, AUC: Area under the curve, CI: Confidence interval, [18]F-FCH: [18]F-fluorocholine

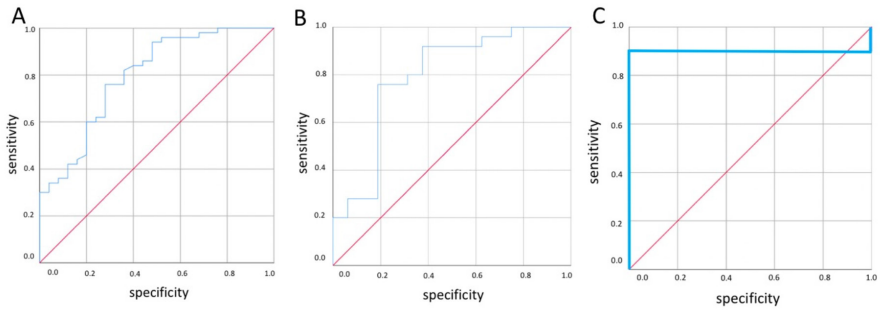

Figure 5. ROC analysis of the SUV_{max} optimal cut-off in predicting the presence of the disease at the outcome; A: total population; B: patients submitted only to PR; C: patients submitted to PR + RT
ROC: Receiver operating curve, SUV_{max}: Maximum standardized uptake value, PR: Prostatectomy, RT: Radiotherapy

Table 4. Results about SUV_{max} in predicting the presence of the disease at the outcome				
	Cut-off	**Sensitivity**	**Specificity**	
Total (n=75)	3.75	87.5%	83.3%	AUC =0.908 (95% CI 0.802-1.000)
PR (n=41)	3.45	90%	75%	AUC =0.850 (95% CI 0.629-1.000)
PR + RT (n=21)	4.7	90%	100%	AUC =0.900 (95% CI 0.714-1.000)
PR: Prostatectomy, RT: Radiotherapy, AUC: Area under the curve, CI: Confidence interval, SUV_{max}: Maximum standardized uptake value				

inflammation. In recent years, RT with curative intent has expanded the fields of application, and approximately 41% of PC patients are treated by it alone (1,6).

Recurrence after curative treatment varies according to the procedure applied although the level of risk retains the most important role. Disease recurrence occurs in approximately 30% of patients who were treated for PC. Agarwal et al. (7) analyzed the United States database of "The Cancer of the Prostate Strategic Urological Research Endeavour" and reported 23% rate of recurrences in patients submitted to PR and 63% in the RT group. They also reported that their results are in line with the literature for the PR group (range 15-33%) and higher in the RT group (range 37-48%) (7). This therefore makes ever present the necessity of diagnosing the presence of relapses. Our results showed relapses in 61% of patients in the PR group and 77% in the RT group, while it was 66.7% in the entire population analyzed. However, these higher results are certainly influenced by the selection of patients who were submitted to [18]F-FCH PET/CT for biochemical recurrence.

It is well known that metabolic/functional changes commonly precede anatomical changes; thus, PET/CT is being increasingly used in clinical oncological settings (8). In this regard, [18]F-FCH PET/CT has emerged as a method for disease localization in PC patients with biochemical relapse after primary treatment. The greatest advantage of PET/CT is that it is a whole-body, non-invasive imaging capable of assessing disease recurrence in multiple anatomical sites. Currently, even though prostate-specific membrane antigen (PSMA) tracers are downsizing the importance of the clinical use [18]F-FCH PET/CT, the literature available for it is much more abundant than for recent PSMA tracers; thus, it is much more supported for clinical routine execution. The more recent guidelines still propose [18]F-FCH PET/CT in patients with PC after PR and/or RT with increasing PSA levels (9,10).

In early studies from 1998, [18]F-FCH PET/CT showed several positive detection rates (30-80% of patients) because of the heterogeneity of the sample population recruited. In 2003, there was a boom in clinical studies in patients with biochemical recurrences after PR and less frequently after RT, but these studies were abandoned in the next decade (11). The aim of this study was to evaluate the role of [18]F-FCH PET/CT in PC patients with suspected recurrences by distinguishing them by type of treatment performed. Our results confirm better results in the positive detection rate of metastases in all groups analyzed, showing results from 47.7% in patients of the PR + RT group to 77% in patients of the RT group.

The prostate bed, lymph nodes (mostly pelvic ones), and the skeleton are the most frequently affected sites of relapses, relating to 34%, 66%, and 29% of PC patients, respectively.

Local recurrences occur in 30-50% of patients after PR, but the ^{18}F-FCH PET/CT evaluation of the postsurgical prostatic bed may be limited by the small size of recurrent lesions and the presence of radioactive urine; even after RT, the inflammatory uptake at the prostatic site can be limited. In the case of recurrence in the prostatic bed, ^{18}F-FCH PET/CT reached a pooled sensitivity of 75.4% (66.9-82.6%) and a pooled specificity of 82.0% (68.6-91.4%) (12,13,14,15).

Evangelista et al. (13), in their meta-analysis of literature from 2000 to 2013, concluded that ^{18}F-FCH PET/CT was highly sensitive and specific, especially for lymph node evaluation in PC patients with biochemical recurrence. In lymph node metastases, ^{18}F-FCH PET/CT showed a pooled sensitivity of 100% (90.5-100%) and a pooled specificity of 81.8% (48.2-97.7%); despite these data, false positives may be possible because of inflammatory changes or artifacts of small bowel activity (13,16,17).

Skeletal metastases are more frequent in the spine and pelvis, and ^{18}F-FCH PET/CT showed elevated specificity (11).

The pattern of relapse sites of ^{18}F-FCH PET/CT observed in this analysis was consistent with the natural spread of the disease involving predominantly lymph nodes followed by bones and the prostate bed, both in the whole population and in the groups analyzed. It should be noted that there were no discrepancies in the identification and interpretation of bone lesions in this analysis.

In this study, only 6/75 patients resulted in false positives, 4 of them were in the PR group and 2 in the PR + RT group; in all of these patients, single lymph nodes in the iliac or inguinal region were indicated as sites of disease, but they were reactive on biopsies results.

Ten/75 patients were false negative, 5 of them were in the PR group and 5 in the PR + RT group; the patients of the PR group had PSA values between 0.92 and 2.40 ng/dL when they underwent ^{18}F-FCH PET/CT, and the subsequent follow-up showed the presence of local recurrence, whereas in the 5 patients of the PR + RT group (PSA between 1.04 and 2.00 ng/dL), subsequent investigations showed the presence of disease in the iliac lymph nodes.

The most effective factor that linearly influences the sensitivity of ^{18}F-FCH PET/CT is the PSA level.

Conventionally, increasing PSA levels are considered the most sensitive tool for detecting PC recurrence, even if it cannot distinguish between local and distant recurrences (13). The definition of biochemical recurrence differs according to the primary treatment: in patients treated with PR, PSA levels greater than 0.2 ng/mL and rising on at least two consecutive measurements performed 3 months apart signify biochemical failure; in patients treated with RT, PSA value 2 ng/mL higher than the lowest (nadir) post-therapeutic represents biochemical failure (18,19). For this reason, in the population analyzed, the PSA levels reported have wide variability.

Numerous articles have shown a significant relationship between ^{18}F-FCH PET/CT positive detection rate and PSA value with a trend toward a more "systemic" disease with increasing PSA; however, there is not a cut-off value that can distinguish local or distant metastases (1,13). Chondrogiannis et al. (1) reported an elevated positive detection rate for PSA levels higher than 6 ng/mL (100%). Giovacchini et al. (12) showed that the detection rate reached a plateau for higher PSA values (84% for PSA >10 ng/mL), but Graziani et al. (20) in their most numerous study showed a fair positive detection rate of about 55% with a mean PSA of 4.9 ng/mL (1).

^{18}F-FCH PET/CT positive detection rate worsens for PSA values within 1 and 2 ng/mL (about 45.9% and 54%) or mean values around 2.0 ng/mL (67%) after PR. A low detection rate is observed for PSA values less than 1.0 ng/mL (7%) (12,21).

Studies that performed ROC curves revealed similar results for PSA values distinguishing positive ^{18}F-FCH PET/CT from negative independently by the curative treatment performed: Giovacchini et al. (12) showed a best value of 1.37 ng/mL in patients submitted to PR and Graziani et al. (20) showed a value of 1.16 ng/mL in PR + RT patients. Summarizing all these results, it can be deduced that ^{18}F-FCH PET/CT should not be restricted to patients with PSA >5 ng/mL; performing ^{18}F-FCH PET/CT with PSA levels between 1 and 2 ng/mL may imply the possibility of false negatives; instead, for patients with PSA lower than 1 ng/mL, the indication for ^{18}F-FCH PET/CT should be critically discussed in the context of multidisciplinary tumor boards. In any case, the minimum cut-off value that makes ^{18}F-FCH PET/CT invalid in restaging PC patients is not established (1,12,13,22,23).

In our analysis, a mean PSA value of 9.34 ng/dL was observed in true positive patients even if the range was between 0.36 and 79; this value was 8.5 ng/dL in the patients of the PR group with the same range, whereas in the patients of the RT group, the PSA mean value was 5.26 ng/dL and in the PR + RT group it was 15.74 ng/dL.

According to literature results in this study's whole population, a statistically significant difference in PSA values emerged in the case of the presence of multiple metastatic lesions and lymph node metastases, which were in any case the most frequently described sites in our population.

Despite the high mean PSA values described, the ROC curves in our groups of patients showed cut-off values of

1.96 ng/dL, 1.95, 1.81, and 2.96, respectively, confirming that this interval is critical for the validity of ^{18}F-FCH PET/CT, regardless of population size and selection criteria.

The analysis of semi-quantitative parameters has been addressed in numerous studies, but to date there is no unanimous consensus except in considering SUV_{max} as the most reproducible parameter.

However, considering only the literature concerning recurrences and metastases after curative therapies, only a few studies have collected and analyzed data concerning SUV_{max}.

Siminiak et al. (24) considered a population selected similarly in our study, but they described SUV_{max} results distinguishing patients by the sites of relapses: they reported a mean SUV_{max} of 3.0 (2.3-4-0) in 27 patients with only local relapses and of 4.9 (3.8-8.0) in 35 patients involved by distant metastases. Wetter et al. (25) reported a mean SUV_{max} in bone lesions of 5.5 (SD =3.1) independently by staging or restaging of PC. The analysis we report confirms that the mean SUV_{max} values are widely variable regardless of the type of treatment received; furthermore, the ROC curve identified values and cut-offs quite similar to those reported in the literature and very similar in the 3 groups analyzed (3.75 vs. 3.45 vs. 4.7).

Study Limitations

This study remains limited by its retrospective design and small sample size; nevertheless, to the best of our knowledge, it represents the most updated cohort of patients selected with regard to curative treatment. Furthermore, the limit concerning the different number of patients in groups was excluded by the application of statistical tests.

Conclusion

Currently not all radiopharmaceuticals for PC are available in all territorial PET/CT reference operative units; therefore, we consider it suitable to provide updated data on the results of ^{18}F-FCH PET/CT, which is currently more widely diffused.

Our study confirms that ^{18}F-FCH PET/CT is valid in the evaluation of PC patients with suspected biochemical recurrence, regardless of the treatment performed and the PSA values, which are higher in case of multiple lesions, independent of the sites of metastases.

Therefore, we can affirm that it still makes sense to perform ^{18}F-FCH PET/CT in patients with biochemical recurrence both in the presence of high PSA values and lower values.

Ethics

Ethics Committee Approval: A retrospective observational analysis was performed, and the institutional review board did not require ethical committee approval for the review of patient files.

Informed Consent: All patients provided written informed consent to the use of their data for clinical research in an anonymous form.

Authorship Contributions

Surgical and Medical Practices: F.T., A.S., A.C., Concept: C.A., A.N.A., A.R.P., Design: C.A., A.R.P., Data Collection or Processing: F.T., A.S., C.F., Analysis or Interpretation: A.N.A., C.F., Literature Search: A.C., D.R., Writing: C.A., D.R.

Conflict of Interest: No conflict of interest was declared by the authors.

Financial Disclosure: The authors declared that this study has received no financial support.

References

1. Chondrogiannis S, Marzola MC, Ferretti A, Maffione AM, Rampin L, Grassetto G, Nanni C, Colletti PM, Rubello D. Role of ^{18}F-choline PET/CT in suspicion of relapse following definitive radiotherapy for prostate cancer. Eur J Nucl Med Mol Imaging 2013;40:1356-1364.
2. Gauvin S, Cerantola Y, Haberer E, Pelsser V, Probst S, Bladou F, Anidjar M. Initial single-centre Canadian experience with 18F-fluoromethylcholine positron emission tomography-computed tomography (18F-FCH PET/CT) for biochemical recurrence in prostate cancer patients initially treated with curative intent. Can Urol Assoc J 2017;11:47-52.
3. Ferrari C, Mammucci P, Lavelli V, Pisani AR, Nappi AG, Rubini D, Sardaro A, Rubini G. [18F]fluciclovine vs. [18F]fluorocholine positron emission tomography/computed tomography: a head-to-head comparison for early detection of biochemical recurrence in prostate cancer patients. Tomography 2022;8:2709-2722.
4. Mottet N, van den Bergh RCN, Briers E, Van den Broeck T, Cumberbatch MG, De Santis M, Fanti S, Fossati N, Gandaglia G, Gillessen S, Grivas N, Grummet J, Henry AM, van der Kwast TH, Lam TB, Lardas M, Liew M, Mason MD, Moris L, Oprea-Lager DE, van der Poel HG, Rouvière O, Schoots IG, Tilki D, Wiegel T, Willemse PM, Cornford P. EAU-EANM-ESTRO-ESUR-SIOG Guidelines on Prostate Cancer-2020 Update. Part 1: Screening, Diagnosis, and Local Treatment with Curative Intent. Eur Urol 2021;79:243-262.
5. Choueiri TK, Dreicer R, Paciorek A, Carroll PR, Konety B. A model that predicts the probability of positive imaging in prostate cancer cases with biochemical failure after initial definitive local therapy. J Urol 2008;179:906-910; discussion 910.
6. Sardaro A, Ferrari C, Carbonara R, Altini C, Lavelli V, Rubini G. Synergism between immunotherapy and radiotherapy in esophageal cancer: an overview of current knowledge and future perspectives. Cancer Biother Radiopharm 2021;36:123-132.
7. Agarwal PK, Sadetsky N, Konety BR, Resnick MI, Carroll PR; Cancer of the Prostate Strategic Urological Research Endeavor (CaPSURE). Treatment failure after primary and salvage therapy for prostate cancer: likelihood, patterns of care, and outcomes. Cancer 2008;112:307-314.
8. Altini C, Niccoli Asabella A, De Luca R, Fanelli M, Caliandro C, Quartuccio N, Rubini D, Cistaro A, Montemurro S, Rubini G. Comparison of (18)F-FDG

PET/CT methods of analysis for predicting response to neoadjuvant chemoradiation therapy in patients with locally advanced low rectal cancer. Abdom Imaging 2015;40:1190-1202.

9. Altini C, Mammucci P, Pisani AR, D'Alò C, Sardaro A, Rubini D, Ferrari C, Rubini G. ^{18}F-FDG PET/CT in GIST treatment response evaluation beyond Imatinib. Hell J Nucl Med 2021;24:239-246.
10. Mütevelizade G, Sezgin C, Gümüşer G, Sayit E. Unexpected metastatic localizations of prostate cancer determined by ^{68}Ga PSMA PET/CT: series of four cases. Mol Imaging Radionucl Ther 2022;31:223-226.
11. Giovacchini G, Giovannini E, Leoncini R, Riondato M, Ciarmiello A. PET and PET/CT with radiolabeled choline in prostate cancer: a critical reappraisal of 20 years of clinical studies. Eur J Nucl Med Mol Imaging 2017;44:1751-1776.
12. Giovacchini G, Picchio M, Coradeschi E, Bettinardi V, Gianolli L, Scattoni V, Cozzarini C, Di Muzio N, Rigatti P, Fazio F, Messa C. Predictive factors of [(11)C]choline PET/CT in patients with biochemical failure after radical prostatectomy. Eur J Nucl Med Mol Imaging 2010;37:301-309.
13. Evangelista L, Zattoni F, Guttilla A, Saladini G, Zattoni F, Colletti PM, Rubello D. Choline PET or PET/CT and biochemical relapse of prostate cancer: a systematic review and meta-analysis. Clin Nucl Med 2013;38:305-314.
14. Bertagna F, Abuhilal M, Bosio G, Simeone C, Rossini P, Pizzocaro C, Orlando E, Finamanti M, Biasiotto G, Rodella C, Cosciani Cunico S, Giubbini R. Role of ^{11}C-choline positron emission tomography/computed tomography in evaluating patients affected by prostate cancer with suspected relapse due to prostate-specific antigen elevation. Jpn J Radiol 2011;29:394-404.
15. Picchio M, Briganti A, Fanti S, Heidenreich A, Krause BJ, Messa C, Montorsi F, Reske SN, Thalmann GN. The role of choline positron emission tomography/computed tomography in the management of patients with prostate-specific antigen progression after radical treatment of prostate cancer. Eur Urol 2011;59:51-60.
16. Scattoni V, Picchio M, Suardi N, Messa C, Freschi M, Roscigno M, Da Pozzo L, Bocciardi A, Rigatti P, Fazio F. Detection of lymph-node metastases with integrated [11C]choline PET/CT in patients with PSA failure after radical retropubic prostatectomy: results confirmed by open pelvic-retroperitoneal lymphadenectomy. Eur Urol 2007;52:423-429.
17. Husarik DB, Miralbell R, Dubs M, John H, Giger OT, Gelet A, Cservenyàk T, Hany TF. Evaluation of [(18)F]-choline PET/CT for staging and restaging of prostate cancer. Eur J Nucl Med Mol Imaging 2008;35:253-263.
18. Cookson MS, Aus G, Burnett AL, Canby-Hagino ED, D'Amico AV, Dmochowski RR, Eton DT, Forman JD, Goldenberg SL, Hernandez J, Higano CS, Kraus SR, Moul JW, Tangen C, Thrasher JB, Thompson I. Variation in the definition of biochemical recurrence in patients treated for localized prostate cancer: the American Urological Association Prostate Guidelines for Localized Prostate Cancer Update Panel report and recommendations for a standard in the reporting of surgical outcomes. J Urol 2007;177:540-545.
19. Roach M 3rd, Weinberg V, Nash M, Sandler HM, McLaughlin PW, Kattan MW. Defining high risk prostate cancer with risk groups and nomograms: implications for designing clinical trials. J Urol 2006;176:S16-20.
20. Graziani T, Ceci F, Castellucci P, Polverari G, Lima GM, Lodi F, Morganti AG, Ardizzoni A, Schiavina R, Fanti S. (11)C-Choline PET/CT for restaging prostate cancer. Results from 4,426 scans in a single-centre patient series. Eur J Nucl Med Mol Imaging 2016;43:1971-1979.
21. Reske SN, Blumstein NM, Glatting G. [(11)C]Choline PET/CT imaging in occult local relapse of prostate cancer after radical prostatectomy. Eur J Nucl Med Mol Imaging 2008;35:9-17.
22. Heinisch M, Dirisamer A, Loidl W, Stoiber F, Gruy B, Haim S, Langsteger W. Positron emission tomography/computed tomography with F-18-fluorocholine for restaging of prostate cancer patients: meaningful at PSA < 5 ng/ml? Mol Imaging Biol 2006;8:43-48.
23. Heidenreich A, Bastian PJ, Bellmunt J, Bolla M, Joniau S, van der Kwast T, Mason M, Matveev V, Wiegel T, Zattoni F, Mottet N; European Association of Urology. EAU guidelines on prostate cancer. part 1: screening, diagnosis, and local treatment with curative intent-update 2013. Eur Urol 2014;65:124-137.
24. Siminiak N, Wojciechowska K, Miechowicz I, Cholewiński W, Ruchała M, Czepczyński R. 18F-choline positron emission tomography/computed tomography for the detection of prostate cancer relapse: assessment of maximum standardized uptake value correlation with prostate-specific antigen levels. Nucl Med Commun 2019;40:1263-1267.
25. Wetter A, Lipponer C, Nensa F, Heusch P, Rubben H, Schlosser TW, Poppel TD, Lauenstein TC, Nagarajah J. Quantitative evaluation of bone metastases from prostate cancer with simultaneous [18F] choline PET/MRI: combined SUV and ADC analysis. Ann Nucl Med 2014;28:405-410.

Original Article
Mol Imaging Radionucl Ther 2024;33:11-18 DOI:10.4274/mirt.galenos.2023.65002

The Added-value of Staging ^{18}F-FDG PET/CT in the Prediction of Overall Survival in the Patients with Bladder Cancer

Mesane Kanseri Hastalarında Evreleme ^{18}F-FDG PET/BT'nin Genel Sağkalımı Öngörmeye Katkısı

Seda Gülbahar Ateş[1], Bedriye Büşra Demirel[2], Halil Başar[3], Gülin Uçmak[2]

[1]*Hitit University Çorum Erol Olçok Training and Research Hospital, Department of Nuclear Medicine, Çorum, Türkiye*
[2]*University of Health Sciences Türkiye, Ankara Dr. Abdurrahman Yurtaslan Oncology Training and Research Hospital, Clinic of Nuclear Medicine, Ankara, Türkiye*
[3]*University of Health Sciences Türkiye, Ankara Dr. Abdurrahman Yurtaslan Oncology Training and Research Hospital, Clinic of Urology, Ankara, Türkiye*

Abstract

Objectives: This retrospective study aimed to evaluate the prognostic importance of ^{18}F-fluorodeoxyglucose (^{18}F-FDG)-positive pelvic lymph nodes (LNs) and extra-pelvic disease on staging ^{18}F-FDG positron emission tomography/computed tomography (PET/CT) in patients with bladder cancer.

Methods: Bladder cancer patients who underwent staging ^{18}F-FDG PET/CT were included in the study. Histopathologic features of tumors, therapy histories, presence of distinguishable tumors on CT and PET images, sizes and maximum standardized uptake value (SUV_{max}) of primary tumors, total numbers, sizes, and SUV_{max} of ^{18}F-FDG-positive pelvic and extra-pelvic LNs, and total numbers and SUV_{max} of distant metastases (M1a/1b) were recorded. Patients were followed up until death or the last medical visit. Factors predicting overall survival were determined using Cox regression analysis.

Results: Fifty-five patients [median age: 70 (53-84), 48 (87.3%) male, 7 (12.7%) female] with bladder cancer were included in this study. Twenty-nine (52.7%) patients had ^{18}F-FDG positive pelvic LNs, while 24 (43.7%) patients had ^{18}F-FDG positive extra-pelvic disease. Patients with ^{18}F-FDG-positive pelvic LNs had a higher rate of extra-pelvic disease (p=0.003). The median follow-up duration was 13.5 months. The median overall survival was 16.3 months [95% confidence interval (CI) 8.9-23.7]. The primary tumor distinguishability on PET (p=0.011) and CT (p=0.009) images, the presence of ^{18}F-FDG-positive pelvic LNs (p<0.001) and ^{18}F-FDG-positive extra-pelvic disease/distant metastases (M1a/M1b) (p<0.001), and the number of distant metastases (p=0.034) were associated with mortality. The ^{18}F-FDG-positive extra-pelvic disease/distant metastases [p=0.029, odds ratio: 4.15 (95% CI 1.16-14.86)] was found to be an independent predictor of mortality in patients with bladder cancer.

Conclusion: The presence of ^{18}F-FDG-positive extra-pelvic disease in pretreatment ^{18}F-FDG PET/CT is an important prognostic factor in bladder cancer patients.

Keywords: Bladder cancer, ^{18}F-FDG PET/CT, overall survival

Öz

Amaç: Bu çalışmanın amacı mesane kanseri hastalarında evreleme ^{18}F-florodeoksiglikoz (^{18}F-FDG) pozitron emisyon tomografisi/bilgisayarlı tomografide (PET/BT) ^{18}F-FDG pozitif pelvik lenf nodlarının ve ekstra-pelvik hastalığın prognostik önemini değerlendirmektir.

Address for Correspondence: Seda Gülbahar Ateş MD, Hitit University Çorum Erol Olçok Training and Research Hospital, Department of Nuclear Medicine, Çorum, Türkiye
Phone: +90 507 377 85 98 **E-mail:** sdsdglbhr@gmail.com ORCID ID: orcid.org/0000-0003-0422-0863
Received: 15.03.2023 **Accepted:** 05.11.2023

Yöntem: Evreleme ^{18}F-FDG PET/BT çalışması yapılan mesane kanseri tanılı hastalar çalışmaya dahil edildi. Tümörlerin histopatolojik özellikleri, BT ve PET görüntülerinde ayırt edilebilir tümör varlığı, primer tümörün boyut ve maksimum standartlaştırılmış tutulum değeri (SUV_{maks}), ^{18}F-FDG pozitif pelvik ve ekstra-pelvik lenf nodlarının sayı, boyut ve SUV_{maks} değerleri, uzak metastaz sayısı ve SUV_{maks} değerleri kaydedildi. Hastalar ölüme veya son hastane vizitine kadar takip edildi. Genel sağkalımı öngören faktörleri belirlemek amacıyla Cox regresyon analizi yapıldı.

Bulgular: Elli beş [medyan yaş: 70 (53-84), 48 (%87,3) erkek, 7 (%12,7) kadın] mesane kanseri tanılı hasta çalışmaya dahil edildi. Yirmi dokuz (%52,7) hastada ^{18}F-FDG pozitif pelvik lenf nodu, 24 (%43,7) hastada ekstra-pelvik hastalık mevcuttu. ^{18}F-FDG pozitif pelvik lenf nodu olan hastalar daha sık ekstra-pelvik hastalığa sahipti (p=0,003). Medyan izlem süresi 13,5 ay, medyan genel sağkalım 16,3 ay [%95 güven aralığı (GA) 8,9-23,7] bulundu. Univariant analizde PET (p=0,011) ve BT'de (p=0,009) primer tümör ayırt edilebilirliği, ^{18}F-FDG pozitif pelvik lenf nodu varlığı (p<0,001), ^{18}F-FDG pozitif ekstra-pelvik hastalık/uzak metastaz varlığı (M1a/M1b) (p<0,001) ve metastaz sayısı (p=0,034) mortalite ile ilişkili bulundu. Multivariant analizde ^{18}F-FDG pozitif ekstra-pelvik hastalık/uzak metastaz varlığı [p=0,029, olasılık oranı: 4,15 (%95 GA 1,16-14,86)] mesane kanseri hastalarında mortaliteyi öngörmede bağımsız risk faktörü olarak bulundu.

Sonuç: Evreleme ^{18}F-FDG PET/BT çalışmasında ^{18}F-FDG pozitif ekstra-pelvik hastalık varlığı önemli bir prognostik faktördür.

Anahtar kelimeler: Mesane kanseri, ^{18}F-FDG PET/BT, genel sağkalım

Introduction

Bladder cancer (BC) is the tenth most common cancer and the thirteenth leading cause of cancer-related deaths worldwide according to the World Health Organization GLOBOCAN 2020 database (1). It is approximately 4 times more common in men than in women (1). Tobacco smoking is the most critical cause of BC, with an attributable risk of approximately 50% (2). The global geographic and temporal distribution patterns of BC reflect the prevalence of tobacco use (1,3).

Urothelial BC is the most common histopathological subtype. BC is a heterogeneous clinical spectrum that includes non-muscle-invasive and muscle-invasive diseases. Approximately 75% of patients have a non-muscle-invasive disease confined to the bladder mucosa/submucosa, whereas the remaining 25% have a muscle-invasive disease at the time of diagnosis (4). Therapy management and prognosis differ substantially from each other.

Early diagnosis and accurate staging, and individualized treatment and follow-up, are crucial for a successful outcome in BC (5). Computed tomography (CT) and magnetic resonance imaging (MRI) are widely used for local staging, imaging of lymph nodes (LNs), and distant metastases despite some limitations. For instance, the assessment of LN metastases in CT and MRI is based on size; therefore, the identification of metastases in normal-sized or minimally enlarged nodes is limited in these imaging modalities (6). ^{18}F-fluorodeoxyglucose (^{18}F-FDG) positron emission tomography/CT (PET/CT) is widely used for staging, restaging, and treatment response evaluation in various cancers. Initially, its use was limited in patients with BC due to the high urinary excretion activity of the ureters and bladder (7). Nevertheless, several studies have shown that PET/CT has a higher sensitivity in the determination of LN and distant metastases than CT and MRI, and it has caused a therapy management alteration in 19-68% of BC patients (8,9,10). Therefore, ^{18}F-FDG PET/CT is increasingly being used in clinical practice, and its exact role continues to be evaluated (6). Recommendations of guidelines on the use of ^{18}F-FDG PET/CT in BC increase over time. The National Comprehensive Cancer Network (NCCN) suggests that ^{18}F-FDG PET/CT may be beneficial in selected patients with T2 (muscle-invasive disease) and in patients with ≥cT3 disease (11). Moreover, PET/CT should be included in oligometastatic disease staging when considering radical surgery according to consensus statements of the European Association of Urology and European Society of Medical Oncology (12).

In the era of precision oncology, early prediction of prognosis is important in patient management and personalized therapy. Identification of prognostic factors for malignancies is an important research topic in oncology. Several studies have demonstrated various clinicopathological prognostic factors in patients with BC. In addition to these factors, the findings of ^{18}F-FDG PET/CT may have prognostic importance in terms of overall survival (OS). ^{18}F-FDG PET/CT has been shown to be highly sensitive in detecting extravesical tumor deposits in BC patients. However, it is critical to know whether the findings detected in ^{18}F-FDG PET impact prognosis in patients with BC. A limited number of studies have investigated its prognostic value (13). Therefore, our hypothesis was that the presence of ^{18}F-FDG-positive pelvic LNs and extra-pelvic diseases may predict patients with a poorer OS. Treatment management and intensification can be modified in these patients accordingly. This study aimed to evaluate the prognostic importance of the presence of ^{18}F-FDG-positive pelvic LNs and extra-pelvic disease on ^{18}F-FDG PET/CT in patients with BC.

Materials and Methods

Patient Population

This retrospective study was approved by the University of Health Sciences Türkiye, Ankara Dr. Abdurrahman Yurtaslan Oncology Training and Research Hospital Non-invasive Clinical Research Ethics Committee (no: 2022-09/167, date: 22.09.2022), and the requirement for informed consent was waived. Patients with histologically proven BC were included in this study. Patients who underwent a staging ^{18}F-FDG PET/CT due to the presence of muscle-invasive BC, high-risk histopathologic subtype, and/or radiological equivocal findings (lung nodules, bone lesions, etc. on CT or MR images that were evaluated as an equivocal for metastasis by clinicians) were included in the study. However, patients who underwent surgery or received chemotherapy (CTx) and/or radiotherapy (RT) before ^{18}F-FDG PET/CT imaging were excluded from the study. Furthermore, patients with secondary primary cancers were not included in the study.

Clinicopathological Features

Demographic characteristics were evaluated using the hospital information system. Tumor histopathologic subtypes and the presence of muscularis propria invasion were recorded from pathology reports. Therapy histories [CTx, RT, chemoradiotherapy (CRT), and surgery] after PET/CT were recorded. Patients were followed until death or the last medical visit. Follow-up time was calculated from the date of PET/CT to the date of death, lost to follow-up, or the last medical visit.

PET/CT Acquisition

All patients had fasted for at least 6 h before ^{18}F-FDG PET/CT studies. The serum glucose levels measured at the time of ^{18}F-FDG injections were 150 mg/dL. ^{18}F-FDG was intravenously administered at a dose of 5.5 MBq/kg body weight. PET/CT images were obtained using a three-dimensional Siemens Biograph True Point 6 PET/CT device 60 min after ^{18}F-FDG injection. A PET scanner and a 3-mm sliced multidetector CT scanner obtained simultaneous images in the same session. Low-dose CT images without intravenous iodinated contrast were used for attenuation correction and anatomical correlation. If nuclear medicine physicians required, some patients underwent dual-phase ^{18}F-FDG PET/CT with/without intravenous diuretic administration. Patients who underwent dual-phase pelvic imaging and their findings were recorded.

Image Analysis

Primary bladder tumors were assessed using PET/CT images. The presence of irregular wall thickening or mass formation was accepted as a distinguishable tumor on CT images. Primary tumors with distinguishable ^{18}F-FDG uptake from background activity were recorded as distinguishable tumors on PET images. The sizes and maximum standardized uptake value (SUV_{max}) of the primary tumors were recorded. The patients were evaluated for a synchronous tumor in the genitourinary tract on ^{18}F-FDG PET/CT images.

LNs with distinguishable ^{18}F-FDG uptake from background activity were accepted as ^{18}F-FDG positive. The presence, total number, and SUV_{max} of ^{18}F-FDG-positive pelvic and extra-pelvic LNs were recorded. Short-axis sizes of the largest ^{18}F-FDG-positive pelvic and extra-pelvic LNs were measured.

Extra-pelvic ^{18}F-FDG positive disease was accepted as distant metastases. M1a is the presence of ^{18}F-FDG positive extra-pelvic LNs, whereas M1b is other distant metastases according to the 8th TNM staging system (14). The locations, total numbers, and SUV_{max} of distant metastases (M1a/1b) were recorded.

Statistical Analysis

Statistical analyses were performed using SPSS software version 21. The variables were investigated using visual (histogram, probability plots) and analytical methods (Kolmogorov-Smirnov/Shapiro-Wilk's test) to determine whether or not they are normally distributed. Descriptive analyses were performed using frequencies for ordinal/nominal variables, medians, minimum, and maximum values for non-normally distributed variables, and mean ± standard deviation for normally distributed variables. The chi-square test was used to analyze the association between primary tumor distinguishability on PET/CT images, the presence and number of pelvic LNs, and the presence of extra-pelvic ^{18}F-FDG-positive disease (M0/M1a/M1b). The Kruskal-Wallis test was used to compare the features of primary tumors and pelvic LNs between the groups. Cox regression analyses were performed to determine the predictors of mortality in univariate and multivariate analyses. Regression analyses were performed using forward-conditional selection. Survival analysis was performed using the Kaplan-Meier method. An overall 5% type-1 error level was used to infer statistical significance.

Results

Fifty-five patients with BC were included in this study. The median age of the patients was 70 (53-84). In 55 patients, 48 (87.3%) were male and 7 (12.7%) were female. The indication for ^{18}F-FDG PET/CT imaging was the presence of muscle-invasive (muscularis propria) BC in 39 (70.9%) patients, whereas it was radiologically equivocal in 12

(21.8%) patients. Moreover, 4 (7.3%) patients had high-risk pathologic subtypes. Of these 4 patients, 1 had sarcoid subtype, 2 had small cell neuroendocrine carcinoma, and 1 of whom was adenocarcinoma + small cell neuroendocrine carcinoma.

The findings of ^{18}F-FDG PET/CT are summarized in Table 1. The median size of the primary tumor was 25.0 (13.0-168.0) mm. The mean SUV_{max} of the primary tumor was 16.1±6.2. The total number of patients with a distinguishable primary tumor on CT (an irregular wall thickening or a mass formation) was 38 (69.1%). The total number of patients with a distinguishable primary tumor on PET images (higher ^{18}F-FDG uptakes from the background) was 32 (58.2%). Eight (14.5%) patients had dual-phase pelvic PET/CT scans, and three of them had a distinguishable primary tumor on late-phase PET scan. Five patients had a suspicion of synchronous tumors in the genitourinary tract on PET/CT images.

Twenty-nine (52.7%) patients had ^{18}F-FDG-positive pelvic LNs, whereas 24 (43.7%) patients had ^{18}F-FDG-positive extra-pelvic disease (n=9 non-regional LNs, n=15 the other distant metastases). The total number of patients with bone, lung, and liver metastases was 9 (16.4%), 11 (20.0%), and 3 (5.4%), respectively.

There was a significant association between the presence of ^{18}F-FDG-positive pelvic LNs and extra-pelvic disease/distant metastases (M1a/M1b) (p=0.003). While 5 (19.2%) of 26 patients without ^{18}F-FDG positive pelvic LNs, 19 (65.5%) of 29 patients with ^{18}F-FDG positive pelvic LNs had ^{18}F-FDG-positive extra-pelvic disease. Patients with ^{18}F-FDG-positive pelvic LNs had a significantly higher rate of extra-pelvic disease.

There was no significant association between the presence of ^{18}F-FDG positive extra-pelvic disease and patient age (p=0.146), size (p=0.228) and SUV_{max} (p=0.520) of primary tumor, or size (p=0.289) and SUV_{max} (p=0.438) of pelvic LNs. Moreover, there was no significant difference between the presence of ^{18}F-FDG-positive extra-pelvic disease/distant metastases, primary tumor distinguishability on PET (p=0.145) and CT (p=0.225), and the number of ^{18}F-FDG-positive pelvic LNs (p=0.096).

The median follow-up duration was 13.5 months (3.2-78.8, interquartile range: 23.1 months). Four patients underwent cystectomy. The total numbers of patients who

Table 1. The findings of ^{18}F-FDG PET/CT

Features			Median or mean ± SD (min-max) or number (%)
The median size of primary tumor (mm)			25.0 (13.0-168.0)
The mean SUV_{max} of primary tumor (g/dL)			16.1±6.2 (5.4-29.0)
The presence of ^{18}F-FDG positive pelvic lymph node			29 (52.7%)
The number of ^{18}F-FDG positive pelvic lymph node		<5	19 (34.5%)
		5-9	2 (3.6%)
		>9	8 (14.5%)
The median size of ^{18}F-FDG positive pelvic lymph nodes (mm)			9.0 (5.0-42.0)
The median SUV_{max} of pelvic lymph nodes (g/dL)			5.4 (1.7-23.6)
The number of ^{18}F-FDG positive extra-pelvic lymph node		<5	11 (20.0%)
		5-9	4 (7.3%)
		>9	6 (10.9%)
The median size of extra-pelvic lymph nodes (mm)			9.0 (4.0-66.0)
^{18}F-FDG positive extra-pelvic disease/distant metastases (n=24)	Non-regional lymph node metastases (M1a)		9 (16.4%)
	Others distant metastases (M1b)		15 (27.3%)
The number of distant metastases		<5	8 (14.5%)
		5-9	5 (9.1%)
		>9	11 (20.0%)
The median SUV_{max} of distant metastases (g/dL)			7.0 (1.7-27.4)

SUV_{max}: Maximum standardized uptake value, ^{18}F-FDG: ^{18}F-fluorodeoxyglucose, PET/CT: Positron emission tomography/computed tomography, SD: Standard deviation, min-max: Minimum-maximum

received CTx, RT, and CRT were 17 (30.9%), 8 (14.6%), 18 (32.7%), respectively. Twelve (21.8%) patients have no treatment. The patients received CTx and/or RT and/or immunotherapy according to the clinician's decisions. In the follow-up, 36 (65.5%) of 55 patients died. The median OS was 16.3 months [95% confidence interval (CI) 8.9-23.7]. OS was 59.7% at 1 year, 42.4% at 2 years, and 30.8% at 3 years.

The results of the univariate and multivariate analyses are shown in Table 2. In the univariate analyses, primary tumor distinguishability on PET (p=0.011) and CT (p=0.009) images, the presence of ^{18}F-FDG-positive pelvic LNs (p<0.001) and ^{18}F-FDG-positive extra-pelvic disease/distant metastases (M0/M1a/M1b) (p<0.001), and the number of distant metastases (p=0.034) were significantly associated with mortality. Consequently, the presence of ^{18}F-FDG-positive extra-pelvic disease/distant metastases [p=0.029, odds ratio: 4.15 (95% CI 1.16-14.86)] was found to be an independent predictor of mortality in patients with BC in the multivariate analysis.

The median OS was significantly lower in patients with ^{18}F-FDG-positive extra-pelvic disease than in those without ^{18}F-FDG-positive extra-pelvic disease (Figure 1). The median OS of M0, M1a, and M1b patients was 32.9, 30.6, and 5.1 months, respectively (p<0.001).

Discussion

In the era of precision medicine, accurate pretreatment staging is essential for better outcomes in patients with BC, similar to other malignancies. Despite the initial hesitation due to the high urinary ^{18}F-FDG activity, ^{18}F-FDG PET/CT is increasingly used in clinical practice in BC patients with growing evidence-based data (7). In this study, we found that the presence of ^{18}F-FDG-positive extra-pelvic disease/distant metastases is an independent predictor of poorer OS in patients with BC.

Table 2. The results of the univariate and multivariate analyses

Parameters	Univariate			Multivariate		
	OR	95% CI	p-value	OR	95% CI	p-value
Patient age	-	-	p=0.988	-	-	-
Patient gender	-	-	p=0.582	-	-	-
High-risk pathologic subtype	-	-	p=0.909	-	-	-
Muscularis propria invasion	-	-	p=0.728	-	-	-
The distinguishability of primary tumor on CT	4.03	(1.41-11.51)	p=0.009*	-	-	-
The distinguishability of primary tumor on PET	2.87	(1.28-6.44)	p=0.011*	-	-	-
Primary tumor size	-	-	p=0.242	-	-	-
The SUV_{max} of primary tumor	-	-	p=0.369	-	-	-
The presence of ^{18}F-FDG positive pelvic LN	4.00	(1.87-8.57)	p<0.001*	-	-	-
The number of ^{18}F-FDG positive pelvic LN	-	-	p=0.256	-	-	-
The size of ^{18}F-FDG positive pelvic LN	-	-	p=0.363	-	-	-
The SUV_{max} of ^{18}F-FDG positive pelvic LN	-	-	p=0.721	-	-	-
The number of ^{18}F-FDG positive extra-pelvic LN	-	-	p=0.140	-	-	-
The size of ^{18}F-FDG positive extra-pelvic LN	-	-	p=0.259	-	-	-
The presence of ^{18}F-FDG positive extra-pelvic disease/distant metastases (M)	-	-	p<0.001*	4.15	(1.16-14.86)	p=0.029*
• M1a (extra-pelvic lymph node)	1.99	(0.75-5.24)	p=0.165	-	-	-
• M1b (others distant metastases)	6.18	(2.70-14.14)	p<0.001	-	-	-
The SUV_{max} of distant metastases	-	-	p=0.092	-	-	-
The number of distant metastases	-	-	p=0.034*	-	-	-
Surgery	-	-	p=0.110	-	-	-
CTx/RT/CRT	-	-	p=0.288	-	-	-

*Statistically significant parameters. OR: Odds ratio, CI: Confidence interval, CT: Computed tomography, PET: Positron emission tomography, SUV_{max}: Maximum standardized uptake value, ^{18}F-FDG: ^{18}F-fluorodeoxyglucose, LN: Lymph node, CTx: Chemotherapy, RT: Radiotherapy, CRT: Chemoradiotherapy

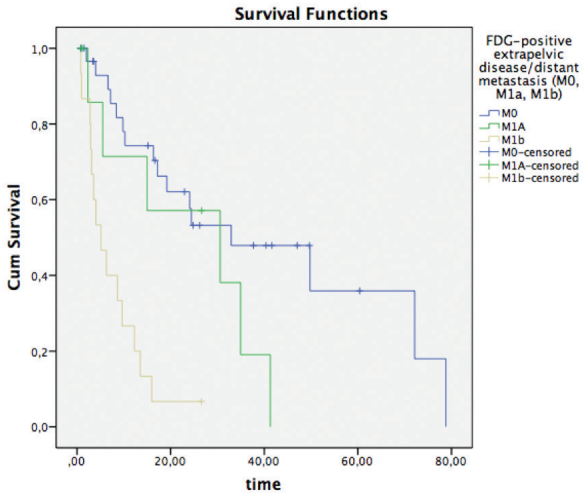

Figure 1. Kaplan-Meier survival analysis according to the presence of extra-pelvic [18]F-FDG positive disease in BC patients
[18]F-FDG: [18]F-fluorodeoxyglucose, BC: Bladder cancer

In this study, it was shown that patients with [18]F-FDG-positive pelvic LNs had a significantly higher rate of [18]F-FDG-positive extra-pelvic disease/distant metastases. LN involvement in BC has a prognostic implication (15). The presence, location, and number of involved LNs can help predict the prognosis of patients with BC This finding could be due to the prognostic importance of pelvic LNs, and the presence of these might be related to a more advanced disease. A prospective study to assess primary lymphatic landing sites from the bladder by Roth et al. (16) showed that the major lymphatic landing sites are pelvic (regional and common iliac) LNs, whereas only 4% of cases showed drainage initially to more distal LNs-para-aortic regions. All patients with para-aortic LNs had additional LNs in the pelvis (external iliac, internal iliac, or obturator fossa regions) (16). Based on this study, our findings may be due to lymphatic drainage pathways for extra-pelvic LNs (M1a) and the prognostic significance of pelvic LNs. Considering this finding of our study, patients with suspected pelvic LN positivity in conventional imaging modalities should be carefully evaluated for the presence of extra-pelvic disease in clinical practice. Consequently, these patients may be staged by [18]F-FDG PET/CT because of their higher sensitivity in the evaluation of LNs and distant metastases. In addition, [18]F-FDG PET/CT has an advantage in determining metastatic LNs regardless of the size.

In our study, the presence of [18]F-FDG positive pelvic LNs and [18]F-FDG positive extra-pelvic disease were associated with mortality in univariate analysis; however, only the presence of [18]F-FDG-positive extra-pelvic disease was found to be an independent predictor of mortality in BC patients in multivariate analysis. The median OS was significantly poorer in patients with [18]F-FDG-positive extra-pelvic disease than in those without [18]F-FDG-positive extra-pelvic disease. In parallel to our study, although their study designs and patient populations were somewhat different, a study on the prognostic value of [18]F-FDG PET/CT in muscle-invasive BC by Mertens et al. (13) found that extravesical [18]F-FDG-positive disease was an independent indicator of mortality in multivariate analysis. Furthermore, the studies demonstrated that OS was significantly poorer in patients with positive [18]F-FDG PET/CT than in those with negative [18]F-FDG PET/CT (17,18). According to the findings, the presence of [18]F-FDG-positive disease, especially in extra-pelvic regions, is an important prognostic factor in BC patients. In addition, patients with [18]F-FDG-positive extra-pelvic LNs had significantly better outcomes than patients with distant metastases, consistent with the literature (19). Contrary to the belief in clinical practice regarding the limitation of [18]F-FDG PET in BC, it is a valuable tool for the determination of pretreatment prognosis and stage, especially in selected BC patients. The presence and location of [18]F-FDG-positive disease has a critical prognostic value for patients with BC. [18]F-FDG PET/CT may contribute to treatment management and personalized therapy decisions by early determination of extra-pelvic disease in patients with BC.

The primary tumor distinguishability on PET and CT was associated with mortality in patients with BC in univariate analysis. It is known that the size of the primary tumor in BC is a prognostic factor (20,21). Patients with larger primary tumors might have more distinguishable tumors on PET and/or CT; therefore, their prognosis might be poorer than others. Moreover, aggressive tumors have a higher [18]F-FDG uptake (22,23), which may contribute to the distinction of primary tumors from urinary activity in PET images.

In our study, there was no association between the presence of [18]F-FDG-positive extra-pelvic disease, OS, and the sizes and SUV_{max} of primary tumors and pelvic LNs. These findings might be due to various factors such as a heterogeneous study population, difficulties such as high bladder activity in interpretation of primary tumor and pelvic LNs on PET/CT, and aggressive tumor behaviors independent of tumor sizes. However, to the best of our knowledge, metabolic prognostic factors such as SUV_{max} have not been reported in BC patients (24).

Study Limitations

This study has some main limitations. First, this was a retrospective study with a limited number of patients. Because of the nature of the study, some clinical information

such as clinical T-stages could not be obtained. Moreover, our patient population was heterogeneous in terms of clinicopathological features and therapies. Although it has been shown that ^{18}F-FDG PET/CT identifies more pelvic and extra-pelvic diseases, the number of studies investigating its prognostic value is limited. Therefore, our study has provided valuable information. Multicenter randomized prospective studies with more patients are needed on this topic.

Conclusion

^{18}F-FDG PET/CT is a valuable tool for staging and determining pretreatment prognosis in selected BC patients. The presence of ^{18}F-FDG-positive extra-pelvic disease in pretreatment ^{18}F-FDG PET/CT is an important prognostic factor in BC patients.

Ethics

Ethics Committee Approval: This retrospective study was approved by the University of Health Sciences Türkiye, Ankara Dr. Abdurrahman Yurtaslan Oncology Training and Research Hospital Non-invasive Clinical Research Ethics Committee (no: 2022-09/167, date: 22.09.2022).

Informed Consent: Retrospective study.

Authorship Contributions

Surgical and Medical Practices: H.B., Concept: S.G.A., B.B.D., H.B., G.U., Design: S.G.A., B.B.D., H.B., G.U., Data Collection or Processing: S.G.A., B.B.D., Analysis or Interpretation: S.G.A., B.B.D., G.U., Literature Search: S.G.A., Writing: S.G.A., B.B.D., G.U.

Conflict of Interest: No conflict of interest was declared by the authors.

Financial Disclosure: The authors declared that this study has received no financial support.

References

1. Sung H, Ferlay J, Siegel RL, Laversanne M, Soerjomataram I, Jemal A, Bray F. Global Cancer Statistics 2020: GLOBOCAN estimates of incidence and mortality worldwide for 36 cancers in 185 countries. CA Cancer J Clin 2021;71:209-249.
2. Cumberbatch MG, Rota M, Catto JW, La Vecchia C. The role of tobacco smoke in bladder and kidney carcinogenesis: a comparison of exposures and meta-analysis of incidence and mortality risks. Eur Urol 2016;70:458-466.
3. Teoh JY, Huang J, Ko WY, Lok V, Choi P, Ng CF, Sengupta S, Mostafid H, Kamat AM, Black PC, Shariat S, Babjuk M, Wong MC. Global trends of bladder cancer incidence and mortality, and their associations with tobacco use and gross domestic product per capita. Eur Urol 2020;78:893-906.
4. Cumberbatch MGK, Jubber I, Black PC, Esperto F, Figueroa JD, Kamat AM, Kiemeney L, Lotan Y, Pang K, Silverman DT, Znaor A, Catto JWF. Epidemiology of bladder cancer: a systematic review and contemporary update of risk factors in 2018. Eur Urol 2018;74:784-795.
5. Kamat AM, Hahn NM, Efstathiou JA, Lerner SP, Malmström PU, Choi W, Guo CC, Lotan Y, Kassouf W. Bladder cancer. Lancet 2016;388:2796-2810.
6. Witjes J, Bruins M, Cathomas R, Compérat E, Cowan N, Gakis G, van der Heijden AG, Hernández V, Lebret T, Lorch A, Ribal MJ. EAU guidelines on muscle-invasive and metastatic bladder cancer. EAU Guidelines (2019 Edn) 2022.
7. Omorphos NP, Ghose A, Hayes JDB, Kandala A, Dasgupta P, Sharma A, Vasdev N. The increasing indications of FDG-PET/CT in the staging and management of invasive bladder cancer. Urol Oncol 2022;40:434-441.
8. Apolo AB, Riches J, Schöder H, Akin O, Trout A, Milowsky MI, Bajorin DF. Clinical value of fluorine-18 2-fluoro-2-deoxy-D-glucose positron emission tomography/computed tomography in bladder cancer. J Clin Oncol 2010;28:3973-3978.
9. Bertolaso P, Brouste V, Cazeau AL, de Clermont-Gallerande H, Bladou F, Cabart M, Lefort F, Gross-Goupil M. Impact of 18 FDG- PET CT in the management of muscle invasive bladder cancer. Clin Genitourin Cancer 2022;20:297-297.e6.
10. Frączek M, Kamecki H, Kamecka A, Sosnowski R, Sklinda K, Czarniecki M, Królicki L, Walecki J. Evaluation of lymph node status in patients with urothelial carcinoma-still in search of the perfect imaging modality: a systematic review. Transl Androl Urol 2018;7:783-803.
11. Flaig TW, Spiess PE, Abern M, Agarwal N, Bangs R, Boorjian SA, Buyyounouski MK, Chan K, Chang S, Friedlander T, Greenberg RE, Guru KA, Herr HW, Hoffman-Censits J, Kishan A, Kundu S, Lele SM, Mamtani R, Margulis V, Mian OY, Michalski J, Montgomery JS, Nandagopal L, Pagliaro LC, Parikh M, Patterson A, Plimack ER, Pohar KS, Preston MA, Richards K, Sexton WJ, Siefker-Radtke AO, Tollefson M, Tward J, Wright JL, Dwyer MA, Cassara CJ, Gurski LA. NCCN Guidelines® Insights: Bladder Cancer, Version 2.2022. J Natl Compr Canc Netw 2022;20:866-878.
12. Witjes JA, Babjuk M, Bellmunt J, Bruins HM, De Reijke TM, De Santis M, Gillessen S, James N, Maclennan S, Palou J, Powles T, Ribal MJ, Shariat SF, Der Kwast TV, Xylinas E, Agarwal N, Arends T, Bamias A, Birtle A, Black PC, Bochner BH, Bolla M, Boormans JL, Bossi A, Briganti A, Brummelhuis I, Burger M, Castellano D, Cathomas R, Chiti A, Choudhury A, Compérat E, Crabb S, Culine S, De Bari B, De Blok W, J L De Visschere P, Decaestecker K, Dimitropoulos K, Dominguez-Escrig JL, Fanti S, Fonteyne V, Frydenberg M, Futterer JJ, Gakis G, Geavlete B, Gontero P, Grubmüller B, Hafeez S, Hansel DE, Hartmann A, Hayne D, Henry AM, Hernandez V, Herr H, Herrmann K, Hoskin P, Huguet J, Jereczek-Fossa BA, Jones R, Kamat AM, Khoo V, Kiltie AE, Krege S, Ladoire S, Lara PC, Leliveld A, Linares-Espinós E, Løgager V, Lorch A, Loriot Y, Meijer R, Mir MC, Moschini M, Mostafid H, Müller AC, Müller CR, N'Dow J, Necchi A, Neuzillet Y, Oddens JR, Oldenburg J, Osanto S, J G Oyen W, Pacheco-Figueiredo L, Pappot H, Patel MI, Pieters BR, Plass K, Remzi M, Retz M, Richenberg J, Rink M, Roghmann F, Rosenberg JE, Rouprêt M, Rouvière O, Salembier C, Salminen A, Sargos P, Sengupta S, Sherif A, Smeenk RJ, Smits A, Stenzl A, Thalmann GN, Tombal B, Turkbey B, Lauridsen SV, Valdagni R, Van Der Heijden AG, Van Poppel H, Vartolomei MD, Veskimäe E, Vilaseca A, Rivera FAV, Wiegel T, Wiklund P, Williams A, Zigeuner R, Horwich A. EAU-ESMO consensus statements on the management of advanced and variant bladder cancer-an international collaborative multistakeholder effort: under the auspices of the EAU-ESMO guidelines committees. Eur Urol 2020;77:223-250.
13. Mertens LS, Mir MC, Scott AM, Lee ST, Fioole-Bruining A, Vegt E, Vogel WV, Manecksha R, Bolton D, Davis ID, Horenblas S, van Rhijn BW, Lawrentschuk N. 18F-fluorodeoxyglucose–positron emission tomography/computed tomography aids staging and predicts mortality in patients with muscle-invasive bladder cancer. Urology 2014;83:393-398.
14. Paner GP, Stadler WM, Hansel DE, Montironi R, Lin DW, Amin MB. Updates in the eighth edition of the tumor-node-metastasis staging classification for urologic cancers. Eur Urol 2018;73:560-569.

15. Shankar PR, Barkmeier D, Hadjiiski L, Cohan RH. A pictorial review of bladder cancer nodal metastases. Transl Androl Urol 2018;7:804-813.
16. Roth B, Wissmeyer MP, Zehnder P, Birkhäuser FD, Thalmann GN, Krause TM, Studer UE. A new multimodality technique accurately maps the primary lymphatic landing sites of the bladder. Eur Urol 2010;57:205-211.
17. Drieskens O, Oyen R, Van Poppel H, Vankan Y, Flamen P, Mortelmans L. FDG-PET for preoperative staging of bladder cancer. Eur J Nucl Med Mol Imaging 2005;32:1412-1417.
18. Kibel AS, Dehdashti F, Katz MD, Klim AP, Grubb RL, Humphrey PA, Siegel C, Cao D, Gao F, Siegel BA. Prospective study of [18F]fluorodeoxyglucose positron emission tomography/computed tomography for staging of muscle-invasive bladder carcinoma. J Clin Oncol 2009;27:4314-4320.
19. Galsky MD, Moshier E, Krege S, Lin CC, Hahn N, Ecke T, Sonpavde G, Godbold J, Oh WK, Bamias A. Nomogram for predicting survival in patients with unresectable and/or metastatic urothelial cancer who are treated with cisplatin-based chemotherapy. Cancer 2013;119:3012-3019.
20. Cheng L, Neumann RM, Scherer BG, Weaver AL, Leibovich BC, Nehra A, Zincke H, Bostwick DG. Tumor size predicts the survival of patients with pathologic stage T2 bladder carcinoma: a critical evaluation of the depth of muscle invasion. Cancer 1999;85:2638-2647.
21. Abudurexiti M, Ma J, Li Y, Hu C, Cai Z, Wang Z, Jiang N. Clinical outcomes and prognosis analysis of younger bladder cancer patients. Curr Oncol 2022;29:578-588.
22. Hofman MS, Hicks RJ. How We Read Oncologic FDG PET/CT. Cancer Imaging 2016;16:35.
23. Ziai P, Hayeri MR, Salei A, Salavati A, Houshmand S, Alavi A, Teytelboym OM. Role of optimal quantification of FDG PET imaging in the clinical practice of radiology. Radiographics 2016;36:481-496.
24. Girard A, Vila Reyes H, Shaish H, Grellier JF, Dercle L, Salaün PY, Delcroix O, Rouanne M. The role of 18F-FDG PET/CT in guiding precision medicine for invasive bladder carcinoma. Front Oncol 2020;10:565086.

Original Article
Mol Imaging Radionucl Ther 2024;33:19-27 DOI:10.4274/mirt.galenos.2023.04880

Evaluation of the Relationship Between Mobile Phone Usage and miRNA-574-5p and miRNA-30C-5p Levels in Thyroid Cancer Patients

Tiroid Kanserli Hastalarda Cep Telefonu Kullanımı ile miRNA-574-5p ve miRNA-30 Düzeyleri Arasındaki İlişkinin Değerlendirilmesi

Zekiye Hasbek[1], Ayça Taş[2], Seyit Ahmet Ertürk[3], Barış Sarıakçalı[4], Özge Ulaş Babacan[5], Gülhan Duman[6], Yavuz Silig[7]

[1]*Sivas Cumhuriyet University Faculty of Medicine, Department of Nuclear Medicine, Sivas, Türkiye*
[2]*Sivas Cumhuriyet University Faculty of Faculty of Health Sciences, Department of Nutrition and Dietetics, Sivas, Türkiye*
[3]*Karadeniz Technical University Faculty of Medicine, Department of Nuclear Medicine, Trabzon, Türkiye*
[4]*Sivas Cumhuriyet University Faculty of Medicine, Department of Endocrinology and Metabolism, Sivas, Türkiye*
[5]*Tokat Gaziosmanpaşa University Faculty of Medicine, Department of Nuclear Medicine, Tokat, Türkiye*
[6]*Medical Park Seyhan Hospital, Clinic of Endocrinology and Metabolism, Adana, Türkiye*
[7]*Sivas Cumhuriyet University Faculty of Medicine, Department of Biochemistry, Sivas, Türkiye*

Abstract

Objectives: This study aimed to evaluate the relationship between mobile phone usage and miRNA-574-5p and miRNA-30C-5p levels in patients diagnosed with differentiated thyroid cancer (DTC).

Methods: Fifty patients diagnosed with DTC and 50 healthy volunteers were included in the study. miRNA-574-5p and miRNA-30C-5p gene expression levels in the blood of all subjects were analyzed by real time-polymerase chain reaction, and a questionnaire including various questions was administered to both groups.

Results: Although there was a 7.60-fold increase in miRNA-30C-5p gene expression levels in the patient group compared with the control group, it was not found to be statistically significant. Considering the miRNA-574-5p gene expression levels, although there was a 2.96-fold increase in the patient group compared with the control group, no significant relationship was found. In our study, 85% of our patients were using mobile phones with internet access, whereas 98% of our healthy volunteers were using mobile phones ($p<0.05$). While 53.5% of the patients had their mobile phones with them while they were sleeping, this rate was 83.7% in healthy volunteers ($p<0.05$). However, 93.9% of the healthy volunteers did not have a Wi-Fi device in their bedrooms, and this rate was 75% in the patient group ($p<0.05$).

Conclusion: Although miRNA-30C-5p and miRNA-574-5p gene expression levels were higher in patients than in healthy volunteers, the differences were not statistically significant. Although there was no significant difference in miRNA levels, we believe that due to the higher rate of Wi-Fi device presence in bedrooms in patients compared with healthy volunteers, the effects of electromagnetic radiation on the thyroid can be reduced by paying attention to this simple change.

Keywords: Thyroid cancer, radioiodine, miRNA-574-5p, miRNA-30C-5p

Address for Correspondence: Prof. Dr. Zekiye Hasbek, Sivas Cumhuriyet University Faculty of Medicine, Department of Nuclear Medicine, Sivas, Türkiye
Phone: +90 346 258 02 53 **E-mail:** hasbekz@yahoo.com ORCID ID: orcid.org/0000-0002-8119-3363
Received: 14.08.2023 **Accepted:** 26.11.2023

Öz

Amaç: Bizim bu çalışmada amacımız, diferansiye tiroid kanseri (DTK) tanısı konulan hastalarda cep telefonu kullanımının, miRNA-574-5p ve miRNA-30C-5p ile ilişkisini değerlendirmekti.

Yöntem: Çalışmaya DTK tanılı 50 hasta ve 50 sağlıklı gönüllü dahil edildi. Tüm deneklerin kanlarındaki miRNA-574-5p ve miRNA-30C-5p gen ekspresyon seviyeleri gerçek zamanlı polimeraz zincir reaksiyonu yöntemi ile analiz edildi ve her iki gruba çeşitli sorular içeren bir anket uygulandı.

Bulgular: Kontrol grubuna göre hasta grubunda miRNA-30C-5p gen ekspresyon düzeylerinde 7,60 kat artış olmasına rağmen istatistiksel olarak anlamlı bulunmadı. miRNA-574-5p gen ekspresyon seviyelerine bakıldığında hasta grubunda kontrol grubuna göre 2,96 kat artış olmasına rağmen anlamlı bir ilişki bulunmadı. Çalışmamızda hastalarımızın %85'i internet erişimi olan cep telefonu kullanırken, sağlıklı gönüllülerimizin %98'i cep telefonu kullanmaktaydı ($p<0,05$). Hastaların %53,5'i uyurken cep telefonunu yanında bulundururken, sağlıklı gönüllülerde bu oran %83,7 idi ($p<0,05$). Ancak sağlıklı gönüllülerin %93,9'unun yatak odalarında Wi-Fi cihazı bulunmadığı, hasta grubunda ise bu oranın %75 olduğu saptandı ($p<0,05$).

Sonuç: miRNA-30C-5p ve miRNA-574-5p gen ekspresyon seviyeleri hastalarda sağlıklı gönüllülere göre daha yüksek olmasına rağmen istatistiksel olarak anlamlı değildi. miRNA düzeylerinde anlamlı bir fark olmasa da sağlıklı gönüllülere göre hastaların yatak odalarında Wi-Fi cihazı bulunma oranının daha yüksek olması nedeniyle elektromanyetik radyasyonun tiroid üzerindeki etkilerinin bu basit değişikliğe dikkat edilerek azaltılabileceğini düşünüyoruz.

Anahtar kelimeler: Tiroid kanser, radyoiyot, miRNA-574-5p, miRNA-30C-5p

Introduction

Thyroid cancer is the most common endocrine system malignancy, and its incidence is increasing, which can be noticed by all departments working on thyroid gland diseases. Some authors believe that this increase is associated with more frequent health check-ups and increased diagnostic possibilities (1). The etiology of thyroid cancer is currently unknown. However, obesity, smoking, hormonal exposure, and some environmental factors may play a role, especially in childhood exposure to ionizing radiation (2). In addition to diagnostic technological developments against diseases, technological developments that cause electromagnetic radiation exposure, especially mobile phones, have accelerated and become indispensable in our daily lives. The increase in the incidence of thyroid cancer and the parallel increase in mobile phone use raise the question of whether electromagnetic radiation (EMR) plays a role in the etiology of thyroid cancer.

Radiation is divided into two groups, ionizing and non-ionizing radiation, according to its effects on the tissue. Ionizing radiation is also divided into two groups: photon radiation (X and γ-rays) and particulate radiation (such as protons, neutrons, ß and α rays). Non-ionizing radiation consists of ultraviolet, visible light, infrared, microwaves, and radio waves. Biological effects of radiation such as cancer occur mainly with ionizing radiation types. Mobile phones are also a source of non-ionizing radiation. There is an increased risk of developing thyroid cancer in those exposed to high-dose ionizing radiation (3). However, the relationship between the effects of non-ionizing EMR and cancer development has not been definitively proven. According to the results of the INTERPHONE study, no increase was found in the incidence of glioma, meningioma, and acoustic neuroma in long-term mobile phone users (4). The thyroid gland is close to the location where mobile phones are used and is located in the electromagnetic field. Studies have shown that EMR can cause thyroid dysfunction (5). Although Milham and Morgan (6) stated that the incidence of thyroid cancer increases in people with excessive cell phone use, according to most studies in the literature, EMR does not show a carcinogenic effect (7).

Exosomes are extracellular vesicles that are produced and released by different cells, have a size of approximately 30-100 nm, consist of proteins, DNA, mRNAs, microRNAs (miRNAs), and lipids, and provide intercellular communication. Because of the presence of miRNAs located in exosome vesicles in biological fluids, many studies have been conducted on their use as non-invasive biomarkers in cancers (8,9). It plays crucial roles in biological processes, including apoptosis, proliferation, differentiation, and cell growth, with a role in the regulation of gene expression. Each miRNA molecule can bind to several mRNAs and different miRNAs in the mRNA. This may be an important reason why we see different clinical conditions in each patient, even though they have the same tumor type. Numerous studies are ongoing regarding the potential of miRNAs to be used as biomarkers in oncology because of their important role in directing mRNA and subsequent gene expression in both normal and tumor tissues. Changes in the regulation of miRNAs can cause carcinogenesis and cancer progression, and miRNA molecules function as oncogenes in some cancers and as tumor suppressor genes in others. For this purpose, several studies have been conducted on different miRNA panels. For example, it has been reported that miRNA-30 is downregulated after EMR and activates autophagy (10). Recently, the

issue of miRNAs associated with thyroid cancers has also been investigated. Recently, Zhang et al. (11); reported that miR-574-5p/FOXN3 is important in the progression of thyroid cancers. In two other studies conducted with the same miRNA, it was reported that the upregulation of miRNA-574-5p was oncogenic for thyroid cancers (12,13). In studies related to ionizing radiation and miRNA, Li et al. (14) showed that miR-30 plays an important role in radiation-induced apoptosis by directly targeting hematopoietic cells. According to Hao et al. (10), the downregulation of miRNA-30 after EMR exposure is provided by the expression modulation of Beclin, which activates autophagy.

Our aim in this study was to evaluate the relationship between mobile phone use and miRNA-574-5p and miRNA-30 in patients with thyroid cancer.

Materials and Methods

Patient and Healthy Volunteer Selection

Patients diagnosed with differentiated thyroid cancer and evaluated for radioactive iodine treatment by the Departments of Nuclear Medicine and Endocrinology and Metabolism were included in the study. Patients who had received radioactive iodine treatment before and did not agree to participate in the survey were excluded from the study. In addition, patients with another cancer history were not included in the study. While blood was drawn for routine tests during hospitalization for RAI treatments, additional blood was taken to determine miRNA-574-5p and miRNA-30C-5p gene expression levels.

Healthy volunteers were included in the study and the number of patients. Healthy volunteers were selected from those who had not been diagnosed with thyroid cancer and who had no thyroid nodules. The healthy volunteers included in the study were selected from people who were similar to the thyroid cancer patient group in terms of age and gender. Before being included in the study, neck ultrasonography was performed by specialist physicians in the Department of Endocrinology on all healthy volunteers. Blood was collected from healthy volunteers who met the study criteria to determine the gene expression levels of miRNA-574-5p and miRNA-30C-5p.

In addition, questions related to the use of mobile phones by patients and healthy volunteers were answered orally.

Ethical approval for this study was obtained from the Cumhuriyet University Clinical Research Ethics Committee (decision no: 2020-05/02, date: 21.05.2020).

Collection of Blood Samples From the Patient and Healthy Volunteer Groups

During the radioactive iodine treatment of the patients, while routine blood tests (serum thyroid stimulating hormone, thyroglobulin and anti-thyroglobulin antibody) were performed before hospitalization, approximately 2 mL of blood was taken into Paxgene tubes, which will provide RNA stabilization, in the same session, and these blood were stored at -80 °C until all patients were completed. Blood was collected from a similar number of healthy volunteers in the same way as in the patient group and stored.

Gene Expression Analysis Using Real Time-polymerase Chain Reaction (RT-PCR)

RNA Isolation From Blood

RNA isolation was performed according to the manufacturer's protocol using the RNeasy Plus mini isolation kit.

ComplementaryDNA (cDNA) Synthesis

To determine the expression levels of miRNA-574-5p and miRNA-30C-5p by RT-PCR, cDNA synthesis from RNA was performed in accordance with the appropriate kit protocol.

RT-PCR Analysis

RT-PCR analysis of *miRNA-574-5p (YP02116206, A.B.T/ABT-PRMR)* and *miRNA-30C-5p (YP00204783, A.B.T/ABT-PRMR)* genes was performed using the ABT 2X Q-PCR SYBR-Green MasterMix (Without ROX) kit. All cDNA samples were run 3 times under the same conditions. The mean of these three measurements was used in the analyses. In the study, the housekeeping gene *glyceraldehyde 3-phosphate dehydrogenase (GAPDH)* (PPH00150F, Qiagen) was used as an internal control to determine the differences in expression levels between the control and study groups.

Analysis of the RT-PCR Data

Analysis of all RT-PCR data of gene expression experiments was performed using Rotor-gene 6000 Series Software Version 1.7. Statistical analysis of the data with the ΔΔCT method was performed using the software "RT2 profiler RT-PCR Array Data Analysis version 3.5" (http://pcrdataanalysissabiosciences.com/pcr/arrayanalysis.php).

Statistical Analysis

SPSS version 24 software was used for statistical analysis. Descriptive quantitative data are expressed as median values, and qualitative data are expressed as percentages. Fisher's exact test and chi-square test were used to compare variables. Whether the variables showed normal

distribution was evaluated by visual (histogram and probability graphs) and analytical methods (Kolmogorov-Smirnov/Shapiro-Wilk tests). Descriptive analyses were performed using median and interquartile range for non-normally distributed variables. Student's t-test was used in the analysis of normally distributed data, whereas the Mann-Whitney U test was used in the evaluation of data that did not show normal distribution. A p-value of 0.05 was considered to indicate a statistically significant result.

Results

Similar to the literature, the frequency of female patients was much higher, and 41 (82%) of the 50 patients included in the study were female and 9 (18%) were male. The median age was 47 years (range: 17-71 years) in the patients, 46 years (range: 17-71 years) in women, and 51 years (range: 17-81 years) in men. Of the patients, 47 (94%) were papillary and 3 (6%) were follicular. The median tumor size was 17.5 mm (range: 8-70). Of the patients, 23 (46%) were under the age of 45, and 27 (54%) were ≥45 years old. Tumor size was ≤2 cm in 30 (60%) patients, and tumor size was greater than 2 cm in 20 (40%) patients. While the tumor was in one focus in 22 (44%) patients, the tumor was in 2 foci in 10 (20%) patients, the tumor was in 3 foci in 7 patients (14%), and the tumor was in more than 3 foci in 11 (22%) patients. All demographic and clinicopathological data of the patients are presented in Table 1.

When the answers given to the questionnaire in the patient group were evaluated, seven of the patients (14%) had a family history of thyroid cancer. A patient (railroad worker) said he had worked in the radiation field for several years. Except for this patient, the other patients had no history of radiation. Seven of our patients (14%) did not have a history of using mobile phones with internet access. Of these 7 patients, 2 had no history of cell phone use. The median mobile phone usage time of the patients was 10 years (range: 1-25 years), and the median daily cell phone usage time was 3 h (range: 0.5-15 hours). While 81.4% of the patients did not use headphones during long conversations, 83.7% did not turn off their phones while sleeping. 53.5% of the patients had a mobile phone with them while they were sleeping. 5 of the patients did not have a Wi-Fi device at home. In 25.6% of the patients, the Wi-Fi device was in the bedroom, and 90.2% of the patients did not turn off the Wi-Fi device while they were sleeping.

Our study included 50 healthy volunteers. Of these, 33 (66%) were female and 17 (34%) were male. The median age of healthy volunteers was 47.5 (range: 18-66 years). When the

Table 1. Demographic and clinicopathological data of patients

Patient characteristics	**n (%)**
Gender	
Female	41 (82)
Male	9 (18)
Histopathological classification	
Papillary carcinoma	47 (94)
Follicular carcinoma	3 (6)
Age	Median: 47 (range: 17-71)
<45	23 (46)
≥45	27 (54)
Tumor size	Median: 17.5 mm (range: 8-70 mm)
Number of tumor foci	
1	22 (44)
2	10 (20)
3	7 (14)
>3	11 (22)
Presence of lymphovascular invasion	
Present	8 (16)
Absent	42 (84)
Presence of perineural invasion	
Present	3 (6)
Absent	47 (94)
Tumor capsule invasion	
Present	8 (16)
Absent	42 (84)
Thyroid capsule invasion	
Present	14 (28)
Absent	36 (72)
Soft tissue invasion	
Present	14 (28)
Absent	36 (72)
Thyroid parenchyma invasion	
Present	4 (8)
Absent	46 (92)
Lymph node metastasis	
Present	5 (10)
Absent	45 (90)
Distant metastasis	
Present	5 (10)
Absent	45 (90)

responses of healthy volunteers to the questionnaire were evaluated, 9 (18%) had a family history of thyroid cancer. None of the healthy volunteers had a history of high-dose radiation exposure to the neck region. However, 4 patients had a history of laser epilation in the neck area. Only 1 (2%) of the healthy volunteers had a history of using a mobile phone with internet access. The median phone usage time of healthy volunteers was 13 years (range: 2-23 years), and the daily median phone usage time was 4 h (range: 0.5-15 hours). Of the healthy volunteers, 86% did not have a history of using headphones for prolonged conversations, and 90% did not turn off their phones while sleeping. In 83.7% of the healthy volunteers, their mobile phone was with them while they were sleeping. 1 of the healthy volunteers did not have a Wi-Fi device at home. Of the healthy volunteers, 6.1% had a Wi-Fi device in the bedroom, and 93.9% did not turn off the Wi-Fi device while sleeping. The results of the questionnaire answers of the patients and healthy volunteers are given in Table 2.

Statistical Analysis of RT-PCR Results

Expression levels of *miRNA-30C-5p* and *miRNA-574-5p* genes were analyzed by RT-PCR in the differentiated thyroid cancer patient group and healthy volunteer group. *GAPDH* was used as a housekeeping gene in our study. Normalization of the expression levels of genes was achieved with GAPDH.

Table 2. Comparison of the survey results of patient and healthy volunteer groups

	Patient n (%)	**Healthy volunteer n (%)**	**p-value**
Family history of thyroid cancer			
Present	7 (43.8)	9 (56.3)	
Absent	43 (51.2)	41 (48.8)	0.585
High-dose radiation exposure to the neck			
Present	-	-	
Absent	50 (100)	50 (100)	0.315
Smartphone usage			
Present	43 (46.7)	49 (53.3)	
Absent	7 (87.5)	1 (12.5)	0.027*
Phone usage time (years) Median (range)/year	10 (1-25)	13 (2-23)	0.115
Daily usage time (hour) Median (range)/hour	3 (0.5-15)	4 (0.5-15)	0.667
Headphone use			
Present	8 (57.1)	6 (42.9)	
Absent	35 (44.9)	43 (55.1)	0.397
Do you turn off the phone while sleeping?			
Yes	7 (63.6)	4 (36.4)	
No	36 (44.4)	45 (55.6)	0.231
Is the phone with you while you sleep?			
Yes	23 (35.9)	41 (64.1)	
No	20 (71.4)	8 (28.6)	0.002*
Is there a Wi-Fi device in the bedroom?			
Yes	11 (78.6)	3 (21.4)	
No	33 (41.8)	46 (58.2)	0.011*
Do you turn off the Wi-Fi device while sleeping?			
Yes	4 (57.1)	3 (42.9)	
No	37 (44.6)	46 (55.4)	0.522

*Sign indicates p<0.05. Seven patients and one healthy volunteer did not use smartphones. In addition, 5 patients and 1 healthy volunteer did not have a Wi-Fi device at home. For this reason, the number of subjects was missing in some analyses

Statistical analysis of RT-PCR data was performed using Rotor-Gene 6000 software, RT² SYBRGreen qPCR Array Data Analysis version 3.5. The data obtained because of the experiment were analyzed using the ΔΔCT method in the RT-PCR device. RT-PCR data were evaluated using Student's t-test. If the fold change value (Fold change =2-ΔΔCt) is greater than one, it means that the gene expression level is increased, but if the fold change value is less than one, it indicates that the gene expression level is decreased. Fold regulation is the adaptation of fold change results to biological systems. If the fold change value (2-ΔΔCt) is greater than one, it is equal to the fold regulation value; however, if the fold change value (2-ΔΔCt) is less than one, the fold regulation value is the negative inverse of the fold change value. Because of the analysis of the data, the average Ct, fold change, and fold regulation values of each gene region are shown in Table 3.

Although there was a 7.60-fold increase in miRNA-30C-5p gene expression levels in the patient group compared with the healthy volunteer group, it was not found to be statistically significant (p=0.142). Considering the miRNA-574-5p gene expression levels, although there was a 2.96-fold increase in the patient group compared with the healthy volunteer group, no significant relationship was found (p=0.464) (Table 3, Figure 1).

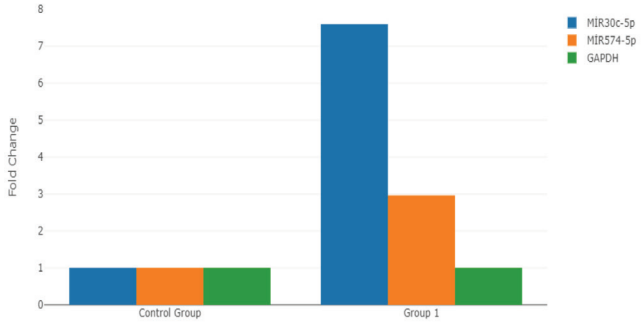

Figure 1. Comparison of expression levels of *miRNA-30C-5p* and *miRNA-574-5p* genes in patient and control groups

GAPDH: Glyceraldehyde 3-phosphate dehydrogenase

*Fold change = $2^{(-\Delta\Delta Ct)}$

**Fold regulation = -1/ΔΔCt

ΔCt tumor = Mean Ct target gene tumor - Mean Ct GAPDH tumor

ΔCt control = Mean Ct target gene control - Mean Ct GAPDH control

ΔΔCt = ΔCt (target gene tumor - GAPDH tumor) - ΔCt (target gene control - GAPDH control)

When the histopathological data of the patients were compared with the expression levels of *miRNA-30C-5p* and *miRNA-574-5p* genes, thyroid cancer patients with positive lymph node metastasis, lymphovascular invasion, blood vessel invasion, perineural invasion, tumor capsule invasion, surrounding soft tissue invasion, and thyroid parenchyma invasion were compared with the negative group. Although there were fold increases in miRNA-30C-5p and miRNA-574-5p expression levels in the positive group, these parameters were not statistically significant (Table 4).

"Smartphone usage", "Do you turn off the phone while sleeping?", "Is the phone with you while you sleep?", "Is there a Wi-Fi device in the bedroom?" and "Do you turn off the Wi-Fi device while sleeping?" questions were asked, and the answers given to these questions were evaluated in the patient group. In the patient group who answered yes to the questions, when evaluated in terms of miRNA-30C-5p and miRNA-574-5p expression levels, although there were fold increases, no statistically significant relationship was found. When evaluated in terms of miRNA-30C-5p and miRNA-574-5p expression levels in the control group with the same questions, although there were fold increases, no statistically significant relationship was found. When the answers given to the same questions were evaluated by considering the patient and control groups together, when evaluated in terms of miRNA-30C-5p and miRNA-574-5p expression levels, although there were fold increases, no statistically significant relationship was found (Table 5).

Table 3. CT, fold change, and fold regulation results of RT-PCR data from thyroid cancer and healthy volunteer groups

Genes	Group	Median CT	Standard deviation	Fold-change	p-value
miRNA-30C-5p	Patient Control	21.63 22.69	1.21 1.12	**7.60**	0.142
miRNA-574-5p	Patient Control	18.02 8.11	2.22 3.41	**2.96**	0.464
GAPDH	Patient Control	24.50 22.21	2.51 3.79	1.00	N/A

GAPDH: Glyceraldehyde 3-phosphate dehydrogenase, RT-PCR: Real time-polymerase chain reaction, CT: Cycle threshold

Discussion

miRNAs are a group of small, single-stranded, non-coding RNAs approximately 22 nucleotides long. According to various studies, irregularities in miRNAs have been implicated in various pathological processes, including tumorigenesis, making miRNAs a promising diagnostic and therapeutic target in the future (15). Changes in miRNAs cause genetic and epigenetic changes by activating proto-oncogenes or inactivating tumor suppressor genes. Thyroid cancers are the most common endocrine system malignancies, and the aim of this study was to evaluate the relationship between cell phone use and miRNA-574-5p and miRNA-30C-5p expression levels in patients diagnosed with differentiated thyroid cancer.

Human miR-574-5p is encoded by miR-574 (gene ID: 693159) on human chromosome 4p14 and is produced in a multi-step process (16). miR-574-5p is a candidate oncogenic target for different types of cancer (17,18). The first study investigating the relationship between this gene expression and thyroid cancer was conducted in 2013 by Fan et al. (19). According to this in vitro study, an inverse correlation was observed with miRNA-574-5p in thyroid cancer cells. Zhang et al. (13) found that abnormal upregulation of miR-574-5p had an oncogenic effect by regulating the Wnt/β-catenin pathway by targeting quaking proteins (QKI). According to the data of our study, miR-574-5p gene expression levels in the differentiated thyroid cancer patient group were found to be higher than those in healthy volunteers, although the difference was not statistically significant. When the patients were evaluated according to histopathological parameters, although there was an increase in miRNA-30C-5p and miRNA-574-5p expression levels in those with positive lymph node metastasis, lymphovascular invasion, blood vessel invasion, perineural invasion, tumor capsule invasion, peripheral soft tissue invasion, and thyroid parenchyma invasion, there was no statistically significant relationship (Table 4).

The miRNA-30 family is known as a tumor suppressor and plays an important role in the development of many cancer types (20). It has been reported that miRNA-30 is downregulated after EMR and activates autophagy (10). Braun et al. (21) reported that miRNA-30 can reduce the invasive potential of anaplastic thyroid carcinoma

Table 4. Comparison of the expression levels of *miRNA-30C-5p* and *miRNA-574-5p* genes in patients with histopathological parameters

	miRNA-30C-5p		miRNA-574-5p		GAPDH	
	Fold-change	p-value	Fold-change	p-value	Fold-change	p-value
Lymph node metastasis (+/-)	7.21	0.51	9.79	0.56	1.00	N/A
Lymphovascular invasion (+/-)	0.62	0.56	1.06	0.75	1.00	N/A
Blood vessel invasion (+/-)	0.45	0.50	2.10	0.50	1.00	N/A
Perineural invasion (+/-)	3.19	0.95	13.19	0.15	1.00	N/A
Tumor capsule invasion (+/-)	1.76	0.67	1.02	0.30	1.00	N/A
Thyroid capsule invasion (+/-)	2.20	0.98	1.31	0.48	1.00	N/A
Soft tissue invasion (+/-)	1.95	0.84	1.39	0.62	1.00	N/A
Thyroid parenchyma invasion (+/-)	0.82	0.88	0.58	0.54	1.00	N/A

GAPDH: Glyceraldehyde 3-phosphate dehydrogenase

Table 5. When the patients and healthy volunteers were evaluated together, the relationship between the expression levels of *miRNA-30C-5p* and *miRNA-574-5p* genes was determined according to their responses to smartphone and Wi-Fi usage

	miRNA-30C-5p		miRNA-574-5p		GAPDH	
	Fold-change	p-value	Fold-change	p-value	Fold-change	p-value
Smartphone usage (+/-)	**6.06**	0.45	**2.58**	0.50	1.00	N/A
Do you turn off the phone while sleeping?	**8.07**	0.31	**3.12**	0.75	1.00	N/A
Is the phone with you while you sleep? (+/-)	**7.70**	0.33	**2.82**	0.72	1.00	N/A
Is there a Wi-Fi device in the bedroom? (+/-)	**8.85**	0.46	0.99	0.40	1.00	N/A
Do you turn off the Wi-Fi device while sleeping?	**8.73**	0.33	**3.28**	0.71	1.00	N/A

GAPDH: Glyceraldehyde 3-phosphate dehydrogenase

cells. According to the data of our study, miRNA-30C-5p expression levels in patients with differentiated thyroid cancer were found to be higher than those in healthy volunteers, although the difference was not statistically significant.

Epidemiological studies have shown that the incidence of thyroid papillary carcinoma has been increasing since the 1980s. At the same time, a rapid increase is observed in the use of mobile phones (7). Because exposure to ionizing radiation has an important role in the development of cancer, many studies have been conducted and continue to be conducted on whether EMR exposure due to mobile phones will cause cancer. In a study conducted on rats, exposure of the whole body to 900 MHz pulse-modulated RF radiation similar to that emitted by the Global System for Mobile Communications (GSM) caused pathological changes in the thyroid gland (22). According to the results of the INTERPHONE study, no increase was found in the incidence of glioma, meningioma, and acoustic neuroma in long-term mobile phone users (4). According to the results of the prospective study by Benson et al. (23), no association was found between cell phone use and glioma, meningioma, or other cancers not originating from the central nervous system. Silva et al. (7) studied thyroid cells using radiofrequency energy and found that this type of radiation did not show a potential carcinogenic effect. Luo et al. (24) found no relationship between cell phone use and the development of thyroid cancer in their study, which included 462 patients and 498 control groups. However, there was an increased risk of microcarcinoma (tumor size ≤10 mm) in those with a higher frequency of mobile phone use. Wi-Fi is a technology that has an important place in human life. In our study, 85% of our patients were using mobile phones with internet access, whereas 98% of our healthy volunteers were using mobile phones ($p<0.05$). Contrary to our expectations, according to the questionnaire, the habit of keeping a mobile phone in the bedroom while sleeping was higher in healthy volunteers than in patients ($p<0.05$). On the other hand, while there was a Wi-Fi device in their bedrooms in 78.6% of the patients, this rate was much lower (21.4%) in healthy volunteers ($p<0.011$). No difference was detected by turning off the Wi-Fi device while sleeping.

Study Limitations

The biggest limitation of our study was the small number of patients. In addition, some responses to survey studies were not certain (for example, how many hours of phone usage per day? etc).

Conclusion

Although there was a 7.60-fold increase in miRNA-30C-5p gene expression levels in the patient group compared with the control group, it was not found to be statistically significant. When miRNA-574-5p gene expression levels were evaluated, although there was a 2.96-fold increase in the patient group compared with the control group, no significant relationship was detected. Differentiated thyroid cancer patients and their healthy volunteers were asked about "Do you have smart mobile phone use?", "Do you turn off the phone while sleeping?, "Do you have mobile phones near while sleeping?", "Is there Wi-Fi device in bedroom?", "Do you turn off Wi-Fi device while sleeping?" When the answers given to the questions miRNA-30C-5p and miRNA-574-5p expression levels were evaluated, although there were fold increases, no statistically significant relationship was detected. However, because of the limited number of patients, which is the biggest limitation of our study, we recommend that these studies be conducted with larger numbers of patients and healthy volunteers.

Although there was no significant difference between miRNA levels, we believe that the effects of EMR on the thyroid gland can be reduced by paying attention to this simple precaution, since there is a higher rate of Wi-Fi devices in the bedrooms than in healthy volunteers.

Ethics

Ethics Committee Approval: Ethics Committee approval was obtained from Cumhuriyet University Clinical Research Ethics Committee (decision no: 2020-05/02, date: 21.05.2020).

Informed Consent: Written informed consent forms were obtained from patients who agreed to participate in the study.

Authorship Contributions

Surgical and Medical Practices: Z.H., S.A.E., B.S., Ö.U.B., G.D., Concept: Z.H, A.T., S.A.E., B.S., Ö.U.B., Y.S., Design: Z.H., A.T., Ö.U.B., Y.S., Data Collection or Processing: Z.H., A.T., S.A.E., B.S., Ö.U.B., G.D., Y.S., Analysis or Interpretation: Z.H., A.T., Literature Search: Z.H., A.T., Writing: Z.H., A.T., S.A.E.

Conflict of Interest: No conflicts of interest were declared by the authors.

Financial Disclosure: This project was supported by grants from Sivas Cumhuriyet University Scientific Research Project Unit (T-897).

References

1. Vaccarella S, Franceschi S, Bray F, Wild CP, Plummer M, Dal Maso L. Worldwide Thyroid-cancer epidemic? The increasing impact of overdiagnosis. N Engl J Med 2016;375:614-617.
2. Kitahara CM, Schneider AB, Brenner AV. Thyroid cancer. Cancer epidemiology and prevention 2018;839-860.
3. Albi E, Cataldi S, Lazzarini A, Codini M, Beccari T, Ambesi-Impiombato FS, Curcio F. Radiation and thyroid cancer. Int J Mol Sci 2017;18:911.
4. INTERPHONE Study Group. Brain tumour risk in relation to mobile telephone use: results of the INTERPHONE international case-control study. Int J Epidemiol 2010;39:675-694.
5. Bergamaschi A, Magrini A, Ales G, Coppeta L, Somma G. Are thyroid dysfunctions related to stress or microwave exposure (900 MHz)? Int J Immunopathol Pharmacol 2004;17(2 Suppl):31-36.
6. Milham S, Morgan LL. A new electromagnetic exposure metric: high frequency voltage transients associated with increased cancer incidence in teachers in a California school. Am J Ind Med 2008;51:579-586.
7. Silva V, Hilly O, Strenov Y, Tzabari C, Hauptman Y, Feinmesser R. Effect of cell phone-like electromagnetic radiation on primary human thyroid cells. Int J Radiat Biol 2016;92:107-115.
8. Simonian M, Mosallayi M, Mirzaei H. Circulating miR-21 as novel biomarker in gastric cancer: diagnostic and prognostic biomarker. J Cancer Res Ther 2018;14:475.
9. Mirzaei H, Khataminfar S, Mohammadparast S, Sales SS, Maftouh M, Mohammadi M, Simonian M, Parizadeh SM, Hassanian SM, Avan A. Circulating microRNAs as potential diagnostic biomarkers and therapeutic targets in gastric cancer: current status and future perspectives. Curr Med Chem 2016;23:4135-4150.
10. Hao YH, Zhao L, Peng RY. Effects of electromagnetic radiation on autophagy and its regulation. Biomed Environ Sci 2018;31:57-65.
11. Zhang ZJ, Xiao Q, Li XY. MicroRNA-574-5p directly targets FOXN3 to mediate thyroid cancer progression via Wnt/β-catenin signaling pathway. Pathol Res Pract 2020;216:152939.
12. Wang X, Lu X, Geng Z, Yang G, Shi Y. LncRNA PTCSC3/miR-574-5p governs cell proliferation and migration of papillary thyroid carcinoma via Wnt/β-catenin signaling. J Cell Biochem 2017;118:4745-4752.
13. Zhang Z, Li X, Xiao Q, Wang Z. MiR-574-5p mediates the cell cycle and apoptosis in thyroid cancer cells via Wnt/β-catenin signaling by repressing the expression of Quaking proteins. Oncol Lett 2018;15:5841-5848.
14. Li XH, Ha CT, Xiao M. MicroRNA-30 inhibits antiapoptotic factor Mcl-1 in mouse and human hematopoietic cells after radiation exposure. Apoptosis 2016;21:708-720.
15. Esteller M. Non-coding RNAs in human disease. Nat Rev Genet 2011;12:861-874.
16. Huang W, Zhao Y, Xu Z, Wu X, Qiao M, Zhu Z, Zhao Z. The regulatory mechanism of miR-574-5p expression in cancer. Biomolecules 2022;13:40.
17. Lin Z, Chen M, Wan Y, Lei L, Ruan H. miR-574-5p targets FOXN3 to regulate the invasion of nasopharyngeal carcinoma cells via Wnt/β-catenin pathway. Technol Cancer Res Treat 2020;19:1533033820971659.
18. Tong R, Zhang J, Wang C, Li X, Yu T, Wang L. LncRNA PTCSC3 inhibits the proliferation, invasion and migration of cervical cancer cells via sponging miR-574-5p. Clin Exp Pharmacol Physiol 2020;47:439-448.
19. Fan M, Li X, Jiang W, Huang Y, Li J, Wang Z. A long non-coding RNA, PTCSC3, as a tumor suppressor and a target of miRNAs in thyroid cancer cells. Exp Ther Med 2013;5:1143-1146.
20. Braun J, Hoang-Vu C, Dralle H, Hüttelmaier S. Downregulation of microRNAs directs the EMT and invasive potential of anaplastic thyroid carcinomas. Oncogene 2010;29:4237-4244.
21. Braun J, Hoang-Vu C, Dralle H, Hüttelmaier S. Downregulation of microRNAs directs the EMT and invasive potential of anaplastic thyroid carcinomas. Oncogene 2010;29:4237-4244.
22. Eşmekaya MA, Seyhan N, Ömeroğlu S. Pulse modulated 900 MHz radiation induces hypothyroidism and apoptosis in thyroid cells: a light, electron microscopy and immunohistochemical study. Int J Radiat Biol 2010;86:1106-1116.
23. Benson VS, Pirie K, Schüz J, Reeves GK, Beral V, Green J; Million Women Study Collaborators. Mobile phone use and risk of brain neoplasms and other cancers: prospective study. Int J Epidemiol 2013;42:792-802.
24. Luo J, Deziel NC, Huang H, Chen Y, Ni X, Ma S, Udelsman R, Zhang Y. Cell phone use and risk of thyroid cancer: a population-based case-control study in Connecticut. Ann Epidemiol 2019;29:39-45.

Original Article
Mol Imaging Radionucl Ther 2024;33:28-37 DOI:10.4274/mirt.galenos.2023.82653

Care Pathway at a Cancer Center for the Administration of Radiometabolic Therapy with 177Lu-PSMA in Patients with Metastatic Castration-resistant Prostate Cancer

Metastatik Kastrasyona Dirençli Prostat Kanserli Hastalarda 177Lu-PSMA ile Radyometabolik Tedavinin Uygulanmasına Yönelik Kanser Merkezinde Bakım Yolu

Carlos Avila[1], *Tatiana Cadavid*[1], *Maria Cristina Martínez*[2], *Humberto Varela*[2], *Nathalie Hernández-Hidalgo*[2]

[1]*Fundación Universitaria Sanitas, Bogotá, Colombia*
[2]*Instituto Nacional de Cancerología, Department of Nuclear Medicine, Bogotá, Colombia*

Abstract

Objectives: To present a clinical care model for the administration of 177Lu-labeled prostate-specific membrane antigen (PSMA) in radiometabolic therapy for metastatic castration-resistant prostate cancer (mCRPC) at the National Cancer Institute (NCI) of Bogotá, Colombia.

Methods: A care model was designed for patients with mCRPC based on the VISION study, a prospective, phase III, multicenter, open-label, randomized study in patients with positive ^{68}Ga-PSMA positron emission tomography/computed tomography who had progressed to taxane and androgen therapy, to receive 177Lu-PSMA-617 combined with the best standard of care vs. the best standard of care alone. The care pathway provided to patients was developed by the Nuclear Medicine Group of the NCI and is the result of adjustments and improvements in the care process and the updating of the literature.

Results: A systematic and efficient care model was formalized and implemented for the administration of 177Lu-PSMA therapy in patients with mCRPC who had previously been treated with at least one androgen receptor pathway inhibitor and one or two taxane regimens, with evidence of disease progression.

Conclusion: An optimized process of care based on the determinants of clinical outcomes was developed for patients who received this type of radiometabolic therapy.

Keywords: Prostatic neoplasms, prostate-specific antigen, lutetium, nuclear medicine radiopharmaceutical delivery of health care, integrated

Address for Correspondence: Nathalie Hernández-Hidalgo MD, Instituto Nacional de Cancerología, Department of Nuclear Medicine, Bogotá, Colombia
Phone: +57 3508919905 **E-mail:** natha8830@gmail.com ORCID ID: orcid.org/0000-0002-7471-9566
Received: 01.07.2023 **Accepted:** 27.12.2023

Öz

Amaç: Bogotá, Kolombiya Ulusal Kanser Enstitüsü'nde (NCI) metastatik kastrasyona dirençli prostat kanserinin (mCRPC) radyometabolik tedavisinde 177Lu etiketli prostat spesifik membran antijeninin (PSMA) uygulanmasına yönelik bir klinik bakım modeli sunmaktır.

Yöntem: ^{68}Ga-PSMA pozitron emisyon tomografisi/bilgisayarlı tomografisi pozitif olan ve taksan ve androjen tedavisi almış hastalarda yapılan prospektif, faz III, çok merkezli, açık etiketli, randomize bir çalışma olan VISION çalışmasını temel alarak mCRPC'li hastalar için 177Lu-PSMA-617 ve en iyi bakım standardını tek başına en iyi bakım standardı ile karşılaştıracak bir bakım modeli tasarlandı. Hastalara sağlanan bakım yolu, bakım sürecindeki ayarlamalar ve iyileştirmeler ile literatürün güncellenmesinin sonucunda NCI'nın Nükleer Tıp Grubu tarafından geliştirilmiştir.

Bulgular: Daha önce en az bir androjen reseptör yolağı inhibitörü ve bir veya iki taksan rejimi ile tedavi edilmiş ve hastalık ilerlemesinin kanıtı bulunan mCRPC'li hastalarda 177Lu-PSMA tedavisinin uygulanması için sistematik ve etkili bir bakım modeli şekillendirildi ve uygulandı.

Sonuç: Bu tip radyometabolik tedavi alan hastalar için klinik sonuçların belirleyicilerine dayalı optimize edilmiş bir bakım süreci geliştirilmiştir.

Anahtar kelimeler: Prostat neoplazmaları, prostat spesifik antijen, lutesyum, nükleer tıp radyofarmasötik sağlık hizmeti sunumu, entegre

Introduction

The National Cancer Institute of the United States (NIH) defines prostate cancer as a neoplasm originating in prostate tissues and is the second most commonly diagnosed neoplasm in the male population worldwide (1).

The incidence of prostate cancer diagnosis varies widely between different geographic areas, being highest in Australia/New Zealand and North America, with age-standardized rates of 111.6 and 97.2 per 100,000 population, respectively (1). According to data reported by the NIH, the rate of new cases was 106.8 per 100,000 people in 2018, with an estimated new case rate of 248,530 (13.1%) for 2021 (2). Likewise, the World Health Organization records a worldwide incidence of 30.1 for the year 2020, estimating 1,628,781 new cases in Latin America and 49.8 in Colombia for the same year (3). Regarding the records of the National Cancer Institute (NCI) of Bogotá, patients with prostate cancer (n=5,430) were evaluated between 2017 and 2020, approximately 1,000 patients per year.

Metastatic castration-resistant prostate cancer (mCRPC) is established in patients with suppressed testosterone levels <50 ng/dL with at least one of the following criteria: biochemical progression understood as an increase in prostate-specific antigen (PSA) in studies spaced at least one week apart, with two increases of 50% over the nadir value and with PSA >2 ng/mL (4); or radiological progression with two or more new lesions on bone scan or soft tissue lesions.

Prostate-specific membrane antigen (PSMA) is a transmembrane protein mainly expressed in prostate cancer cells; its high expression is an independent biomarker of poor prognosis during the disease. Most patients with mCRPC have positive PSMA levels, and its high expression has been associated with reduced survival (5).

Radiolabeled PSMA is an effective tool for treating mCRPC. Its usefulness, safety, and low toxicity have been verified because it limits radiation to target organs and reduces the presentation of radiation-related symptoms during tumor cytorduction (5,6,7).

In particular, the use of PSMA radiolabeled with 177Lu has shown an improvement in the overall and progression-free survival of patients and in some cases in tumor regression, both in animal and human studies. Recently, in the VISION study-the only phase III randomized study-it was possible to show the efficacy of 177Lu-PSMA (5), which has led to its inclusion as a therapeutic option in mCRPC after progression despite one or two lines of taxanes according to international guidelines (4).

In the hospital radiopharmacy of NCI (Bogotá, Colombia), radiolabeled PSMA has been developed for the diagnosis and treatment of prostate cancer. In January 2020, 177Lu-PSMA was produced, at which time the first treatment was administered.

To date, 41 therapies have been administered to 19 patients, which has made it possible to adjust an orderly and optimized procedure for the administration of this radionuclide therapy. In Colombia, few institutions have the capacity to administer this type of therapy; thus, this work seeks to document the evolution of a model for the administration of 177Lu-PSMA therapy in patients diagnosed with mCRPC, with the aim that different cancer centers can use it as a guide for the care of this group of patients.

Materials and Methods

To establish a standardized institutional procedure for the administration of 177Lu-PSMA therapies, some key moments were defined (Figure 1).

We don't use statistical analysis in our article.

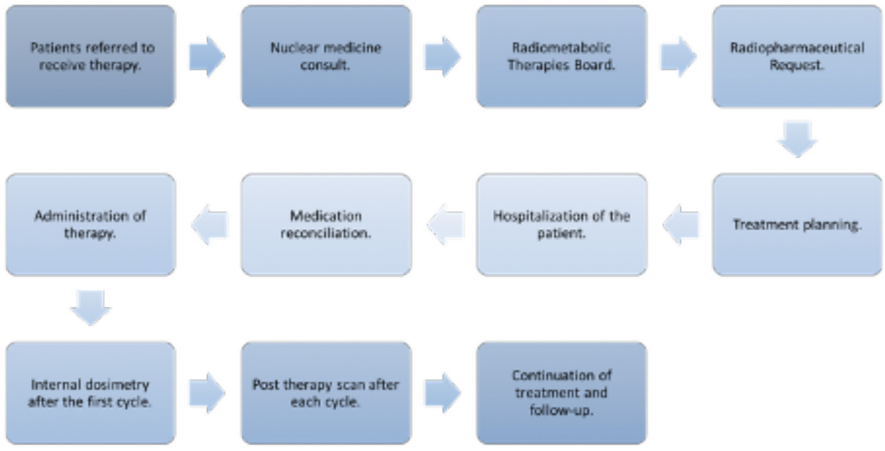

Figure 1. Flowchart 177Lu-PSMA therapy workflow at our institution
177Lu-PSMA: 177Lu-prostate-specific membrane antigen

Results

The Nuclear Medicine Group at NCI has managed to develop a systematic method for the administration of 177Lu-PSMA therapy to patients with mCRPC diagnosis. Figure 2 shows the key stages of the care process in force at the institution.

Patients Eligible for Therapy

Adult patients admitted with a diagnosis of mCRPC, who have been treated with one or two antiandrogens (abiraterone or enzalutamide) and one or two taxane regimens, present biochemical and imaging progression, with evidence of at least one metastatic lesion by computed tomography (CT) scan, magnetic resonance imaging (MRI), or bone scan; additionally, with PSMA-positive metastatic lesions confirmed by positron emission tomography/CT (PET/CT) with ^{68}Ga-PSMA-11 (5,7).

PET/CT with ^{68}Ga-PSMA-11 allows defining PSMA-positive and-negative lesions. A positive lesion presents a maximum standardized uptake value higher (1.5 times) than the mean

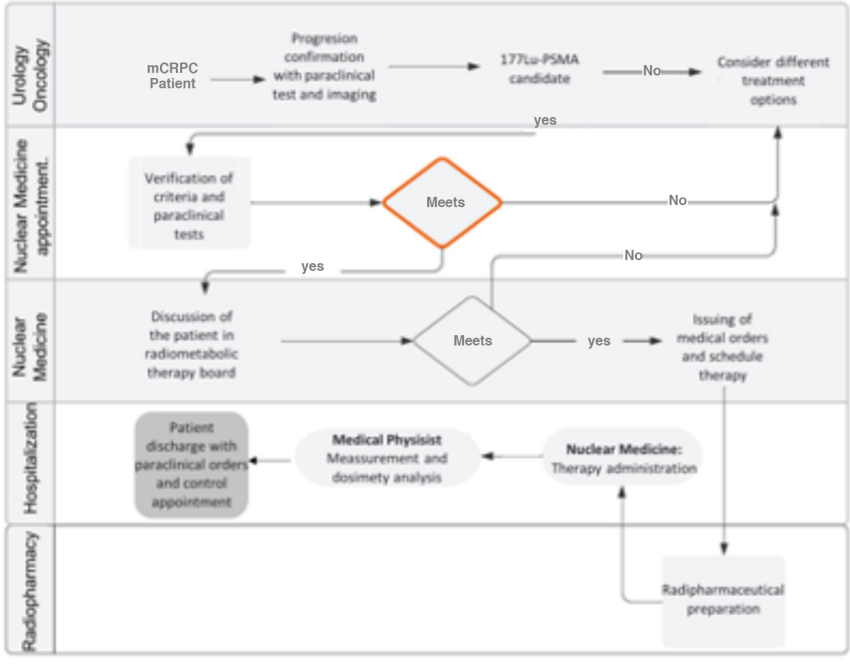

Figure 2. Systematic method for the administration of 177Lu-PSMA therapy
177Lu-PSMA: 177Lu-prostate-specific membrane antigen

standardized uptake value of the liver (7). On the other hand, a PSMA-negative lesion is defined as an uptake equal to or less than that of the liver parenchyma, in any lymph node with a short axis less than 2.5 cm, in any metastatic solid organ tumor with a short axis less than 1 cm, and in any bone lesion with a soft tissue component with a short axis less than 1 cm (Figures 3,4,5,6) (Table 1) (5).

Selection Criteria

Patients with mCRPC and evidence of progression must meet the following criteria to receive 177Lu-PSMA therapy (Tables 2,3).

Nuclear Medicine Consultation

Every patient referred by the oncology or the oncologic urology service undergoes a medical assessment by a

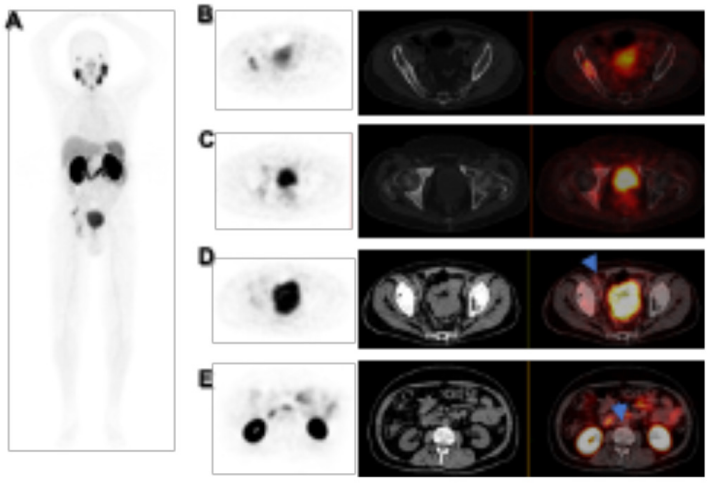

Figure 3. ^{68}Ga-PSMA PET/CT restaging in 70-years-old patient with biochemically recurrent prostate cancer and rising level of prostate-specific antigen: PET maximum intensity projection (A), axial PET/CT shows blast involvement in the right hemipelvis with foci showing moderate PSMA expression (SUV_{max}: 4.6, score 2) (By C), lymph nodes with partial calcification at the level of the aortic bifurcation and in the right external iliac region that do not present PSMA expression, probably post-treatment changes (D), lymph nodes in the inter-aortocaval region (up to 10 mm short diameter) and para-aortics without PSMA expression, score 0 (E)
^{68}Ga-PSMA: ^{68}Ga-prostate-specific membrane antigen, PET/CT: Positron emission tomography/computed tomography, SUV_{max}: Maximum standardized uptake value

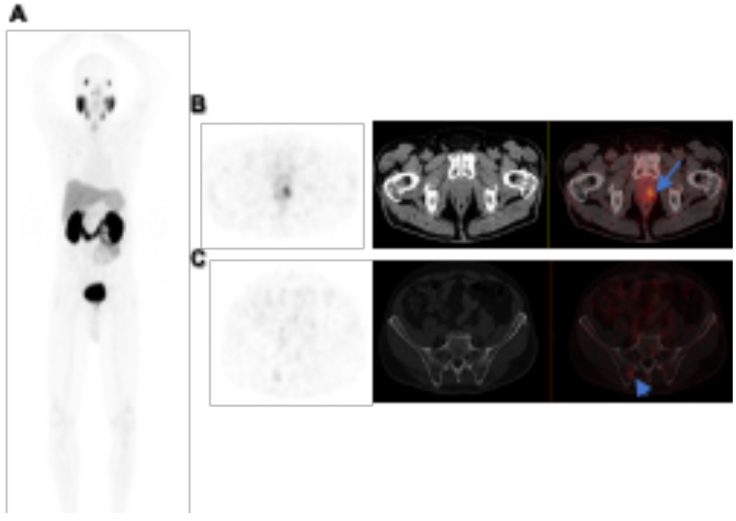

Figure 4. Primary staging using ^{68}Ga-PSMA11 PET/CT in 65-years-old patient with histopathologically proven prostate cancer T3bN0Mx, GG 4, iPSA 7.55 ng/mL: PET maximum intensity projection (A), axial PET/CT showing a focal area of greater intensity at the apex towards the left side with SUV_{max}: 6.4, score 2 (B), focal uptake with low expression of PSMA in the postero-superior region of the right iliac adjacent to the sacroiliac joint (SUV_{max}: 1.6), score 1 (C)
^{68}Ga-PSMA: ^{68}Ga-prostate-specific membrane antigen, PET/CT: Positron emission tomography/computed tomography, SUV_{max}: Maximum standardized uptake value

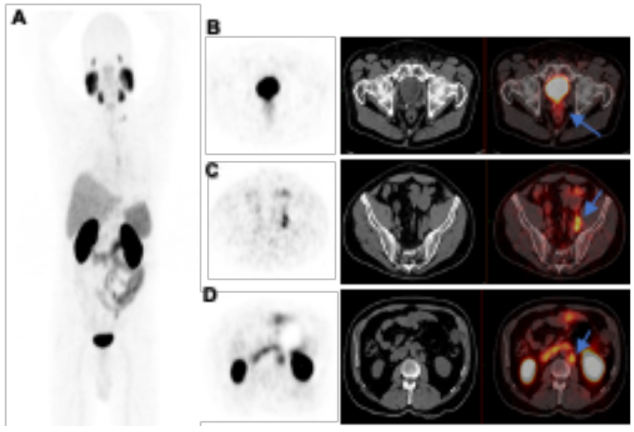

Figure 5. ^{68}Ga-PSMA 11 PET/CT restaging in 62-years-old patient with biochemically recurrent prostate cancer and rising level of prostate-specific antigen: PET maximum intensity projection (A), axial PET/CT post-radical prostatectomy state, low expression of PSMA in the rectovesical septum (SUV_{max}: 3.2, score 1) (B), lymph nodes with moderate expression of PSMA, score 2, in the left internal iliac chain (SUV_{max}: 6) and in the left interiliac region (SUV_{max}: 5.9, score 2) (C), in the left common iliac chain (SUV_{max}: 8.2), para-aortic up to approximately 20 mm in greatest diameter (SUV_{max}: 7.3), interaortocavus (SUV_{max}: 5.3) (D)
^{68}Ga-PSMA: ^{68}Ga-prostate-specific membrane antigen, PET/CT: Positron emission tomography/computed tomography, SUV_{max}: Maximum standardized uptake value

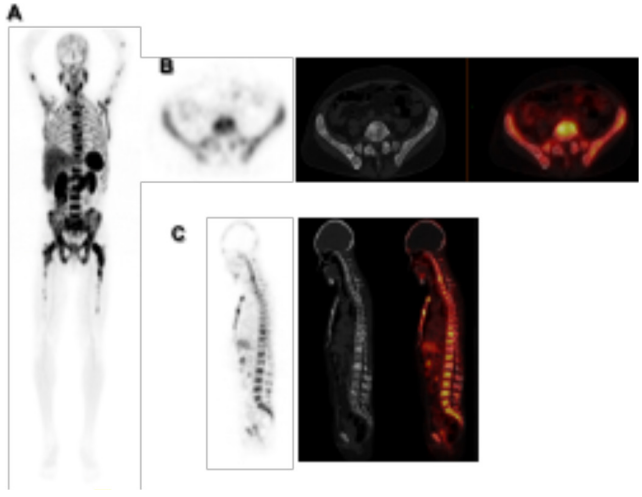

Figure 6. ^{68}Ga-PSMA 11 PET/CT in 73-years-old patient with prostate cancer presenting clinical, biochemical and imaging progression. PET maximum intensity projection (A) axial (B) and sagittal PET/CT (C) osteoblastic polyostotic metastatic compromise with abnormal increased uptake of the radiotracer and high expression of PSMA (score 3) involving the axial and appendicular skeleton, the most dominant located in the left humeral head (SUV_{max}: 6.3), sternal extremity of both clavicles (SUV_{max}: 6.5), manubrium sternal (SUV_{max}: 9.0), left femoral neck (SUV_{max}: 15.5), vertebral body of C6 (SUV_{max}: 9.3)
^{68}Ga-PSMA: ^{68}Ga-prostate-specific membrane antigen, PET/CT: Positron emission tomography/computed tomography, SUV_{max}: Maximum standardized uptake value

Table 1. miPSMA expression score. PSMA imaging can be quantified on the basis of the degree of radiotracer uptake. This is visually evaluated relative to uptake by the liver and parotid gland, which both physiologically take up PSMA expression

Score	Reported PSMA expression	Uptake
0	No	Below blood pool
1	Low	Equal to or above blood pool and lower than liver
2	Intermediate	Equal to or above liver and lower than parotid gland
3	High	Equal to or above parotid gland

PSMA: Prostate-specific membrane antigen

Table 2. These threshold criteria are used to evaluate patients before initiating and while monitoring 177Lu-PSMA. Patients with laboratory values outside the threshold values may be treated after discussion and shared
Selection criteria
Have a ^{68}Ga-PSMA 11 PET/CT with PSMA-positive lesions (SUV_{max} 1.5 times greater than the SUV_{mean} of the liver).
Tumor with histopathological confirmation by the pathology service.
Functional status: ECOG ≤2 and a life expectancy of more >6 months.
Safety criteria
Hemoglobin ≥9.0 g/dL.
Bone marrow reserve: leukocytes ≥2,500/µL ($2.5x10^3$/µL), neutrophils ≥1,500/µL platelets >$75x10^3$/µL.
Glomerular filtration > 30 mL/min, with a creatinine ≤1.5.
Total bilirubin ≤1.5x the upper limit of normal for the institution, in case of known Gilbert's syndrome ≤3x the upper limit of normal is allowed.
Alanine aminotransferase or aspartate aminotransferase ≤3.0 and ≤5.0x the upper limit of normal for the institution, in patients with known liver metastases.
Albumin >3.0 g/dL.
Have discontinued myelosuppression therapy at least 6 weeks before the start of lutetium and have recovered from all toxcities related to the previous therapy (equal to or less than grade 2).
177Lu-PSMA:177Lu-prostate-specific membrane antigen, PET/CT: Positron emission tomography/computed tomography, SUV_{max}: Maximum standardized uptake value, SUV_{mean}: Mean standardized uptake value, ECOG: Eastern Cooperative Oncology Group

Table 3. Contraindication for the administration of the therapy
Contraindications
Life expectancy less than 6 months.
Presence or high risk of urinary obstruction.
Progressive deterioration of renal function (GFR <30 mL/min or creatinine >2 times the ULN).
Liver enzymes >5 times the ULN.
Myelosuppression (leukocytes 2,500 mL or platelets <75,000 mL).
Medical condition requiring urgent intervention.
GFR: Glomerular filtration rate, ULN: Upper limit of normal

nuclear medicine professional, who evaluates the patient's general condition and comorbidities, verifies eligibility criteria, and monitors paraclinical findings. The adverse events, benefits, radioprotection measures, and treatment risks are clearly explained to the patient so that they can accept or reject the therapy.

Regarding paraclinical tests, the maximum validity time for them is the following: ≤4 weeks for blood count; <1 week for renal function tests; ≤3 months (preferably 1 month) for CT or MRI of the study area; and ≤3 months for ^{68}Ga-PSMA-11 PET/CT (8).

After this, the informed consent form is filled out and signed by the patient, who is given this document with the recommendations and information necessary for their treatment. The contact information of the patient and one family member is recorded; medical orders are provided to perform the administrative and authorization procedures for subsequent presentation at the Radiometabolic Therapy Board. If the patient is ineligible or does not accept receiving 177Lu-PSMA therapy, their management must be continued by the treating service.

Radiometabolic Therapies Board

Once the patient is evaluated by the nuclear medicine service in the medical consultation, the case is presented to the Radiometabolic Therapies Board in which at least four nuclear physicians participate, who verify the appropriateness of the treatment, the dose to be administered, and discuss possible complications that the patient may present during therapy. After these aspects have been discussed and analyzed, the administration of the treatment is scheduled.

Radiopharmaceutical

For each cycle of therapy, a dose of 200 mCi of 177Lu-PSMA is administered, which can be modified according to medical criteria considering the specific clinical conditions

of each patient. These doses must be administered at intervals of 6-8 weeks until completion of 4-6 doses.

Scheduling

In Colombia, according to current regulations, preparations must be performed in a high-complexity radiopharmacy, which must have an operating license from the Colombian Geological Service and certification of compliance with Resolution 4245 of 2015 on good practices of radiopharmaceutical manufacturing granted by the National Institute for Drug and Food Surveillance (INVIMA) (9). These master preparations must be prepared by pharmaceutical chemists after receiving the medical prescription given by the nuclear physician. Once the application date is assigned, the preparation of the radiopharmaceutical 177Lu-PSMA-I&T is scheduled at least 15 days in advance.

The radionuclide 177Lu does not have any therapeutic or diagnostic purpose on its own. Therefore, it is not considered a pharmaceutical product, nor is it suitable for use in humans until it is transformed into a radiopharmaceutical. Therefore, it is necessary to perform biomolecular labeling and finally, transform it into an injectable form called a master formula.

For this master preparation, raw materials and excipients are needed in addition to the radioactive radioisotope; in this case, 2.5-dihydroxybenzoic acid, PSMA I&T peptide, acetate, and acetate buffer, among others, which fulfill different functions such as stabilizing and guaranteeing an adequate pH for the desired chemical reaction and thus obtaining a quality radiopharmaceutical for the patient.

Evaluation of Patient Medications

It is not necessary to discontinue medications before 177Lu-PSMA therapy. In the case of receiving medications to control other pathologies, they must be continued during therapy (7).

Therapy Administration

The 177Lu-PSMA radiopharmaceutical is prepared in the radiopharmacy according to institutional protocol on the same day that it has been scheduled for the administration of the therapy.

The patient should be hospitalized in a single room designed to ensure radiation protection for caregivers, other patients, and the environment. After admission, the nurse records the patient's vital signs and canalizes two veins, one in each arm. The patient is hydrated according to individual conditions; if there is no cardiovascular risk, 1-2 L of normal saline solution is administered at 20 cc/min (7).

To reduce 177Lu-PSMA uptake by the salivary glands, cold packs covered with a dry towel are placed for at least 1 h before and up to 4 h after the end of treatment, replacing them every 30 min. This prevents alterations in the salivary glands, although there is no clear evidence of its usefulness (9).

In patients with brain or spinal cord metastases or at risk of edema and mechanical obstruction, the administration of prophylactic corticosteroids may be considered. Similarly, if the patient presents with alterations in elimination, slow urinary flow, or constipation, diuretics and laxatives can be used after therapy administration, allowing for rapid elimination (7).

After all mentioned above, the radiopharmaceutical is administered by the nuclear physician and the therapy technologist, with support from the nursing staff. A shielded infusion pump is used to administer 177Lu-PSMA intravenously over 1 h.

The nuclear medicine professional should evaluate the patient's condition during the administration of therapy. Once it is completed, the nurse should monitor the patient's vital signs. Subsequently, the physicist in charge of radiological protection must take the necessary measures to guarantee the patient's discharge, with a dose rate <25 μSv/h at a 1-meter distance (Figure 7) (10).

Post-therapy Screening

After the therapy, 120-144 h post-injection, whole-body images should be acquired to evaluate the distribution of the radiopharmaceutical with medium-energy collimators, energy window centered at 208 keV ±10%, velocity 16 cm/min, matrix size 256x1024, and zoom 1.0. This screening should be performed after each dose cycle administered to the patient (Figure 8).

Internal Dosimetry

Whole-body planar imaging, abdominal single photon emission computed tomography (SPECT)/CT, and blood samples were taken 24, 48, and 72-166 h after the application of the first therapy to calculate the doses absorbed in the bone marrow, kidneys, parotids, and other organs of interest. Likewise, the dose absorbed by the highest and most avid tumor lesions was calculated. If dosimetry analyses suggest absorbed doses higher than 27 Gy in the kidneys and 2 Gy in the red bone marrow, a correlation should be made with respective functional tests, and it is analyzed whether to suspend therapy or adjust the interval and activity to be administered. In case of retained whole-body activity at 48 h greater than 120 mCi, the nuclear physician should adjust the dose of 177Lu-PSMA for the remaining cycles.

Figure 7. Timeline of the therapy administration

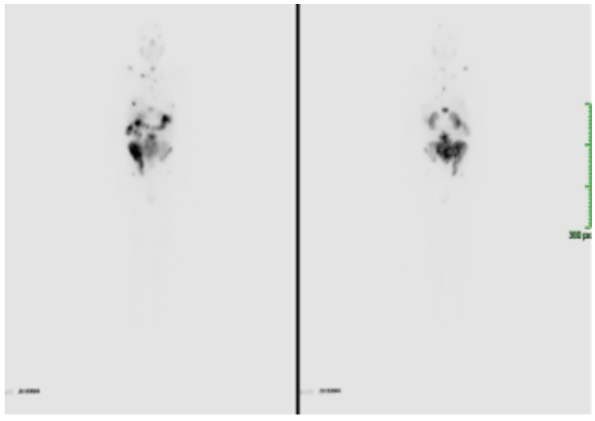

Figure 8. Patient with a history of pT3bN0M1b castration-resistant prostate cancer, with polyostotic bone metastatic involvement and disease in the prostate bed. Two days after administration of 200 mCi of 177Lu-PSMA, a whole body scan was performed in anterior and posterior projections. Physiological distribution of lutetium in liver, spleen and kidneys is observed. In the total body scan, retention of the radiopharmaceutical was observed in multiple bone lesions: right clavicle, thoracic and lumbar vertebral bodies, sacral region, right and left iliac wing, right acetabulum. All the findings show expression of PSMA receptors in the PET/CT ^{68}Ga-PSMA 11
177Lu-PSMA: 177Lu-prostate-specific membrane antigen, PET/CT: Positron emission tomography/computed tomographyc

Once each therapy is finished, a nuclear medicine consultation should be scheduled after 4 to 5 weeks to monitor paraclinical findings (blood count, PSA, alkaline phosphatase, lactate dehydrogenase, albumin, and renal and hepatic function tests) to evaluate possible hematotoxicity generated in the patient and, depending on the results, to reschedule the date of the next therapy (Figure 9) (11).

Continuation of Treatment and Follow-up

The duration of therapy depends on each patient's individual clinical condition, which requires careful evaluation of the absorbed doses accumulated by both the salivary glands and kidneys. The patient's clinical condition, paraclinical findings, and inclusion and exclusion criteria for therapy should be reevaluated before proceeding with the next cycle (7).

In recent observational studies, an average of 7 cycles of 177Lu-PSMA therapy have been performed without exceeding toxicity because repeating therapy every 6 to 8 weeks allows hematologic recovery in most cases (7). For this reason, once consultation has been made after administering the first dose, the dates of the following therapies should be scheduled with intervals of 6 to 8 weeks, completing approximately 6 cycles. Likewise, the patient must continue to be monitored by the oncologic urology service during treatment and after its completion, and in 6-monthly controls by the Nuclear Medicine Group, with laboratory tests (to evaluate late toxicity), imaging studies (RECIST), and tumor biomarkers (PSA), to evaluate response to treatment (7).

Complementary imaging with ^{68}Ga-PSMA-11 is performed at the beginning of treatment and 3 months after completion.

The oncologic urology service will evaluate the patient every 3 months from the beginning of therapy, assess the Eastern Cooperative Oncology score and pain scale, resolve symptoms of urinary obstruction, and request complementary images in case of suspected disease progression or complications secondary to metastatic disease.

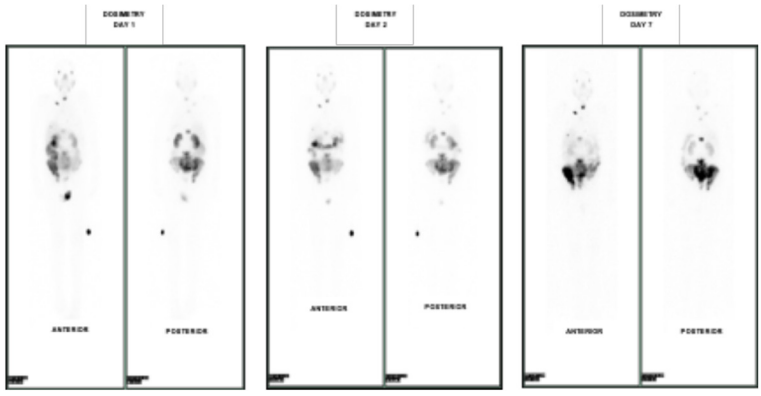

Figure 9. After the administration of 200 mCi of 177Lu-prostate-specific membrane antigen (177Lu-PSMA) I&T therapy, planar images, single photon emission computed tomography (SPECT), and blood samples were acquired at 24, 48, and 170 hours after the administration of the radiopharmaceutical.
• Uptake in the whole body, remnant of the body and parotids, is estimated through planar images following the MIRD 16 methodology.
• The estimation of doses to organs and lesions is estimated with SPECT/computed tomography (CT) and following the MIRD 23 methodology. Regions of interest delimited in CT: liver, kidneys, lumbar and right iliac lesion.
• The estimation of dose to bone marrow follows the methodology described in the European Association of Nuclear Medicine protocol, where the auto-dose in bone marrow is estimated through the dose in blood plasma, and the dose by organs with SPECT/CT and the contribution of the rest of the body with whole body scans.
• S-values are taken from public tabulations of Monte Carlo simulation results for the standardized male (177Lu-PSMA-617 and 177Lu-Octreotate) or female (177Lu-Octreotate) anthropomorphic phantom such as provided, among other dummies, by RADAR and IDAC2.1.
Result:
* Half-life times (bi-exponential fit): Short effective half-life: 0.62 hours. Long effective half-life: 5.27 hours. Whole body retained activity at 48 hours: 30%=59 mCi.
* The doses in Gy, for the organs of main interest due to the therapy with 200 mCi of 177Lu-PSMA, are kidneys: 4.34 Gy, liver: 0.47 Gy, parotids: 1.28 Gy, bone marrow: 1.32 Gy, whole body: 585 mSv.
* Lesion doses, using the sphere method: Right Iliaca (volume =42 cc, density =1.92 g/cm^3): 5.83 Gy, L5 (volume =19 cc, density =1.92 g/cm^3): 5.75 Gy.
Comments:
A high retention of 30% is found at 48 hours, a red bone marrow exposure of 1.32 Gy, generalized bone uptake makes it difficult to estimate the dose to the bone marrow.
The estimated renal dose is 4.34 Gy and 17.4 Gy at the end of treatment, lower than the renal absorbed dose restriction of 23 Gy.
The estimated parotid dose was 1.28 Gy, lower than the dose restriction of 35 Gy.
Dose estimation in SPECT/CT through the sphere method, yields an average dose in bone lesions of 5.78 Gy for the first cycle

Discussion

The most relevant experience worldwide in the administration of 177Lu-PSMA therapy in patients diagnosed with mCRPC has been developed in Europe; it requires a multidisciplinary team, adequate logistics, and appropriate infrastructure. In Latin America, this therapeutic option is offered in countries such as Mexico, Argentina, Chile, Brazil, and Uruguay; however, no literature has shown standardization in the administration of this therapy. The procedure described above results from several years of work at NCI, which conforms to European standards and seeks excellence in the care of this type of pathology.

Since 2009, the NCI has administered therapies with 177Lu-labeled peptides for the treatment of neuroendocrine neoplasms, such as 177Lu-DOTATATE/DOTATOC, which has made it possible to have adequate rooms for therapy, qualified personnel, and experience necessary for the administration of these radiopharmaceuticals, thus facilitating the incorporation of 177Lu-PSMA therapies for treating patients with mCRPC.

In Colombia, the first 177Lu-PSMA therapy was administered at the NCI, in Bogotá, on January 28, 2020. Since then, different training sessions have been conducted to perfect the administration technique, taking as a reference the more extended experience available worldwide, especially in Europe and Australia, using the therapy and the VISION study. Likewise, during this time, the production and quality control processes have been optimized through continuous improvement, and are now in compliance with Resolution 4245 of 2015.

In Colombia, the regulations for the administration of these therapies and the management of radioactive waste are different from those in other countries, whose health systems, in many cases, have different norms, making it easier to administer this therapy.

Although salivary gland protection is a process that is still under study worldwide, we have not had patients with xerostomia so far with the unproven method of cold gel packs (7,8); thus, we continue to apply this technique.

Uptake in the whole body and parotids is estimated through planar imaging following the MIRD 16 methodology. Estimation of doses to organs and lesions are calculated using SPECT/CT and according to MIRD 23 methodology. Regions of interest delimited by CT are liver, kidneys, sternal and femur injury, and visceral soft tissue injury. Bone marrow dose estimation follows the methodology described in the European Association of Nuclear Medicine protocol, where bone marrow self-dose is estimated through blood plasma dose, organ dose with SPECT/CT, and rest-of-body contribution with whole-body scans. S-values are taken from the public tabulations of the Monte Carlo simulation results for the standardized male (177Lu-PSMA-617 and 177Lu-octreotate) or female (177Lu-octreotate) anthropomorphic phantom as provided, among other phantoms, by RADAR and IDAC2.1.

The standardization of image acquisition techniques for dosimetry and the implementation of tomography-based image quantification techniques have made it possible to quantify volumes of interest in a more precise and reproducible way and provide dosimetric information on exposure to bone marrow, kidneys, salivary glands, and lesions, among other organs of interest.

The goal is to consolidate a multidisciplinary team that participates in the Radiometabolic Therapies Board, including an oncologist, urologist, clinical oncologist, radiologist, and nuclear physician, to complement the selection of the best candidate for the administration of the therapy and continue to build knowledge about the best technique for the management and follow-up of patients, seeking to become a center of excellence in radiometabolic therapies. In addition to the above, it is expected that in the coming years, based on the experience at the NCI, more institutions and therefore more patients may benefit from treatment with 177Lu-PSMA therapy.

Conclusion

The Nuclear Medicine Group of NCI has developed an optimized care process for patients receiving this type of radiometabolic therapy for continuous improvement based on the increasing experience in the multidisciplinary management of these patients. Thus, the learning curve achieved by administering these radiopharmaceutical treatments allows us to share this model so that it can be adjusted to the needs and particularities of each institution that requires administering therapies with 177Lu-PSMA.

Ethics

Ethics Committee Approval: As this is an experience as a Nuclear Medicine Group of the National Cancer Institute of Bogota, Colombia, we do not need approval from the ethics committee.

Informed Consent: Informed consent form is filled out and signed by the patient, who is given this document with the recommendations and information necessary for their treatment.

Authorship Contributions

Surgical and Medical Practices: C.A., T.C., M.C.M., H.V., N.H.-H., Concept: C.A., T.C., M.C.M., N.H.-H., Design: C.A., T.C., N.H.-H., Data Collection or Processing: C.A., T.C., Analysis or Interpretation: C.A., T.C., M.C.M., H.V., N.H.-H., Literature Search: C.A., T.C., Writing: C.A., T.C., H.V., N.H.-H.

Conflict of Interest: No conflicts of interest were declared by the authors.

Financial Disclosure: The authors declared that this study has received no financial support.

References

1. Virgolini I, Decristoforo C, Haug A, Fanti S, Uprimny C. Current status of theranostics in prostate cancer. Eur J Nucl Med Mol Imaging 2018;45:471-495.
2. Surveillance, Epidemiology, and End Results Program. Available from: https://seer.cancer.gov/ (accessed 2022 Mar 11).
3. Cancer Today. Available from: https://gco.iarc.fr/today/home (accessed 2022 Mar 11).
4. EAU-EANM-ESTRO-ESUR-ISUP-SIOG guidelines on prostate cancer. Available from: https://d56bochluxqnz.cloudfront.net/documents/pocket-guidelines/EAU-EANM-ESTRO-ESUR-ISUP-SIOG-Pocket-on-Prostate-Cancer-2022.pdf (accessed 2022 Mar).
5. Sartor O, de Bono J, Chi KN, Fizazi K, Herrmann K, Rahbar K, Tagawa ST, Nordquist LT, Vaishampayan N, El-Haddad G, Park CH, Beer TM, Armour A, Pérez-Contreras WJ, DeSilvio M, Kpamegan E, Gericke G, Messmann RA, Morris MJ, Krause BJ; VISION Investigators. Lutetium-177-PSMA-617 for metastatic castration-resistant prostate cancer. N Engl J Med 2021;385:1091-1103.
6. Hofman MS, Emmett L, Violet J, Y Zhang A, Lawrence NJ, Stockler M, Francis RJ, Iravani A, Williams S, Azad A, Martin A, McJannett M; ANZUP TheraP team; Davis ID. TheraP: a randomized phase 2 trial of ^{177} Lu-PSMA-617 theranostic treatment vs cabazitaxel in progressive metastatic castration-resistant prostate cancer (Clinical Trial Protocol ANZUP 1603). BJU Int 2019;124(Suppl 1):5-13.
7. Kratochwil C, Fendler WP, Eiber M, Baum R, Bozkurt MF, Czernin J, Delgado Bolton RC, Ezziddin S, Forrer F, Hicks RJ, Hope TA, Kabasakal L, Konijnenberg M, Kopka K, Lassmann M, Mottaghy FM, Oyen W, Rahbar K, Schöder H, Virgolini I, Wester HJ, Bodei L, Fanti S, Haberkorn U, Herrmann K. EANM procedure guidelines for radionuclide therapy with ^{177}Lu-labelled PSMA-ligands (^{177}Lu-PSMA-RLT). Eur J Nucl Med Mol Imaging 2019;46:2536-2544.
8. Yilmaz B, Nisli S, Ergul N, Gursu RU, Acikgoz O, Çermik TF. Effect of external cooling on ^{177}Lu-PSMA uptake by the parotid glands. J Nucl Med 2019;60:1388-1393.
9. Resolución 4245 de 2015 Ministerio de salud y protección social, República de Colombia. Available from: https://www.minsalud.gov.co/Normatividad_Nuevo/Resoluci%C3%B3n%204245%20de%202015.pdf (accessed 2015 Oct 10).
10. von Eyben FE, Kiljunen T, Joensuu T, Kairemo K, Uprimny C, Virgolini I. ^{177}Lu-PSMA-617 radioligand therapy for a patient with lymph node metastatic prostate cancer. Oncotarget 2017;8:66112-66116.
11. Calais PJ, Turner JH. Radiation safety of outpatient 177Lu-octreotate radiopeptide therapy of neuroendocrine tumors. Ann Nucl Med 2014;28:531-539.

Interesting Image
Mol Imaging Radionucl Ther 2024;33:38-39 DOI:10.4274/mirt.galenos.2023.68815

Metastatic Superscan in ^{18}F PSMA PET/CT of a Patient with Prostate Carcinoma

Prostat Karsinomu Olan Bir Hastanın ^{18}F PSMA PET/BT'sinde Metastatik Superscan

Man Mohan Singh, Shashwat Verma, Lavish Kakkar, Satyawati Deswal, Priyamedha Bose Thakur

Dr. Ram Manohar Lohia Institute of Medical Sciences, Department of Nuclear Medicine, Lucknow, India

Abstract

A biopsy-proven patient with prostate carcinoma aged 70 years was referred to the department of nuclear medicine for radionuclide-based therapy. His prostate-specific antigen levels were >1000 ng/mL, and prostatic magnetic resonance imaging showed an enlarged prostate with a heterogeneous signal and size 3.8x3.7x3.5 cm with few small heterogeneous nodular signals in the transition zone. He was scheduled for ^{18}F prostate-specific membrane antigen (PSMA) positron emission tomography/computed tomography (PET/CT) scan before therapy. ^{18}F PSMA PET/CT revealed PSMA-expressing prostate lesions (maximum standardized uptake value ~10.2) with extension into the urinary bladder along with bilateral supraclavicular, mediastinal, retrocrural, retroperitoneal, and pelvic lymph nodes and sclerotic lesions in the entire axial and appendicular skeleton.

Keywords: Superscan, prostate carcinoma, ^{18}F PSMA PET/CT, ^{18}F prostate-specific membrane antigen

Öz

Biyopsi ile kanıtlanmış 70 yaşındaki prostat karsinomu olan hasta, radyonüklid bazlı tedavi için nükleer tıp bölümüne yönlendirildi. Prostat spesifik antijen düzeyi >1000 ng/mL idi ve prostat manyetik rezonans görüntülemede heterojen sinyalli, 3,8x3,7x3,5 cm boyutunda, geçiş bölgesinde az sayıda küçük heterojen nodüler sinyal içeren büyümüş prostat görüldü. Tedavi öncesinde kendisine ^{18}F prostat spesifik membran antijen (PSMA) pozitron emisyon tomografisi/bilgisayarlı tomografi (PET/BT) taraması yapılması planlandı. ^{18}F PSMA PET/BT'de mesaneye uzanan PSMA eksprese eden prostat lezyonu (maksimum standartlaştırılmış tutulum değeri ~10,2) ile birlikte iki taraflı supraklaviküler, mediastinal, retrokrural, retroperitoneal ve pelvik lenf nodları ve tüm aksiyal ve apendiküler iskelette sklerotik lezyonlar ortaya çıktı.

Anahtar kelimeler: Superscan, prostat karsinomu, ^{18}F PSMA PET/BT, ^{18}F prostat-spesifik membran antijeni

Address for Correspondence: Man Mohan Singh MD, Dr. Ram Manohar Lohia Institute of Medical Sciences, Department of Nuclear Medicine, Lucknow, India
Phone: +918447188205 **E-mail:** drmmsingh007@gmail.com ORCID ID: orcid.org/0000-0001-9153-4697
Received: 03.12.2022 **Accepted:** 02.04.2023

Figure 1. ^{18}F prostate-specific membrane antigen (PSMA) positron emission tomography/computed tomography (PET/CT) scan maximum intensity projection image (A) showing generalized increased patchy tracer uptake throughout the skeleton and reduced tracer uptake in salivary and lacrimal glands, spleen, proximal small gut, and kidneys mimicking a metastatic superscan. The corresponding CT scan showed the sclerotic lesion in the visualized axial and appendicular skeleton with increased radiotracer on PET/CT in sagittal (B) and transaxial sections at the level of the thorax and pelvic regions (C), respectively. Superscan of malignancy is a well-known phenomenon on Tc-99m methylene diphosphonate bone scintigraphy. There is increased patchy/diffuse uptake of radiotracer throughout the skeleton with faint/non-visualization of the kidneys (1). Superscans are often seen in benign conditions (including hyperparathyroidism, renal osteodystrophy and Paget's disease), myeloproliferative disorders (including leukemia lymphoma and Waldenstrom's disease), and malignancies (like prostate, breast and lung) (2,3). Superscans indicate advanced stages of disease and have poor prognoses (4,5). ^{18}F PSMA PET/CT has significant value in staging (6), detection of biochemically recurrent prostate cancer (7), risk stratification, and evaluation of distant metastases in prostate carcinoma (8).

Ethics

Informed Consent: The authors certify that they have obtained all appropriate patient consent forms.

Authorship Contributions

Surgical and Medical Practices: M.M.S., Concept: M.M.S., Design: S.D., Data Collection or Processing: L.K., P.B.T., Analysis or Interpretation: S.V., Literature Search: S.V., Writing: M.M.S.

Conflict of Interest: No conflicts of interest were declared by the authors.

Financial Disclosure: The authors declare that this study has received no financial support.

References

1. Liu Y. Super-superscan on a bone scintigraphy. Clin Nucl Med 2011;36:227-228.
2. Buckley O, O'Keeffe S, Geoghegan T, Lyburn ID, Munk PL, Worsley D, Torreggiani WC. 99mTc bone scintigraphy superscans: a review. Nucl Med Commun 2007;28:521-527.
3. Chan M, Schembri GP. Combined 18F-FDG PET/CT and 68Ga DOTATATE PET/CT "superscan" in metastatic pancreatic neuroendocrine tumor. Clin Nucl Med 2017;42:108-109.
4. Chakraborty PS, Sharma P, Karunanithi S, Bal C, Kumar R. Metastatic superscan on (99m)Tc-MDP bone scintigraphy in a case of carcinoma colon: Common finding but rare etiology. Indian J Nucl Med 2014;29:158-159.
5. Agarwal KK, Tripathi M, Kumar R, Bal C. Metastatic superscan in prostate carcinoma on gallium-68-prostate-specific membrane antigen positron emission tomography/computed tomography scan. Indian J Nucl Med 2016;31:150-151.
6. Awenat S, Piccardo A, Carvoeiras P, Signore G, Giovanella L, Prior JO, Treglia G. Diagnostic role of ^{18}F-PSMA-1007 PET/CT in prostate cancer staging: a systematic review. Diagnostics (Basel) 2021;11:552.
7. Ferrari M, Treglia G. ^{18}F-PSMA-1007 pET in biochemical recurrent prostate cancer: an updated meta-analysis. Contrast Media Mol Imaging 2021;2021:3502389.
8. Wang Z, Zheng A, Li Y, Dong W, Liu X, Yuan W, Gao F, Duan X. ^{18}F-PSMA-1007 PET/CT performance on risk stratification discrimination and distant metastases prediction in newly diagnosed prostate cancer. Front Oncol 2021;11:759053.

Interesting Image
Mol Imaging Radionucl Ther 2024;33:40-42 DOI:10.4274/mirt.galenos.2023.24382

Bone and Parathyroid Scintigraphy Findings in Sagliker Syndrome

Sağlıker Sendromunda Kemik ve Paratiroid Sintigrafisi Bulguları

Çağlagül Erol[1], Özlem Şahin[1], Ahmet Eren Şen[2], Zeynep Aydın[3]

[1]*Necmettin Erbakan University Meram Faculty of Medicine, Department of Nuclear Medicine, Konya, Türkiye*
[2]*Kastamonu Training and Research Hospital, Clinic of Nuclear Medicine, Kastamonu, Türkiye*
[3]*Konya City Hospital, Clinic of Nuclear Medicine, Konya, Türkiye*

Abstract

Sagliker syndrome (SS) is a rare, exaggerated form of chronic kidney disease (CKD)-mineral and bone disorder resulting from untreated secondary hyperparathyroidism due to CKD. Herein, we describe a 34-year-old male patient whose Tc-99m-methylene diphosphonate bone scintigraphy and Tc-99m-sestamibi parathyroid scintigraphy revealed hints of SS and exhibited its defining characteristics.

Keywords: Sagliker syndrome, renal osteodistrophy, secondary hyperparathyroidism

Öz

Sağlıker sendromu (SS), kronik böbrek hastalığına (KBH) bağlı tedavi edilmemiş sekonder hiperparatiroidizm sonucu ortaya çıkan, KBH-mineral ve kemik bozukluğunun nadir görülen, abartılı bir şeklidir. Burada Tc-99m-metilen difosfonat kemik sintigrafisi ve Tc-99m-sestamibi paratiroid sintigrafisinde SS belirtileri gösteren ve SS'yi tanımlayıcı özellikler sergileyen 34 yaşında bir erkek hastayı sunuyoruz.

Anahtar kelimeler: Sağlıker sendromu, renal osteodistrofi, sekonder hiperparatiroidizm

Address for Correspondence: Çağlagül Erol MD, Necmettin Erbakan University Meram Faculty of Medicine, Department of Nuclear Medicine, Konya, Türkiye
Phone: +90 332 223 60 00 **E-mail:** drcaglagulerol@gmail.com ORCID ID: orcid.org/0000-0001-6857-5212
Received: 31.01.2023 **Accepted:** 02.04.2023

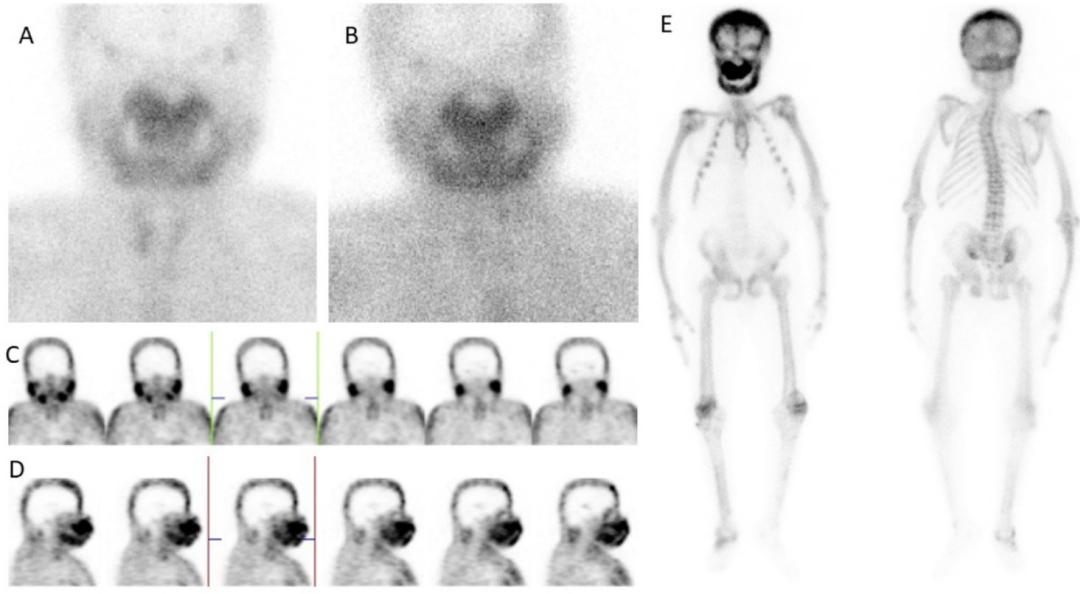

Figure 1. A 34-year-old male patient with secondary hyperparathyroidism was admitted to our department for parathyroid scintigraphy. The patient was in the hemodialysis program for 10 years because of chronic renal failure of unknown cause. Serum intact parathyroid hormone level was 3,521 pg/mL, total calcium level was 9.23 mg/dL, phosphate level was 5.4 mg/dL, 25-OH vitamin D3 level was 15.63 ng/mL, and alkaline phosphatase level was 1,375 U/L. Tc-99m-MIBI biphasic parathyroid scintigraphy (A, B) showed hyperplasia. However, on single-photon emission computerized tomography images (C, D), irregularly increased radioactivity uptake was observed in the maxilla, mandible, and calvarium, with the maxilla showing the greatest intensity. The facial deformity was noticeable, especially in the sagittal section (D). We performed whole-body bone scintigraphy (E) on a separate day to evaluate the head and other skeletal structures. Increased radioactivity uptake was observed in the axial and appendicular bones, most intensely in the maxilla and whole-body bone imaging with Tc-99m-MDP. No radioactivity uptake by the kidneys and bladder was observed. The distance between the anterior ends of the bilateral ribs increased remarkably toward the basal end in the anterior projection. The thorax had morphed into a bell-shaped mouth. There was scoliosis in the vertebral column and bending-bowing deformity in the upper extremities.

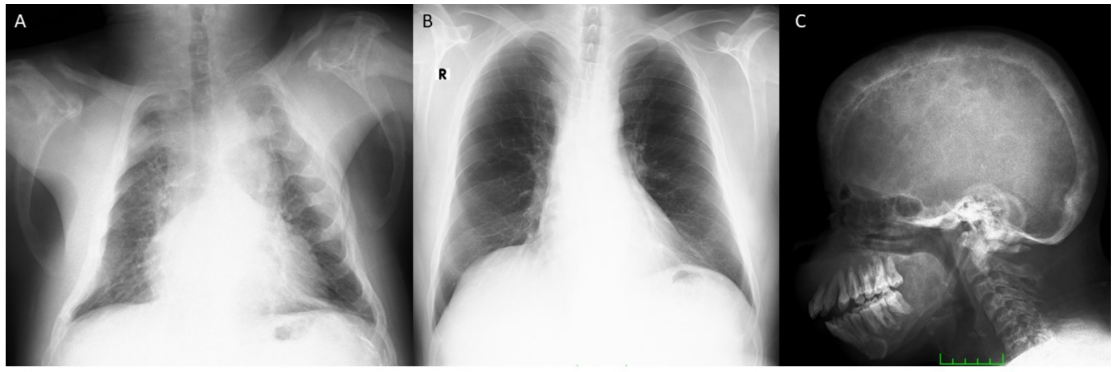

Figure 2. A posteroanterior chest radiograph (A) showed cardiomegaly, decreased lung volumes, rib fractures, and bilateral collapse of the lateral chest walls. The deformity seen in the current chest X-ray was not seen 6 years ago (B). The lateral head X-ray (C) revealed calvarial thickening and multiple lytic irregularly circumscribed lesions. In addition, there was a frontal forward malformation of the maxilla, and the lower and upper incisors were malposition. The patient was determined to have Sagliker syndrome (SS). Recently described SS is an aggravated form of renal osteodystrophy, which is an abnormal bone histology in chronic kidney disease (CKD) (1). In 1953, Cohen and Diamond (2) initially defined the signs of secondary hyperparathyroidism related to prolonged renal failure as uremic leontiasis ossea, which is marked by disfiguring craniomaxillofacial bone overgrowth (3,4). In 2004, Sagliker et al. (1) described this phenomenon in detail and named it SS. The symptoms of SS include a deformed facial appearance, maxillary and mandibular bone overgrowth, nasal bone and cartilage destruction, irregular teeth shape and localization, grade 2 maxillary malocclusion (anterior forward malformation of the upper jaws), short stature, soft and benign tissue deposits, upward curved fingertip changes, and knee and scapula deformities (1,5). In addition, SS affects the immune, neuropsychiatric, and cardiovascular systems as well as the musculoskeletal system (6). The etiology of SS remains unknown. SS is especially seen in developing countries. It is thought that financial deficiency, sociocultural deficiencies, and unwanted iatrogenic late, incomplete, or incorrect treatment methods play an essential role in the development of SS (7). After performing gene mutation studies, Demirhan et al. (8) postulated that SS may be caused by a combination of CKD, hereditary osteodystrophies, and bone dysplasias. Many patients do not notice the onset of SS because the symptoms develop slowly. Early medical and surgical treatment can prevent irreversible musculoskeletal deformities and cardiovascular disorders.

Ethics

Informed Consent: Patient consent was obtained.

Authorship Contributions

Concept: Ç.E., Ö.Ş., Design: Ç.E., Ö.Ş., Data Collection or Processing: Ç.E., Ö.Ş., Analysis or Interpretation: Ç.E., Ö.Ş., Z.A., Literature Search: Ç.E., Ö.Ş., A.E.Ş., Writing: Ç.E.

Conflict of Interest: No conflicts of interest were declared by the authors.

Financial Disclosure: The authors declare that this study has received no financial support.

References

1. Sagliker Y, Balal M, Sagliker Ozkaynak P, Paydas S, Sagliker C, Sabit Sagliker H, Kiralp N, Mumin Adam S, Tuncer I, Gonlusen G, Esenturk M, Gocmez E, Taskapan H, Yeksan M, Kobaner E, Ozkaya O, Yuksekgonul M, Emir I, Cengiz N, Onder Isik I, Bilginer O, Guler T, Yakar H, Sarsmaz N, Dilaver S, Akoglu B, Basgumus M, Chirik E. Sagliker syndrome: uglifying human face appearance in late and severe secondary hyperparathyroidism in chronic renal failure. Semin Nephrol 2004;24:449-455.
2. Cohen J, Diamond I. Leontiasis ossea, slipped epiphyses, and granulosa cell tumor of testis with renal disease; report of a case with autopsy findings. AMA Arch Pathol 1953;56:488-500.
3. Lee VS, Webb MS Jr, Martinez S, McKay CP, Leight GS Jr. Uremic leontiasis ossea: "bighead" disease in humans? Radiologic, clinical, and pathologic features. Radiology 1996;199:233-240.
4. Fisher D, Hiller N, Drukker A. Nephroquiz for the beginner: A swollen face in a girl on haemodialysis. Diagnosis: renal osteodystrophy. Nephrol Dial Transplant 1999;14:1797-1798.
5. Sagliker Y, Acharya V, Ling Z, Golea O, Sabry A, Eyupoglu K, Ookalkar DS, Tapiawala S, Durugkar S, Khetan P, Capusa C, Univar R, Yildiz I, Cengiz K, Bali M, Ozkaynak PS, Sagliker HS, Paylar N, Adam SM, Balal M, Paydas S, Demirhan O, Tasdemir D, Ben Maiz H, Redulescu D, Garneata L, Mircescu G, Hong-Liang R, Lun L, Yildizer K, Emir I, Yuksekgonul M, Yenicerioglu Y, Akar H, Sagliker C, Esenturk M, Kiralp N. International study on Sagliker syndrome and uglifying human face appearance in severe and late secondary hyperparathyroidism in chronic kidney disease patients. J Ren Nutr 2008;18:114-117.
6. Mohebi-Nejad A, Gatmiri SM, Abooturabi SM, Hemayati R, Mahdavi-Mazdeh M. Diagnosis and treatment of Sagliker syndrome: a case series from Iran. Iran J Kidney Dis 2014;8:76-80.
7. Yildiz I, Sagliker Y, Demirhan O, Tunc E, Inandiklioglu N, Tasdemir D, Acharya V, Zhang L, Golea O, Sabry A, Ookalkar DS, Capusa C, Radulescu D, Garneata L, Mircescu G, Ben Maiz H, Chen CH, Prado Rome J, Benzegoutta M, Paylar N, Eyuboglu K, Karatepe E, Esenturk M, Yavascan O, Grzegorzevska A, Shilo V, Mazdeh MM, Francesco RC, Gouda Z, Adam SM, Emir I, Ocal F, Usta E, Kiralp N, Sagliker C, Ozkaynak PS, Sagliker HS, Bassuoni M, Sekin O. International evaluation of unrecognizably uglifying human faces in late and severe secondary hyperparathyroidism in chronic kidney disease. Sagliker syndrome. A unique catastrophic entity, cytogenetic studies for chromosomal abnormalities, calcium-sensing receptor gene and GNAS1 mutations. Striking and promising missense mutations on the GNAS1 gene exons 1, 4, 10, 4. J Ren Nutr 2012;22:157-161.
8. Demirhan O, Arslan A, Sagliker Y, Akbal E, Ergun S, Bayraktar R, Sagliker HS, Dogan E, Gunesacar R, Ozkaynak PS. Gene mutations in chronic kidney disease patients with secondary hyperparathyroidism and Sagliker syndrome. J Ren Nutr 2015;25:176-186.

Interesting Image
Mol Imaging Radionucl Ther 2024;33:43-46 DOI:10.4274/mirt.galenos.2023.02328

Two Rare Benign Lesions on ^{18}F-FDG PET/CT: Peliosis Hepatis and SANT

^{18}F-FDG PET/BT'de Saptanan İki Nadir Benign Lezyon: Peliosis Hepatis ve SANT

Ediz Beyhan[1], Ahu Senem Demiröz[2], İbrahim Taşkın Rakıcı[3], Tevfik Fikret Çermik[1], Esra Arslan[1]

[1]University of Health Sciences Türkiye, İstanbul Training and Research Hospital, Clinic of Nuclear Medicine, İstanbul, Türkiye
[2]İstanbul University-Cerrahpaşa, Cerrahpaşa Faculty of Medicine, Department of Pathology, İstanbul, Türkiye
[3]University of Health Sciences Türkiye, İstanbul Training and Research Hospital, Clinic of Radiology, İstanbul, Türkiye

Abstract

Peliosis hepatis (PH) and sclerosing angiomatoid nodular transformation of the spleen are uncommon benign lesions. Diagnosis can be difficult in some patients. Herein, we present the case of a 28-year-old woman referred with abdominal pain who had spleen lesions. ^{18}F-fluorodeoxyglucose (FDG) positron emission tomography/computed tomography revealed multiple non-FDG avid lesions in the liver and hypermetabolic lesions in the spleen. In addition, abdominal magnetic resonance imaging was performed. Histopathology revealed sclerosing angiomatoid nodular transformation in the spleen and PH in the liver.

Keywords: Peliosis hepatis, splenic lesions, liver lesions, ^{18}F-FDG PET/CT, SANT

Öz

Peliosis hepatis (PH) ve dalağın sklerozan anjiomatoid nodüler transformasyonu nadir görülen benign lezyonlardır. Bazı olgularda tanısı zor olabilir. Bu olguda karın ağrısı şikayeti ile başvuran 28 yaşında, multipl dalak lezyonları saptanan hastayı sunuyoruz. ^{18}F-florodeoksiglikoz (FDG) pozitron emisyon tomografisi/bilgisayarlı tomografide, karaciğerde çok sayıda FDG tutulumu göstermeyen lezyonlar ve dalakta hipermetabolik lezyonlar izlendi. Ayrıca hastaya batın manyetik rezonans görüntüleme yapıldı. Histopatolojik inceleme ile dalakta sklerozan anjiomatoid nodüler transformasyon ve karaciğerde PH saptandı.

Anahtar kelimeler: Peliosis hepatis, splenik lezyonlar, karaciğer lezyonları, ^{18}F-FDG PET/BT, SANT

Address for Correspondence: Ediz Beyhan MD, University of Health Sciences Türkiye, İstanbul Training and Research Hospital, Clinic of Nuclear Medicine, İstanbul, Türkiye
Phone: +90 212 459 68 02 **E-mail:** edizbeyhan@gmail.com ORCID ID: orcid.org/0000-0001-6833-4830
Received: 21.03.2023 **Accepted:** 29.05.2023

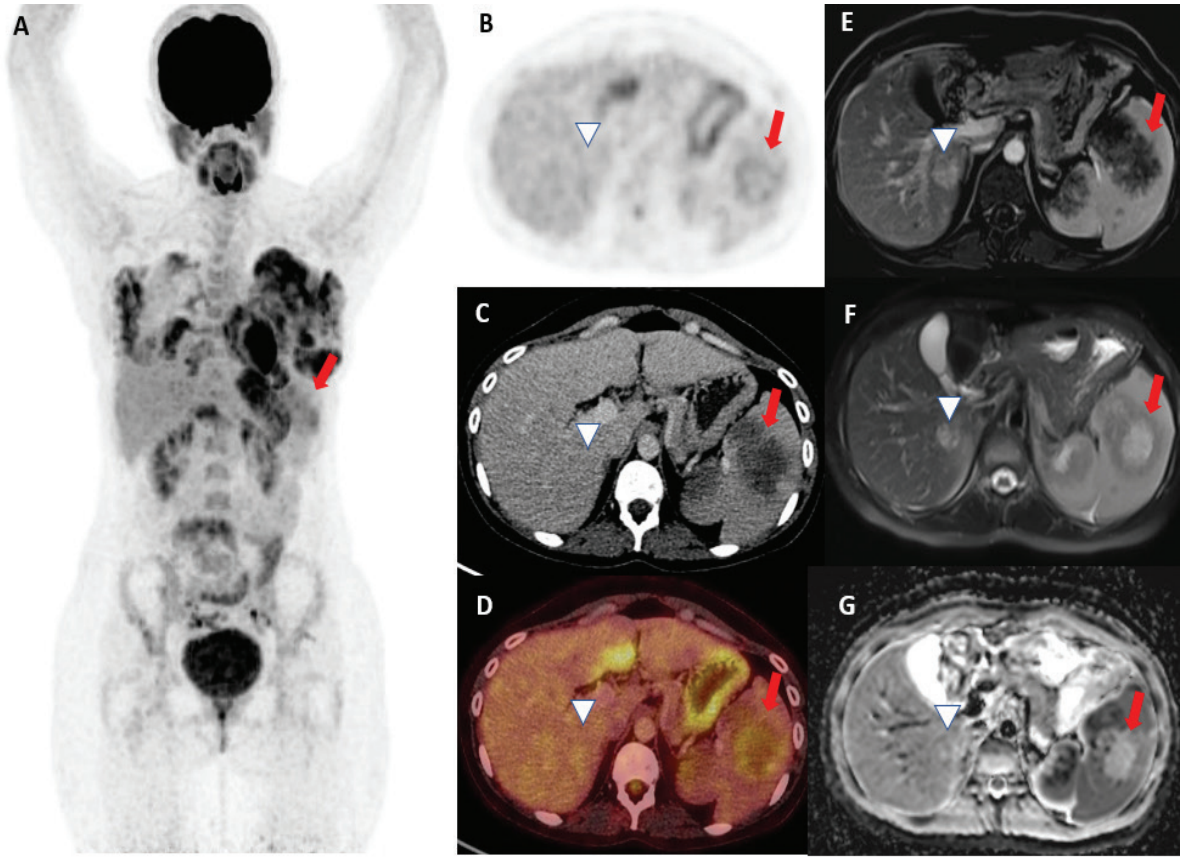

Figure 1. A 28-year-old breastfeeding woman presented with abdominal pain. The patient was referred with multiple spleen lesions for ^{18}F-fluorodeoxyglucose (^{18}F-FDG) positron emission tomography/computed tomography (PET/CT) for suspicion of lymphoma. In PET/CT images, multiple hypodense lesions were observed in spleen axial CT slices (C, arrow). These lesions showed peripheral lacy mild FDG uptake on PET and PET/CT [maximum standardized uptake value (SUV_{max}): 4.7] (A, B, D, arrow). In addition, subcapsular multiple hypodense lesions were observed in the liver in axial CT slices and showed no FDG uptake in PET and PET/CT (B, C, D, arrowhead). Multiple intensity projection images showed intense FDG uptake in the bilateral breast parenchyma due to breastfeeding. Abdominal magnetic resonance imaging (MRI) showed multiple hypointense lesions with septa and peripheral enhancement on the T1 delayed phase and hyperintense lesions on the T2 fast spin echo in the spleen (E, F, arrow). In addition, multiple lesions in the liver showed hyperintense increasing contrast enhancement on the T1 delayed phase (E, arrowhead), hyperintense on T2 fast spin-echo (F), and restricted diffusion (G, arrowhead).

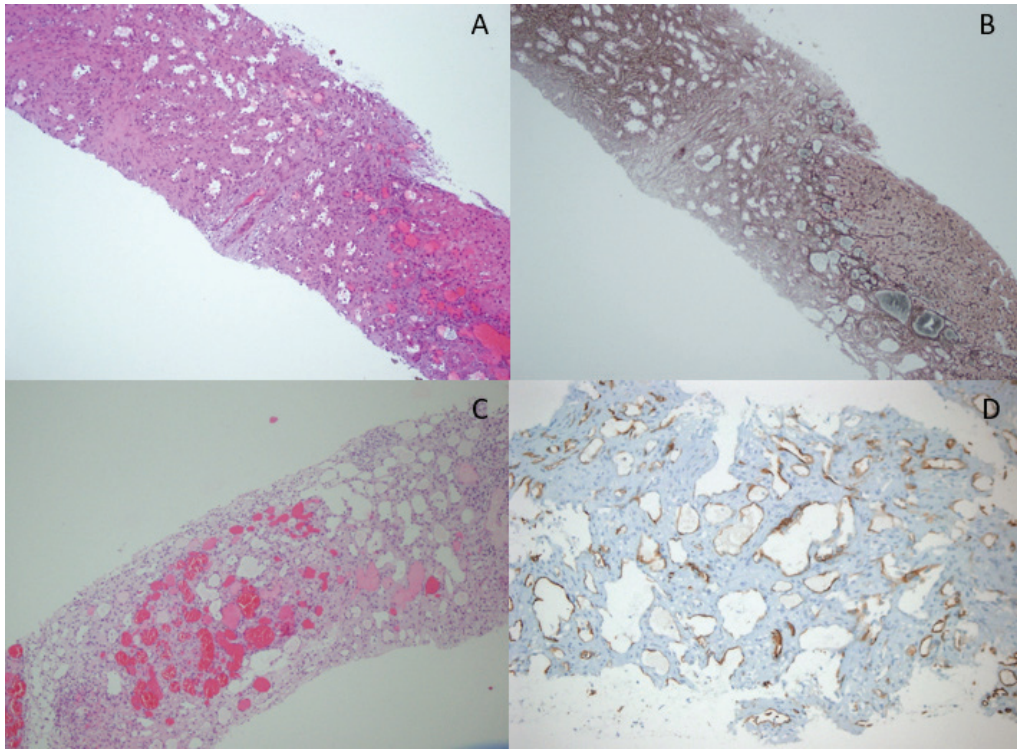

Figure 2. Liver biopsy revealed loss of the parenchyma, proliferated capillary vascular structures within the nodular area characterized by fibrosis in the liver (A, H&E, x200), and reticular fibrosis surrounding the capillary vascular bed (B, reticulin dye x200), and PH diagnosis. In spleen biopsy, pathological examination determined by sclerosing angiomatoid nodular transformation (SANT) showed that vascular capillary proliferation was seen in the spleen (C H&E, x200). The lesion's immunohistochemical staining was positive for CD34 (D, x400). SANT is a benign rare splenic lesion characterized by vascular multi-nodules and presents asymptomatic or abdominal pain (1). SANT in the spleen has a few cases with ^{18}F-FDG PET/CT showing mild to moderate hypermetabolism (2,3). Peliosis hepatis (PH) is rare, and its etiology includes infections, steroids, and organ transplantation, in some cases unknown (4). PH is an uncommon vascular condition characterized by multiple, randomly distributed, blood-filled cavities throughout the liver. The cavities usually range between a few millimeters and 3 cm in diameter (5). It can be challenging to differentiate PH from malignancy or infectious pathologies because of nonspecific radiologic findings. MRI findings of SANT have been described as T1 hypointense, T2 hyperintense, and peripheral and septal contrast enhancement, known as the spoke wheel pattern (6,7). Isometabolic or hypermetabolic uptake patterns in PH on ^{18}F-FDG PET/CT have been reported in the literature (7,8). Asymptomatic and small lesions can be followed, but surgery is recommended for SANT and PH (4). Both pathologies could mimic malignancy, but SANT showed false positive uptake in this case. Faint and peripheral uptake patterns could be descriptive of SANT on ^{18}F-FDG PET/CT.

Ethics

Informed Consent: Patient consent was obtained.

Authorship Contributions

Surgical and Medical Practices: A.S.D., E.B., İ.T.R., T.F.Ç, E.A., Concept: E.A., T.F.Ç, E.B., A.S.D., İ.T.R., Design: T.F.Ç, E.A., E.B., A.S.D., İ.T.R., Data Collection or Processing: İ.T.R., E.B., A.S.D., T.F.Ç, E.A., Analysis or Interpretation: E.A., T.F.Ç, E.B., A.S.D., İ.T.R., Literature Search: E.B., E.A., A.S.D., İ.T.R., T.F.Ç, Writing: E.B., E.A., A.S.D., İ.T.R., T.F.Ç.

Conflict of Interest: No conflicts of interest were declared by the authors.

Financial Disclosure: The authors declare that this study has received no financial support.

References

1. Sangiorgio VFI, Arber DA. Non-hematopoietic neoplastic and pseudoneoplastic lesions of the spleen. Semin Diagn Pathol 2021;38:159-164.
2. Zhang ZB, Li L. Splenic sclerosing angiomatoid nodular transformation in a patient with right renal carcinoma: A case report. Asian J Surg 2021;44:396-397.
3. Feng YM, Huang YC, Tu CW, Kao WS, Tu DG. Distinctive PET/CT features of splenic SANT. Clin Nucl Med 2013;38:e465-e466.
4. Dave YA, Gupta A, Shah MM, Carpizo D. Liver haematoma as a presentation of peliosis hepatis. BMJ Case Rep 2019;12:e226737
5. Holmes JA, Chung RT. Hepatitis C. In: Feldman M, Friedman LS, Brandt LJ (eds). Sleisenger and Foltran's Sleisenger and Fordtranıs Gastrointestinal and Liver Disease: Pathophysiology, Diagnosis, Management. Canada, Elsevier, 2021;1243-1283.
6. Imamura Y, Nakajima R, Hatta K, Seshimo A, Sawada T, Abe K, Sakai S. Sclerosing angiomatoid nodular transformation (SANT) of the spleen:

a case report with FDG-PET findings and literature review. Acta Radiol Open 2016;5:2058460116649799.

7. Seo M, Lee SH, Han S, Sung C, Son DH, Lee JJ. Peliosis hepatis shows isometabolism on (18)F-FDG PET/CT: two case reports. Nucl Med Mol Imaging 2014;48:309-312.
8. Levin D, Hod N, Anconina R, Ezroh Kazap D, Shaco-Levy R, Lantsberg S. Peliosis hepatis simulating metastatic liver disease on FDG PET/CT. Clin Nucl Med 2018;43:e234-e236.

Interesting Image
Mol Imaging Radionucl Ther 2024;33:47-49 DOI:10.4274/mirt.galenos.2023.27576

Detection of Rare Gallbladder Microperforation by ^{18}F-FDG PET/CT in a Patient with Maxillary Sinus Cancer

Maksiller Sinüs Kanserli Hastada Nadir Görülen Safra Kesesi Mikroperforasyonunun ^{18}F-FDG PET/BT ile Saptanması

Zehranur Tosunoğlu[1], Selim Doğan[2], Ceyda Turan Bektaş[3], Tevfik Fikret Çermik[1], Esra Arslan[1]

[1]*University of Health Sciences Türkiye, İstanbul Training and Research Hospital, Clinic of Nuclear Medicine, İstanbul, Türkiye*
[2]*University of Health Sciences Türkiye, İstanbul Training and Research Hospital, Clinic of Surgery, İstanbul, Türkiye*
[3]*University of Health Sciences Türkiye, İstanbul Training and Research Hospital, Clinic of Radiology, İstanbul, Türkiye*

Abstract

Gallbladder perforation is one of the most serious complications of cholecystitis and is rarely seen in 2-11% of cases. Pericholecystic abscesses secondary to gallbladder perforation are rare. Rapid diagnosis is important because of high morbidity and mortalityrates. A subcapsular abscess secondary to gallbladder microperforation is presented on ^{18}F-fluorodeoxyglucose positron emission tomography/computed tomography performed for restaging in a patient with maxillary sinus cancer.

Keywords: Gallbladder micro-perforation, abscess, ^{18}F-FDG PET/CT

Öz

Safra kesesi perforasyonu kolesistitin en ciddi komplikasyonlarından biridir ve %2-11 oranında nadir görülür. Safra kesesi perforasyonuna sekonder gelişen perikolesistik abse nadir görülen bir durumdur. Yüksek morbidite ve mortalite nedeniyle hızlı tanı önemlidir. Maksiller sinüs kanserli olguda yeniden evreleme amacıyla çekilen ^{18}F-florodeoksiglikoz pozitron emisyon tomografisi/bilgisayarlı tomografide safra kesesi mikroperforasyonuna bağlı gelişen subkapsüler abse sunulmaktadır.

Anahtar kelimeler: Safra kesesi mikroperforasyonu, abse, ^{18}F-FDG PET/BT

Address for Correspondence: Zehranur Tosunoğlu MD, University of Health Sciences Türkiye, İstanbul Training and Research Hospital, Clinic of Nuclear Medicine, İstanbul, Türkiye
Phone: +90 507 866 77 85 **E-mail:** zehranurtosunoglu@gmail.com ORCID ID: orcid.org/0000-0002-8509-1583
Received: 08.04.2023 **Accepted:** 14.07.2023

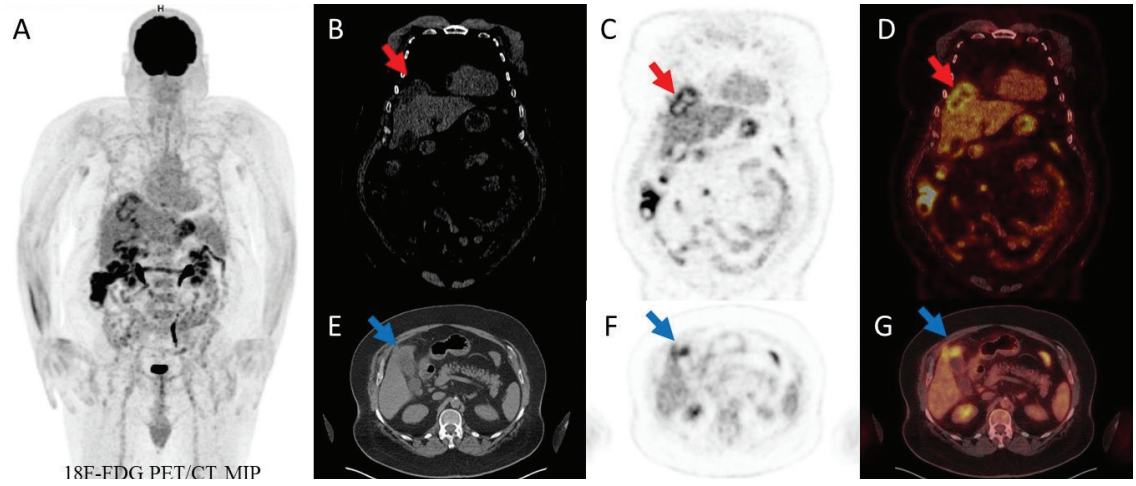

Figure 1. ^{18}F-fluorodeoxyglucose (^{18}F-FDG) positron emission tomography/computed tomography (PET/CT) imaging was performed to restage maxillary sinus cancer in a 67-year-old man with a known history of diabetes mellitus, hypertension, and stroke (A). In coronal CT sections, there was a hypodense area outside the liver parenchyma at the junction of liver segments 4-8 (B). PET and fusion images (C, D) showed linear ^{18}F-FDG uptake [maximum standardized uptake value (SUV_{max}): 6.30] (red arrow). Thickening of the fundus was observed in transaxial CT sections (E). ^{18}F-FDG uptake was observed in PET and fusion images (F, G) (blue arrow). There were several lymph nodes with increased ^{18}F-FDG uptake in the precaval and aortocaval lymphatic regions (SUV_{max}: 5.40). It was evaluated as a subcapsular abscess secondary to gallbladder microperforation. The clinical findings were indistinct. There was no significant abdominal pain due to diabetic neuropathy. In laboratory tests, neutrophils (7,640/µL), C-reactive protein (CRP) (114 mg/L), alkaline phosphatas (ALP) (134 U/L), gamma-glutamyltransferase (GGT) (87 U/L), and direct bilirubin (0.4 mg/dL) were high. Other liver function tests were within the normal range (aspartate aminotransferase, alanine aminotransferase). He was admitted to the surgical service with a preliminary diagnosis of gallbladder microperforation secondary to cholecystitis.

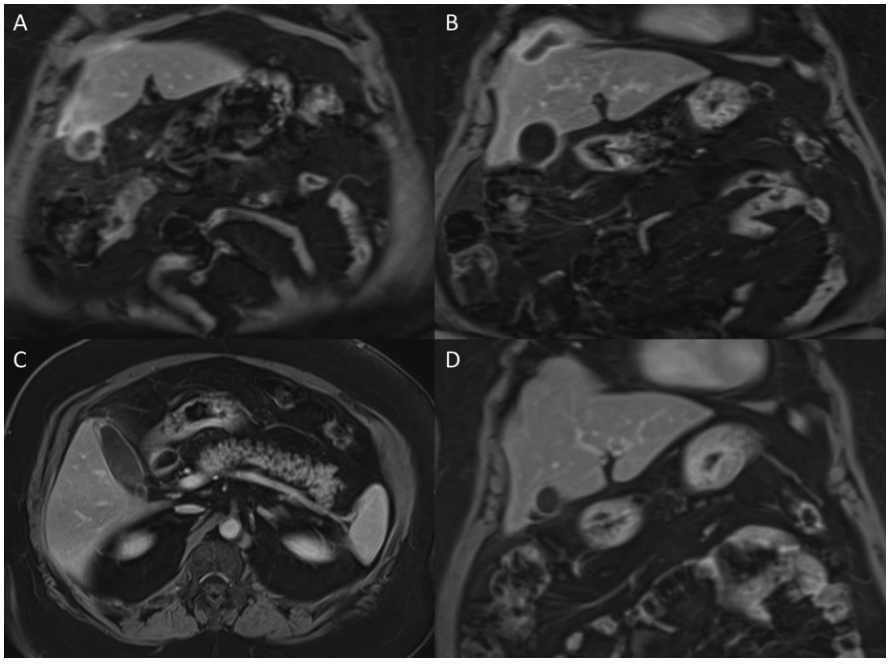

Figure 2. One day later, an extension of the collection, which is continuous with the gallbladder, to the perihepatic region and abscess formation/loculated collection at the subdiaphragmatic level were observed in postcontrast coronal VIBE images in cholangiopancreatic magnetic resonance imaging (MRI). (A, B). Antibiotic and intravenous fluid therapy were initiated. Two weeks later, neutrophil levels (4,200/µL), CRP (4.79 mg/L), direct bilirubin (0.18 mg/dL), ALP (78 U/L), and GGT (57 U/L) decreased. Two months later, a cholangiopancreatic MRI was performed for the control. In the postcontrast axial VIBE image, focal wall thickening and increased contrast were observed at the fundus of the sac (C). In the coronal sections, it was observed that the existing collection in the previous examination was lost in the vicinity of the gallbladder and subdiaphragmatic area (D).

Gallbladder perforation is a serious complication of acute cholecystitis (1). It may develop a few weeks after the onset of acute cholecystitis symptoms (2). There are 3 types according to the Niemer classification: Type 1, chronic perforation with cholecystoenteric fistula; type 2, subacute perforation with pericholecystic abscess; and type 3, acute free perforation into the peritoneal cavity (3,4). The fundus is the most common perforation site (5). Old age, male gender, diabetes, vascular disease, steroid therapy, malignancy, and cholelithiasis are predisposing factors (6). ^{18}F-FDG uptake is a known finding in inflammatory and infectious lesions (7). Abscesses are a benign cause of increased ^{18}F-FDG uptake in the liver. In one review, SUV values of 7.7±2.2 for abscesses were reported (8). In cholecystitis, a ring-like distribution of abnormal ^{18}F-FDG has been observed in the gallbladder (9). It is important to keep in mind the physiological distribution of ^{18}F-FDG, potential benign pitfalls, and the pattern of disease spread to interpret ^{18}F-FDG PET/CT studies correctly. We would like to present a subcapsular abscess secondary to gallbladder microperforation that was detected using ^{18}F-FDG PET/CT.

Ethics

Informed Consent: The patient consent was obtained.

Authorship Contributions

Surgical and Medical Practices: Z.T., S.D., C.T.B., T.F.Ç., E.A., Concept: Z.T., S.D., C.T.B., E.A., T.F.Ç., Design: Z.T., C.T.B., S.D., T.F.Ç., E.A., Data Collection or Processing: Z.T., S.D., C.T.B., T.F.Ç., E.A., Analysis or Interpretation: S.D., C.T.B., T.F.Ç., E.A., Z.T., Literature Search: Z.T., S.D., C.T.B., T.F.Ç., E.A., Writing: Z.T., T.F.Ç., E.A., S.D., C.T.B.

Conflict of Interest: No conflicts of interest were declared by the authors.

Financial Disclosure: The authors declare that this study has received no financial support.

References

1. Kochar K, Vallance K, Mathew G, Jadhav V. Intrahepatic perforation of the gall bladder presenting as liver abscess: case report, review of literature and Niemeier's classification. Eur J Gastroenterol Hepatol 2008;20:240-244.
2. Kim PN, Lee KS, Kim IY, Bae WK, Lee BH. Gallbladder perforation: comparison of US findings with CT. Abdom Imaging 1994;19:239-242.
3. Quiroga-Garza A, Alvarez-Villalobos NA, Angeles-Mar HJ, Garcia-Campa M, Muñoz-Leija MA, Salinas-Alvarez Y, Elizondo-Omaña RE, Guzmán-López S. Localized gallbladder perforation: a systematic review of treatment and prognosis. HPB (Oxford) 2021;23:1639-1646.
4. Smith EA, Dillman JR, Elsayes KM, Menias CO, Bude RO. Cross-sectional imaging of acute and chronic gallbladder inflammatory disease. AJR Am J Roentgenol 2009;192:188-196.
5. Peer A, Witz E, Manor H, Strauss S. Intrahepatic abscess due to gallbladder perforation. Abdom Imaging 1995;20:452-455.
6. Singh K, Singh A, Vidyarthi SH, Jindal S, Thounaojam CK. Spontaneous intrahepatic type II gallbladder perforation: a rare cause of liver abscess - case report. J Clin Diagn Res 2013;7:2012-2014.
7. Pijl JP, Nienhuis PH, Kwee TC, Glaudemans AWJM, Slart RHJA, Gormsen LC. Limitations and pitfalls of FDG-PET/CT in infection and inflammation. Semin Nucl Med 2021;51:633-645.
8. Tan GJ, Berlangieri SU, Lee ST, Scott AM. FDG PET/CT in the liver: lesions mimicking malignancies. Abdom Imaging 2014;39:187-195.
9. Rahman WT, Wale DJ, Viglianti BL, Townsend DM, Manganaro MS, Gross MD, Wong KK, Rubello D. The impact of infection and inflammation in oncologic 18F-FDG PET/CT imaging. Biomed Pharmacother 2019;117:109168.

Interesting Image
Mol Imaging Radionucl Ther 2024;33:50-53 DOI:10.4274/mirt.galenos.2023.91259

^{18}F-FDG PET/CT Imaging for Treatment Response Assessment of Cardiac Primitive Neuroectodermal Tumor

Kardiyak Primitif Nöroektodermal Tümörde Tedavi Yanıtı Değerlendirmede ^{18}F-FDG PET/BT

Mehmet Emin Mavi, Murat Fani Bozkurt

Hacettepe University Faculty of Medicine, Department of Nuclear Medicine, Ankara, Türkiye

Abstract

Primitive neuroectodermal tumors (PNETs) are rare and aggressive members of the small round cell carcinoma family. Generally, PNETs are classified into two main groups: PNETs of the central nervous system and PNETs of the peripheral nervous system. Herein, we report the therapy response assessment of a rare case of isolated cardiac PNET using ^{18}F-fluorodeoxyglucose (^{18}F-FDG) positron emission tomography/computed tomography (PET/CT) imaging. Given that physiological cardiac FDG uptake is typically observed, assessing FDG avid lesions in the myocardium presents a challenge for FDG PET/CT. This case holds significance because of the rarity of the disease and the challenging nature of the site for FDG PET/CT imaging.

Keywords: Primitive, neuroectodermal, cardiac, ^{18}F-fluorodeoxyglucose, positron, emission, tomography, treatment, response

Öz

Primitif nöroektodermal tümörler (PNET) küçük yuvarlak hücreli tümörler ailesinin nadir görülen ve agresif bir üyesidir. PNET'ler genellikle santral sinir sisteminin PNET'leri ve periferik sinir sisteminin PNET'leri olmak üzere iki ana grupta değerlendirilmektedir. Burada, nadir görülen bir izole kardiyak PNET olgusunda tedavi yanıtının ^{18}F-FDG pozitron emisyon tomografisi/bilgisayarlı tomografi (PET/BT) ile değerlendirmesi sunulmuştur. Fizyolojik kardiyak FDG tutulumu göz önünde bulundurulduğunda, miyokarddaki FDG tutan lezyonların değerlendirilmesi FDG PET/BT için zorluk oluşturmaktadır. Bu olgu, hastalığın nadirliği ve FDG PET/BT ile değerlendirilmesi için zorlu doğası nedeniyle önem taşımaktadır.

Anahtar kelimeler: Primitif, nöroektodermal, kardiyak, ^{18}F-fluorodeoksiglikoz, pozitron, emisyon, tomografi, tedavi, yanıtı

Address for Correspondence: Mehmet Emin Mavi MD, Hacettepe University Faculty of Medicine, Department of Nuclear Medicine, Ankara, Türkiye
Phone: +90 312 305 13 36 **E-mail:** mehmeteminmavii@gmail.com ORCID ID: orcid.org/0000-0001-7702-8157
Received: 26.01.2023 **Accepted:** 23.08.2023

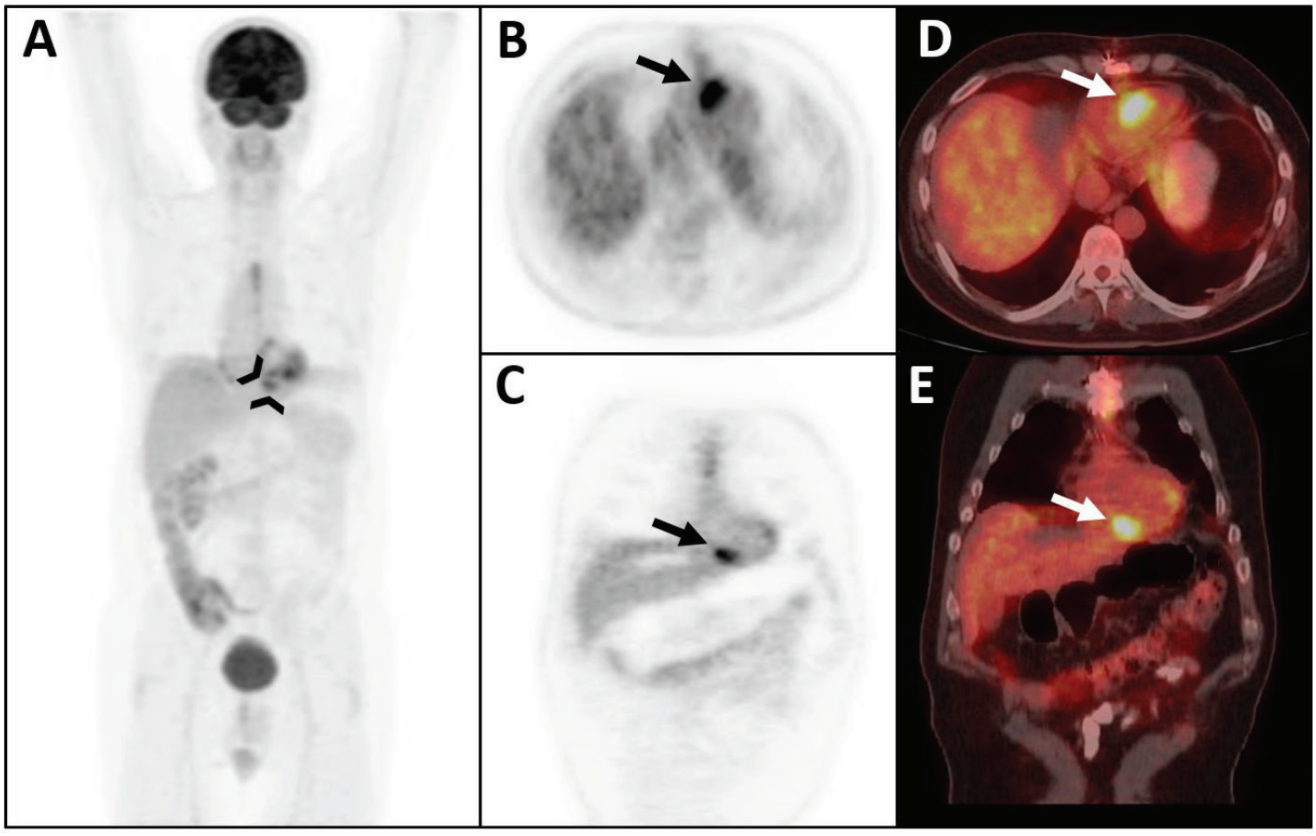

Figure 1. A 45-year-old man with a history of orchiectomy 21 years ago due to yolk sac tumor underwent thoracoabdominal computed tomography (CT) for routine follow-up. A left adrenal mass and a cardiac soft tissue lesion in the right ventricle were detected. After that, the adrenal mass and cardiac lesion were excised surgically. Pathology report of the adrenal mass was consistent with mature teratoma, but the cardiac lesion was diagnosed as primitive neuroectodermal tumor (PNET). One month after surgery, ^{18}F-fluorodeoxyglucose (^{18}F-FDG) positron emission tomography (PET)/CT was performed to evaluate disease status. Maximum intensity projection (MIP) image (A, black arrowheads), axial and coronal PET (B, C, black arrows), and PET/CT fusion (D, E, white arrows) images of PET/CT scan revealed increased FDG uptake in the right ventricle area, previous surgery site, without any marked pathology on CT component of the study, which was interpreted as probable residual malignant disease, indicating that surgery with R0 margin safety cannot be guaranteed in such surgical excision of cardiac tumoral masses. Moreover, it is not usual to observe physiologic FDG uptake in the right ventricle in particular where no physiologic FDG uptake is not seen in the left ventricle or elsewhere in the heart, unless there is an underlying clinical situation of other etiologies such as right ventricular hyperthrophia and cardiac failure, which are not present in this patient. There was no other abnormal FDG uptake in the rest of the body in favor of metastasis.

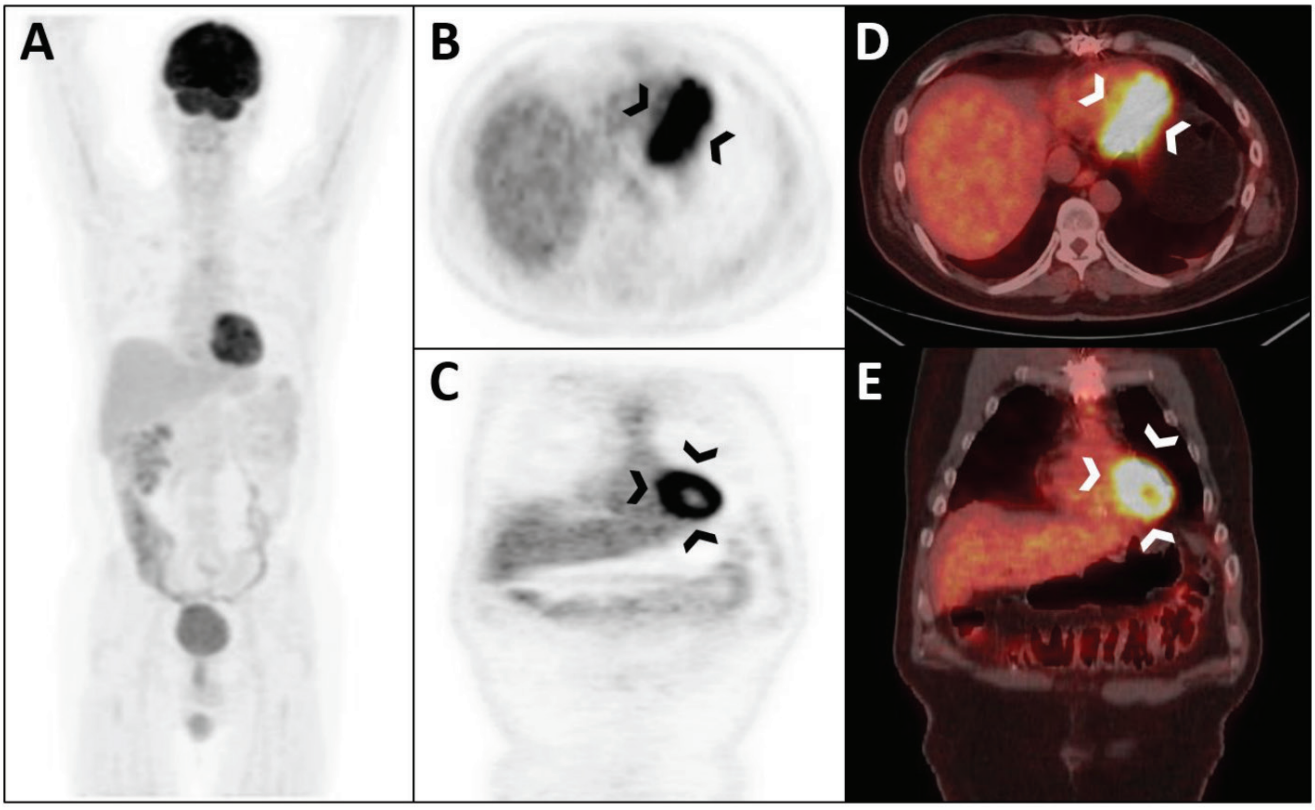

Figure 2. The patient was treated with chemotherapy after detection of residual malignant disease. Following chemotherapy, another [18]F-FDG PET/CT scan was performed to evaluate the therapy response. MIP image (A), axial and coronal PET (B, C), and PET/CT fusion (D, E) images of the second scan revealed no abnormal FDG activity in the right ventricle. However, unlike the first scan, there was physiological FDG uptake in the left ventricle (arrowheads). PNETs are rare and aggressive members of the small round cell carcinoma family and primarily stem from neural crest cells (1). When mentioning PNETs, the distinction between PNETs of the central nervous system (cPNETs) and PNETs of the peripheral nervous system (pPNETs) must be considered first, since they are fairly different from each other both clinically and pathologically (2). The term cPNETs no longer exists in the World Health Organization classification of tumors of the central nervous system as it was removed from the 4th edition which was publihed in 2016 (3). pPNETs and Ewing's sarcoma are considered to be on two edges of the neuroectodermal differentiation spectrum, with pPNETs on the most differentiated side and Ewing's sarcoma on the least differentiated side (4). A limited number of cases of demonstration of pPNETs occurring at different sites of the body by FDG PET/CT, generally with high FDG avidity, have been reported in the literature (5,6,7,8,9). Considering the rarity of pPNETs, cardiac pPNETs, especially isolated cardiac pPNETs, are even rarer. Only a few cases of isolated cardiac pPNETs have been reported in the literature (10,11,12); among them, only one case demonstrated the disease with FDG PET/CT (10). In this case, both the detection of probable residual disease and the therapy response of an isolated cardiac pPNET was demonstrated by FDG PET/CT imaging. Because physiological cardiac FDG uptake is usually observed, evaluation of the FDG avid lesions of the myocardium is challenging for FDG PET/CT (13). However, although FDG uptake is usually seen in the left ventricle, owing to relatively high muscle content and contractile activity, it is not common to observe physiological cardiac FDG uptake solely in the right ventricle, unless there is an underlying disease status affecting the right ventricle, such as in our case (14). Therefore, this case is quite important for such a rare disease in a challenging site for FDG PET/CT imaging.

Ethics

Informed Consent: Since the information provided is anonymous, obtaining informed consent from the patients was deemed not required.

Authorship Contributions

Surgical and Medical Practices: M.E.M., M.F.B., Concept: M.E.M., M.F.B., Design: M.E.M., M.F.B., Data Collection or Processing: M.E.M., M.F.B., Analysis or Interpretation: M.E.M., M.F.B., Literature Search: M.E.M., M.F.B., Writing: M.E.M., M.F.B.

Conflict of Interest: No conflicts of interest were declared by the authors.

Financial Disclosure: The authors declare that this study has received no financial support.

References

1. Gao L, Zhu Y, Shi X, Gao Z, Chen X. Peripheral primitive neuroectodermal tumors: A retrospective analysis of 89 cases and literature review. Oncol Lett 2019;18:6885-6890.
2. Vogel H, Fuller GN. Primitive neuroectodermal tumors, embryonal tumors, and other small cell and poorly differentiated malignant neoplasms of the central and peripheral nervous systems. Ann Diagn Pathol 2003;7:387-398.
3. Chhabda S, Carney O, D'Arco F, Jacques TS, Mankad K. The 2016 World Health Organization Classification of tumours of the central nervous system: what the paediatric neuroradiologist needs to know. Quant Imaging Med Surg 2016;6:486-489.
4. Kumar V, Singh A, Sharma V, Kumar M. Primary intracranial dural-based Ewing sarcoma/peripheral primitive neuroectodermal tumor mimicking a meningioma: A rare tumor with review of literature. Asian J Neurosurg 2017;12:351-357.
5. Wang J, Li J, Zhang X, Zhang X, Xiao Y. Primitive neuroectodermal tumor of the pericardium: a case report and literature review. BMC Cardiovasc Disord 2021;21:305.
6. Bae SH, Hwang JH, Da Nam B, Kim HJ, Kim KU, Kim DW, Choi IH. Multiple ewing sarcoma/primitive neuroectodermal tumors in the mediastinum: a case report and literature review. Medicine (Baltimore) 2016;95:e2725.
7. Dong A, Wang Y, Lu J, Zuo C. FDG PET/CT in peripheral primitive neuroectodermal tumor of the retroperitoneum. Clin Nucl Med 2014;39:707-710.
8. Musana KA, Raja S, Cangelosi CJ, Lin YG. FDG PET scan in a primitive neuroectodermal tumor. Ann Nucl Med 2006;20:221-225.
9. Sharma P, Ghosh I, Khan EM. 18F-FDG PET/CT for staging and response evaluation in a rare case of childhood ovarian primitive neuroectodermal tumor. Clin Nucl Med 2021;46:e266-e267.
10. Fan C, Kong D, Tan C, Yang J. Isolated cardiac peripheral primitive neuroectodermal tumor: A case report. Cancer Biol Ther 2017;18:4-7.
11. Chai Y, Huang L, Yue L. Peripheral primitive neuroectodermal tumour of left ventricular wall origin: a rare case. Acta Cardiol 2007;62:523-524.
12. Kath R, Krack A, Schneider C, Katenkamp D, Höffken K. Kardiale Manifestation eines peripheren primitiven neuroektodermalen Tumors (pPNET)–eine Rarität [Cardiac manifestations of peripheral primitive neuroectodermal tumor (pPNET): a rare case]. Dtsch Med Wochenschr 2000;125:1192-1194.
13. Boellaard R, Delgado-Bolton R, Oyen WJ, Giammarile F, Tatsch K, Eschner W, Verzijlbergen FJ, Barrington SF, Pike LC, Weber WA, Stroobants S, Delbeke D, Donohoe KJ, Holbrook S, Graham MM, Testanera G, Hoekstra OS, Zijlstra J, Visser E, Hoekstra CJ, Pruim J, Willemsen A, Arends B, Kotzerke J, Bockisch A, Beyer T, Chiti A, Krause BJ; European Association of Nuclear Medicine (EANM). FDG PET/CT: EANM procedure guidelines for tumour imaging: version 2.0. Eur J Nucl Med Mol Imaging 2015;42:328-354.
14. Maurer AH, Burshteyn M, Adler LP, Steiner RM. How to differentiate benign versus malignant cardiac and paracardiac 18F FDG uptake at oncologic PET/CT. Radiographics 2011;31:1287-1305.

Interesting Image
Mol Imaging Radionucl Ther 2024;33:54-56 DOI:10.4274/mirt.galenos.2023.47855

^{68}Ga Prostate-specific Membrane Antigen Uptake in Metastatic Medullary Thyroid Carcinoma

Metastatik Medüller Tiroid Kanserinde ^{68}Ga Prostat-spesifik Membran Antijen Tutulumu

Kübra Şahin, Ali Kibar, Cansu Güneren, Muhammet Sait Sağer, Kerim Sönmezoğlu

İstanbul University-Cerrahpaşa, Cerrahpaşa Faculty of Medicine, Department of Nuclear Medicine, İstanbul, Türkiye

Abstract

We present the case of a 58-year-old man with advanced medullary thyroid carcinoma who had a treatment history with different types of modalities. In the follow-up, the patient had rising calcitonin and CEA levels. Metastatic lymph nodes, liver, and bone metastases with varying degrees of uptake were detected on ^{18}F-fluorodeoxyglucose (FDG) and ^{68}Ga-DOTATATE positron emission tomography/computed tomography (PET/CT). ^{68}Ga prostate-specific membrane antigen (PSMA) PET/CT was performed to explore whether the patient might have a chance for PSMA-targeted radionuclide therapy, and increased PSMA expression was noted in most of the metastatic lesions, even some of which have higher PSMA uptake than ^{18}F-FDG and ^{68}Ga-DOTATATE.

Keywords: Medullary thyroid carcinoma, prostate-specific membrane antigen, PSMA, ^{18}F-FDG, ^{68}Ga-DOTA, ^{68}Ga-PSMA

Öz

Farklı modalitelerle tedavi öyküsü olan 58 yaşında ileri evre medüller tiroid kanseri tanılı bir erkek hastayı sunuyoruz. Hastanın takiplerinde kalsitonin ve CEA düzeylerinde artış saptandı. Yapılan ^{18}F-fluorodeoksiglukoz (FDG) ve ^{68}Ga-DOTATATE pozitron emisyon tomografisi/bilgisayarlı tomografi (PET/BT) görüntülemelerinde değişen derecelerde tutulum gösteren metastatik lenf nodları, karaciğer ve kemik metastazları tespit edildi. Hastanın prostat-spesifik membran antijeni (PSMA) hedefli radyonüklid tedavi şansı olup olmadığını araştırmak için yapılan ^{68}Ga-PSMA PET/BT görüntülemesinde metastatik lezyonlarda artmış PSMA ekspresyonu görülmekle birlikte bazı lezyonlarda ^{18}F-FDG ve ^{68}Ga-DOTATATE'den daha yüksek aktivite tutulumu saptandı.

Anahtar kelimeler: Medüller tiroid kanseri, prostat spesifik membran antijeni, PSMA, ^{18}F-FDG, ^{68}Ga-DOTA, ^{68}Ga-PSMA

Address for Correspondence: Kübra Şahin MD, İstanbul University-Cerrahpaşa, Cerrahpaşa Faculty of Medicine, Department of Nuclear Medicine, İstanbul, Türkiye
Phone: +90 532 664 17 97 **E-mail:** kubra.sahin@iuc.edu.tr ORCID ID: orcid.org/0009-0004-9020-7482
Received: 03.07.2023 **Accepted:** 25.09.2023

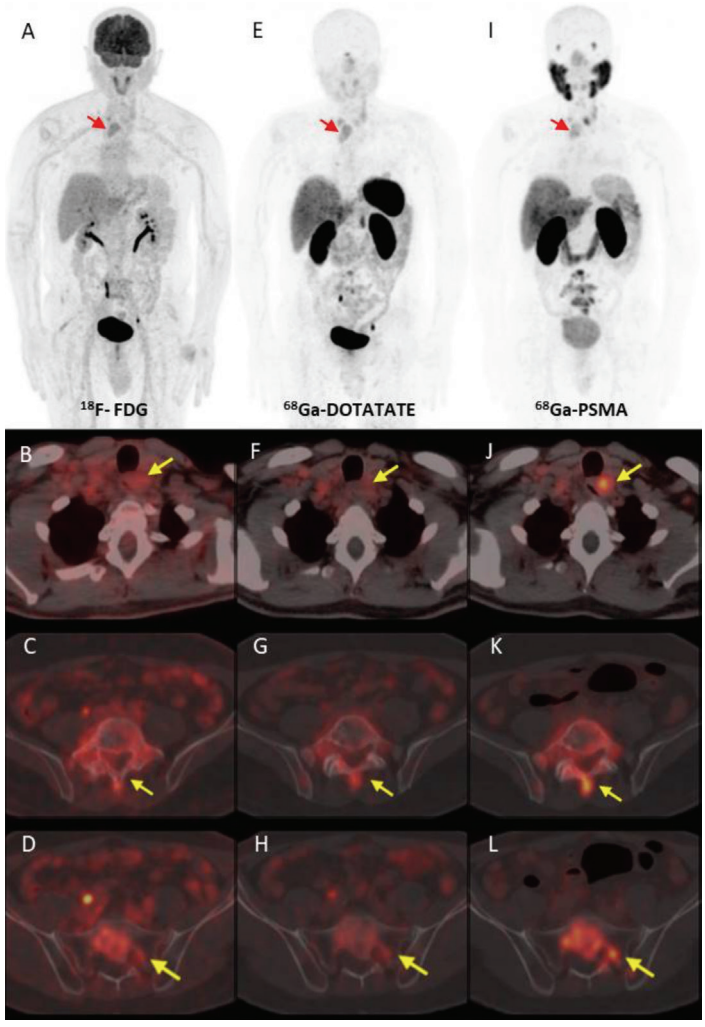

Figure 1. We present the case of a 58-year-old man with medullary thyroid carcinoma (MTC) who underwent total thyroidectomy and bilateral lymph node dissection 7 years ago. In the follow-up, different types of tyrosine kinase inhibitors (TKI) (sorafenib, vandetanib, sunitinib, and cabozantinib) and four cycles of ^{177}Lu-DOTATATE treatments were also administered because of the presence of metastatic disease. The patient had rising calcitonin (up to 15,622 pg/mL) and CEA levels (up to 727 ng/mL) while using TKI treatments. ^{18}F-fluorodeoxyglucose (^{18}F-FDG) and ^{68}Ga-DOTATATE positron emission tomography/computed tomography (PET/CT) were performed for restaging purposes. ^{18}F-FDG PET/CT imaging revealed metastatic conglomerated lymph nodes with mildly increased ^{18}F-FDG uptake in the right upper mediastinum [multiple intensity projection image (MIP) in A, red arrow] and in the left upper paraesophageal region (fused transaxial PET/CT view, arrow); B) as well as metastases in the liver parenchyma (not shown) and bones (i.e., the lumbar vertebrae and sacrum, shown images on C and D). The metastatic lymph nodes in the right upper mediastinum (MIP in E, red arrow) and bone metastases (G and H) also had mildly increased ^{68}Ga-DOTATATE levels, despite no uptake in the left metastatic paraesophageal lymph node (F) and liver metastases (not shown). Because of disease progression, we also performed ^{68}Ga prostate-specific membrane antigen (PSMA) PET/CT to explore whether the patient would be a candidate for PSMA-targeted radionuclide therapy. PSMA uptake was higher than that of ^{18}F-FDG and ^{68}Ga-DOTATATE in the metastatic lymph nodes in the left upper paraesophageal region (J) and bone metastases (K and L), whereas the metastatic lymph nodes in the right upper mediastinum (MIP in I, red arrow) had mild PSMA uptake and no discernible PSMA accumulation in the liver metastases (not shown). MTC is a rare neuroendocrine tumor with an unfavorable prognosis, and the management of the metastatic disease is complex (1).^{18}F-FDG and ^{68}Ga-somatostatin receptor (SSTR) PET/CT are recommended for detecting recurrent or metastatic disease in MTC with 72.4% and 88.1% sensitivity, respectively (1,2). ^{68}Ga-SSTR PET/CT imaging demonstrates SSTR-avid lesions leading to targeted peptide receptor radionuclide therapy with radiolabeled somatostatin analogs, which are well-tolerated and possibly beneficial treatment alternatives in advanced MTC (3). It has also been shown that PSMA expression is present in some aggressive non-prostatic malignancies, including MTC as a biomarker of angiogenesis, and this observation suggests that PSMA-based radionuclide treatment might be beneficial (4,5,6,7). Moreover, ^{177}Lu-PSMA therapy has been reported in a few patients with non-MTC (8). In this case, because of the presence of progression with TKI treatment and higher uptake of some lesions on ^{68}Ga-PSMA PET/CT compared with ^{18}F-FDG and ^{68}Ga-DOTATATE, ^{177}Lu-PSMA could be considered as a palliative therapy. By presenting this particular case, we speculate that further studies related to the theranostic application of PSMA are needed in patients with MTC who have limited treatment options.

Ethics

Informed Consent: Informed consent was obtained from the patient.

Authorship Contributions

Surgical and Medical Practices: K.Ş., M.S.S., Concept: M.S.S., Design: M.S.S., K.S., Data Collection or Processing: K.Ş., A.K., C.G., Analysis or Interpretation: K.Ş., M.S.S., K.S., Literature Search: K.Ş., A.K., C.G., Writing: K.Ş., K.S.

Conflict of Interest: No conflicts of interest were declared by the authors.

Financial Disclosure: The authors declare that this study has received no financial support.

References

1. Haddad RI, Bischoff L, Ball D, Bernet V, Blomain E, Busaidy NL, Campbell M, Dickson P, Duh QY, Ehya H, Goldner WS, Guo T, Haymart M, Holt S, Hunt JP, Iagaru A, Kandeel F, Lamonica DM, Mandel S, Markovina S, McIver B, Raeburn CD, Rezaee R, Ridge JA, Roth MY, Scheri RP, Shah JP, Sipos JA, Sippel R, Sturgeon C, Wang TN, Wirth LJ, Wong RJ, Yeh M, Cassara CJ, Darlow S. Thyroid Carcinoma, Version 2.2022, NCCN Clinical Practice Guidelines in Oncology. J Natl Compr Canc Netw 2022;20:925-951.
2. Şahin OE, Uslu-Beşli L, Asa S, Sağer S, Sönmezoğlu K. The role of ^{68}Ga-DOTATATE PET/CT and ^{18}F-FDG PET/CT in the follow-up of patients with medullary thyroid cancer. Hell J Nucl Med 2020;23:321-329.
3. Liu Q, Kulkarni HR, Zhao T, Schuchardt C, Chen X, Zhu Z, Zhang J, Baum RP. Peptide receptor radionuclide therapy in patients with advanced progressive medullary thyroid cancer: efficacy, safety, and survival predictors. Clin Nucl Med 2023;48:221-227.
4. Lodewijk L, Willems SM, Dreijerink KMA, de Keizer B, van Diest PJ, Schepers A, Morreau H, Bonenkamp HJ, Van Engen-van Grunsven IACH, Kruijff S, van Hemel BM, Links TP, Nieveen van Dijkum E, van Eeden S, Valk GD, Borel Rinkes IHM, Vriens MR. The theranostic target prostate-specific membrane antigen is expressed in medullary thyroid cancer. Hum Pathol 2018;81:245-254.
5. Arora S, Prabhu M, Damle NA, Bal C, Kumar P, Nalla H, Arun Raj ST. Prostate-specific membrane antigen imaging in recurrent medullary thyroid cancer: a new theranostic tracer in the offing? Indian J Nucl Med 2018;33:261-263.
6. Arora S, Damle NA, Parida GK, Singhal A, Nalli H, Dattagupta S, Bal C. Recurrent medullary thyroid carcinoma on 68Ga-Prostate-Specific membrane antigen PET/CT: exploring new theranostic avenues. Clin Nucl Med 2018;43:359-360.
7. Hasenauer N, Higuchi T, Deschler-Baier B, Hartrampf PE, Pomper MG, Rowe SP, Fassnacht M, Buck AK, Werner RA. Visualization of tumor heterogeneity in advanced medullary thyroid carcinoma by dual-tracer molecular imaging: revealing the theranostic potential of SSTR- and PSMA-directed endoradiotherapy. Clin Nucl Med 2022;47:651-652.
8. Uijen MJM, Derks YHW, Merkx RIJ, Schilham MGM, Roosen J, Privé BM, van Lith SAM, van Herpen CML, Gotthardt M, Heskamp S, van Gemert WAM, Nagarajah J. PSMA radioligand therapy for solid tumors other than prostate cancer: background, opportunities, challenges, and first clinical reports. Eur J Nucl Med Mol Imaging 2021;48:4350-4368.

Interesting Image
Mol Imaging Radionucl Ther 2024;33:57-62 DOI:10.4274/mirt.galenos.2023.13471

Atypical Presentation of Metastatic Castrate-resistant Prostate Cancer in a Middle Aged African Male with Good Response to Radioligand Therapy

Radyoligand Tedavisine İyi Yanıt Veren Orta Yaşlı Afrikalı Bir Erkekte Metastatik Kastrasyon Dirençli Prostat Kanserinin Atipik Prezentasyonu

Osayande Evbuomwan, Walter Endres, Tebatso Tebeila, Gerrit Engelbrecht

University of The Free State, Department of Nuclear Medicine, Bloemfontein, South Africa

Abstract

Prostate cancer typically follows a characteristic pattern of metastatic spread to the pelvic lymph nodes and bone. Atypical patterns of metastasis are rare but have been documented. In African men, this disease tends to follow a more aggressive course, with the possibility of an atypical site of metastatic spread. We present a case of a 58-year- old African male with metastatic castrate-resistant prostate cancer who presented with both typical and atypical patterns of metastatic disease detected by a fluorine 18 prostate-specific membrane antigen positron emission tomography/computed tomography scan. This patient also had a good response to radioligand therapy.

Keywords: Metastatic castrate-resistant prostate cancer, atypical metastases, ^{18}F-PSMA

Öz

Prostat kanseri tipik olarak pelvik lenf düğümlerine ve kemiğe metastatik yayılım yapar. Atipik metastaz paterni nadirdir ancak daha önce gösterilmiştir. Afrikalı erkeklerde bu hastalık, atipik metastatik yayılma olasılığıyla birlikte daha agresif bir seyir izleme eğilimindedir. Flor 18 prostat spesifik membran antijeni pozitron emisyon tomografisi/bilgisayarlı tomografi taraması ile tespit edilen hem tipik hem de atipik metastatik hastalık paterniyle başvuran, metastatik kastrasyon dirençli prostat kanseri olan 58 yaşında Afrikalı bir erkek olguyu sunuyoruz. Bu hasta aynı zamanda radyoligand tedavisine de iyi yanıt vermiştir.

Anahtar kelimeler: Metastatik kastrasyon dirençli prostat kanseri, atipik metastazlar, ^{18}F-PSMA

Address for Correspondence: Osayande Evbuomwan MD, Universitas Academic Hospital, Department of Nuclear Medicine, Bloemfontein, South Africa
Phone: +27742869731 **E-mail:** moreli14@yahoo.com ORCID ID: orcid.org/0000-0003-3670-8556
Received: 12.04.2023 **Accepted:** 15.10.2023

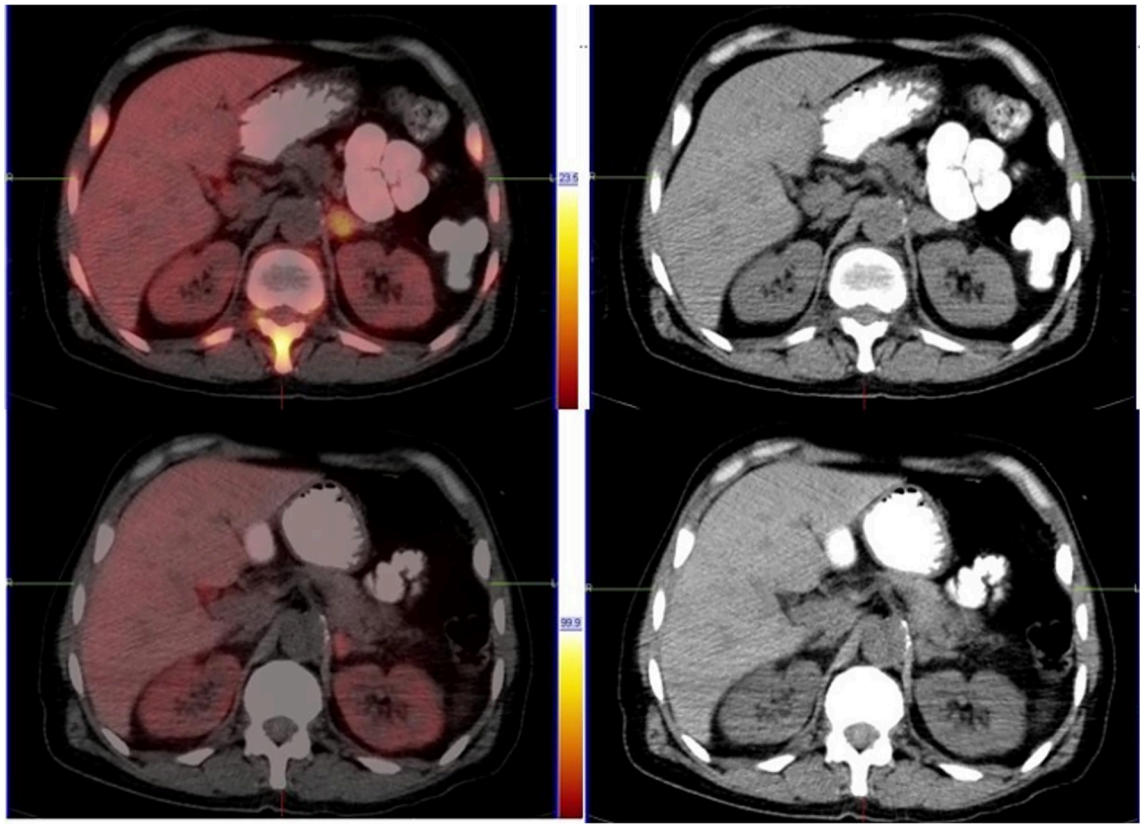

Figure 1. Fluorine 18 (^{18}F) positron emission tomography/computed tomography (PET/CT) and CT only images of a 58-year-old African male with high-risk adenocarcinoma [Gleason score 5+4 and prostate-specific antigen (PSA) 4, 441 ug/L] referred to our facility for radioligand therapy workup. The images in the top row reveal increased prostate-specific membrane antigen (PSMA) expression in the medial limb of the left adrenal gland [standardized uptake value (SUV): 15.04], which is confirmed to be bulky on the CT-only images. The images below are post 4 cycles of 177Lu-PSMA radioligand therapy images, revealing a reduction in PSMA expression (SUV: 5.30) and the size of the previously affected adrenal gland, confirming the response to therapy. The adrenal gland is one of the atypical sites for metastatic prostate cancer (1). In a retrospective study involving 620 patients with biopsy-proven prostate cancer, adrenal metastases were observed in 12 of the 82 patients (15%) with an atypical site of metastatic disease (2). However, adrenal metastases are considered extremely rare, accounting for 1% of all metastatic cases (3).

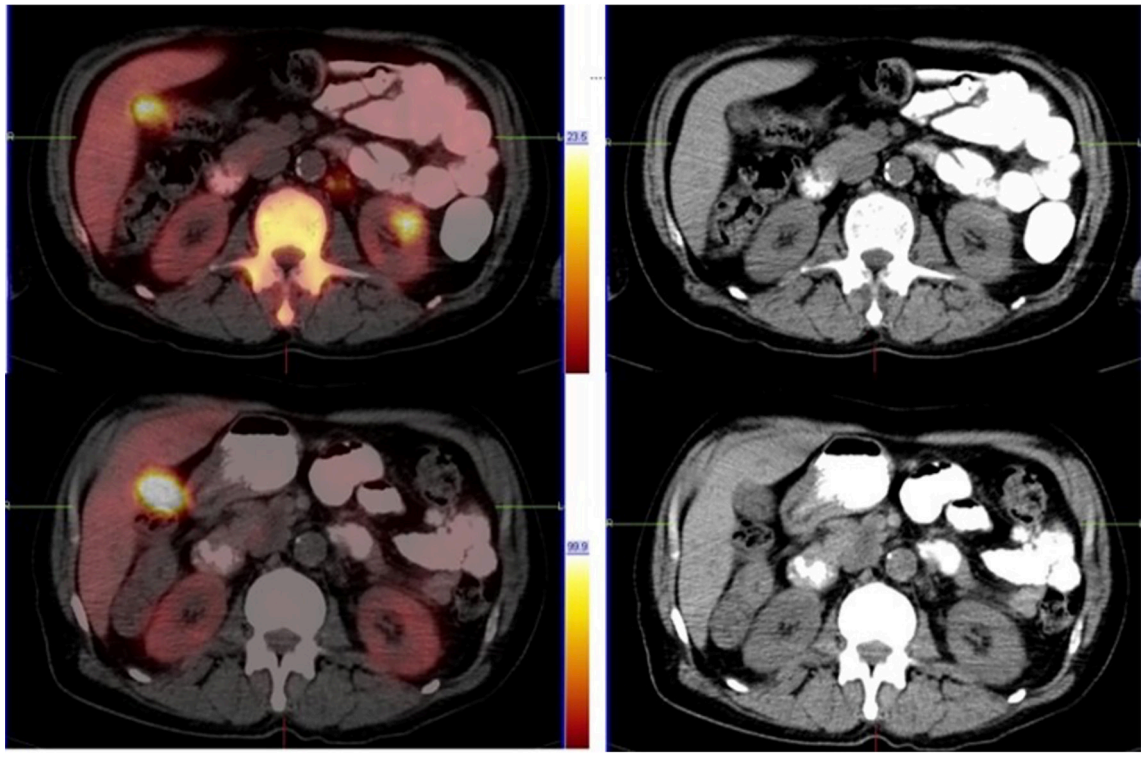

Figure 2. ^{18}F PET/CT and CT only images of the same patient. The images in the top row reveal increased PSMA expression in the left kidney (SUV: 24.7), with no obvious CT changes. The images below are after 4 cycles of 177Lu-PSMA radioligand therapy, which demonstrate complete resolution of the disease in the left kidney (SUV: 6.5). Few cases of prostate cancer metastasizing to the kidney have been reported (4,5,6). Chen et al. (6) described renal metastases in the setting of prostate cancer as an extremely rare entity.

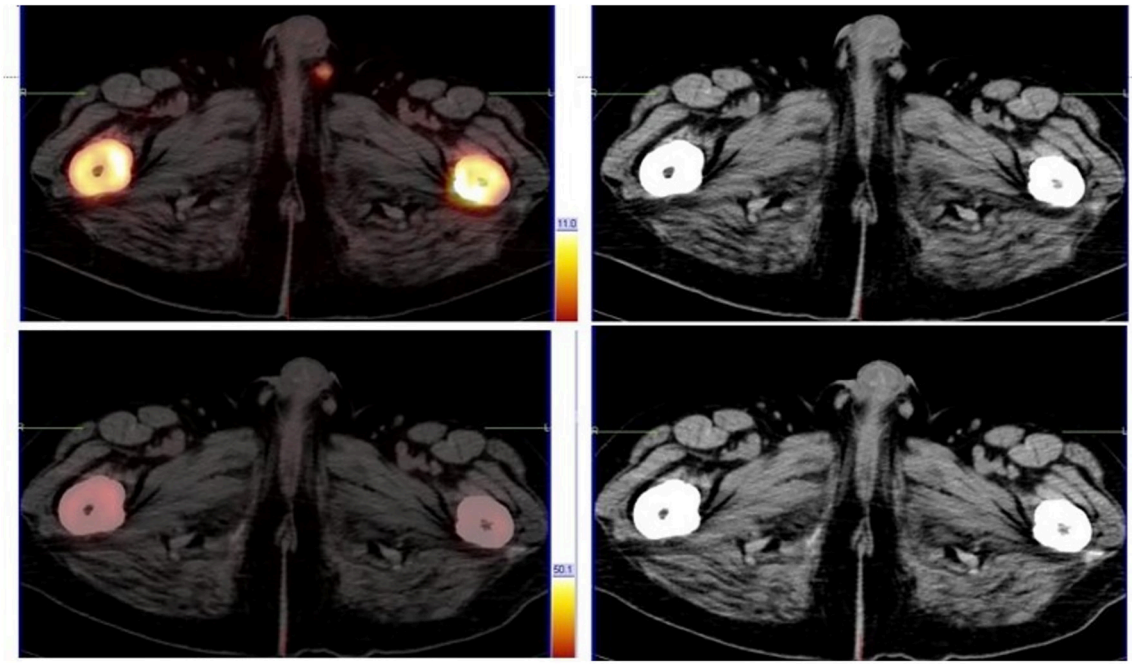

Figure 3. ^{18}F PET/CT and CT only images of the same patient. The images in the top row reveal increased PSMA expression in the left spermatic cord (SUV: 6.06), with no obvious CT changes. The images below are after 4 cycles of 177Lu-PSMA radioligand therapy, which demonstrate complete resolution (SUV: 1.39). Metastatic spread of prostate cancer to the spermatic cord is extremely rare, with Gergelis et al. (7) reporting the third case in the literature in 2019. Similar to renal metastases, there are no obvious CT changes in the affected left spermatic cord to suspect metastatic disease.

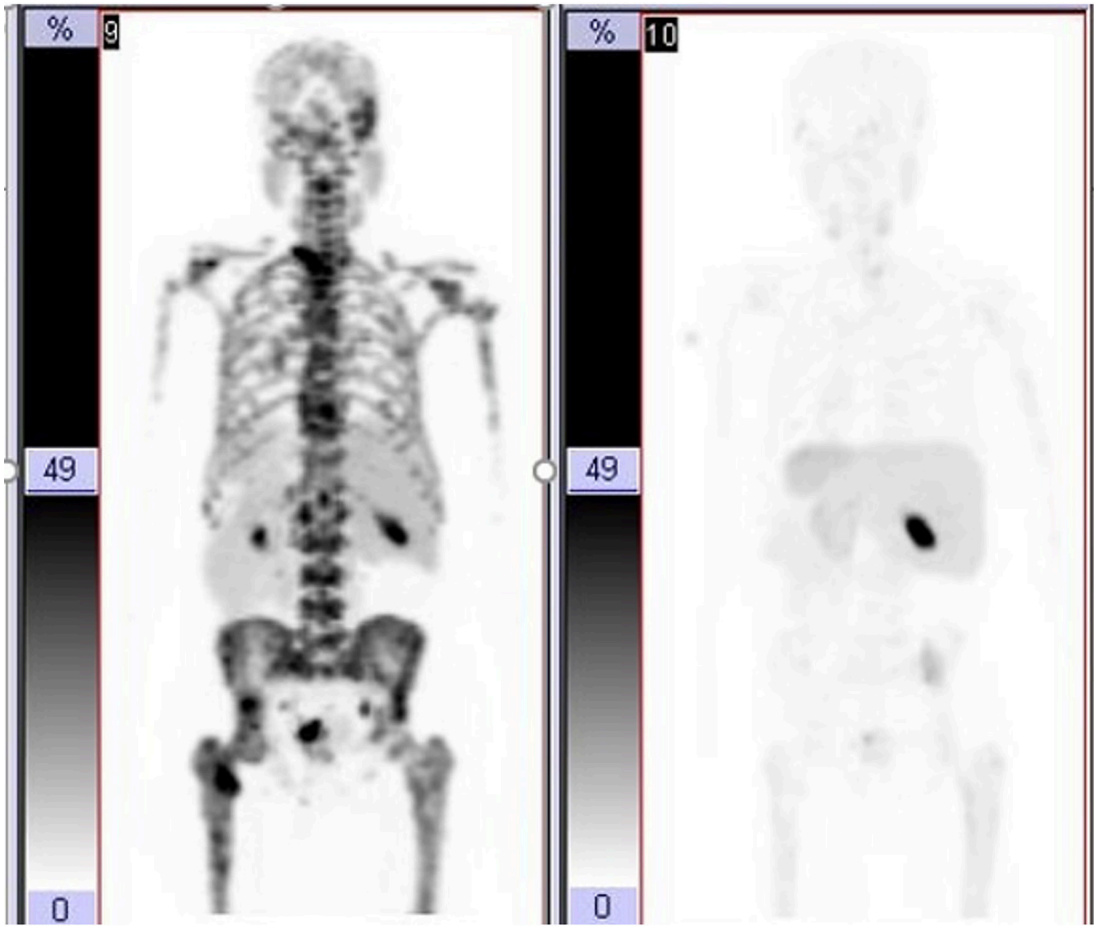

Figure 4. The image on the left is the patient's baseline maximum intensity projection (MIP) before 177Lu-PSMA therapy, showing widespread metastatic disease. The image on the right is an MIP image after radioligand therapy showing evidence of response to treatment. His PSA level pre and post therapy was 4,441 ug/L and 55 ug/L, respectively. The value of ^{18}F-PSMA PET/CT imaging has also been shown here because some of these atypical sights might have been missed on anatomical imaging because of little or no obvious anatomical changes. The testes and urethra are also known atypical sites for metastatic disease (8); however, this was absent in our patient. This case also shows the effectiveness of radioligand therapy with 177Lu-PSMA, even in patients with an atypical pattern of metastatic disease. Although we do not have histological confirmation of these atypical metastatic sights, the fact that they were associated with high PSMA expression that showed a very good response to 177Lu-PSMA therapy gives us a very high index of suspicion for metastatic disease.

Ethics

Informed Consent: Informed consent was obtained from the patient.

Authorship Contributions

Surgical and Medical Practices: O.E., Concept: O.E., G.E., Design: O.E., W.E., T.T., Data Collection or Processing: O.E., W.E., T.T., Analysis or Interpretation: O.E., W.E., T.T., G.E., Literature Search: O.E., Writing: O.E.

Conflict of Interest: No conflicts of interest were declared by the authors.

Financial Disclosure: The authors declare that this study has received no financial support.

References

1. Ss M, Masood N. Prostatic Adenocarcinoma - A Case with adrenal gland and bone metastasis. iMedPub Journals 2018;1-2.
2. Vinjamoori AH, Jagannathan JP, Shinagare AB, Taplin ME, Oh WK, Van den Abbeele AD, Ramaiya NH. Atypical metastases from prostate cancer: 10-year experience at a single institution. AJR Am J Roentgenol 2012;199:367-372.
3. Gandaglia G, Abdollah F, Schiffmann J, Trudeau V, Shariat SF, Kim SP, Perrotte P, Montorsi F, Briganti A, Trinh QD, Karakiewicz PI, Sun M. Distribution of metastatic sites in patients with prostate cancer: A population-based analysis. Prostate 2014;74:210-216.
4. Kurtul N, Resim S, Koçarslan S. Giant renal metastasis from prostate cancer mimicking renal cell carcinoma. Turk J Urol 2018;44:367-369.
5. Khan F, Mahmalji W, Sriprasad S, Madaan S. Prostate cancer with metastases to the kidney: a rare manifestation of a common disease. BMJ Case Rep 2013;2013:bcr2012008388.

6. Chen C, He H, Yu Z, Qiu Y, Wang X. Renal and retroperitoneal metastasis from prostate adenocarcinoma: a case report. World J Surg Oncol 2016;14:74.
7. Gergelis KR, Remme DS, Choo CR. Isolated biopsy-proven recurrence of prostate carcinoma in the spermatic cord after radical prostatectomy detected with 11C-Choline PET/CT. Urol Case Rep 2019;26:100985.
8. Kasai Y, Sawada N, Yamagishi T, Kamiyama M, Mitsui T, Takeda M. A case of urethral metastasis of castration-resistant prostate cancer successfully cured with CyberKnife radiosurgery. Urol Case Rep 2020;33:101346.

Interesting Image
Mol Imaging Radionucl Ther 2024;33:63-65 DOI:10.4274/mirt.galenos.2023.74507

Exceptionally Rare Isolated Thyroidal Metastasis of Pulmonary Carcinosarcoma: A Tale of ^{18}F-FDG-positive Thyroid Nodule

Pulmoner Karsinosarkomun Son Derece Nadir İzole Tiroid Metastazı: Bir ^{18}F-FDG Pozitif Tiroid Nodülü Öyküsü

Mehmet Emin Mavi[1], Fariba Amini[2], Seyfettin Ilgan[3]

[1]*Karaman Training and Research Hospital, Clinic of Nuclear Medicine, Karaman, Türkiye*
[2]*Güven Hospital, Clinic of Pathology, Ankara, Türkiye*
[3]*Güven Hospital, Clinic of Nuclear Medicine, Ankara, Türkiye*

Abstract

Pulmonary carcinosarcomas (PCS) are uncommon and aggressive malignant tumors with epithelial and mesenchymal components and have a worse prognosis than other non-small-cell lung cancers. Metastases of non-thyroidal malignancies to the thyroid are rare. We reported a unique case of isolated thyroidal metastasis of PCS and discussed ^{18}F-fluorodeoxyglucose (^{18}F-FDG) positivity in incidentally found thyroid nodules on ^{18}F-FDG positron emission tomography scan.

Keywords: ^{18}F-fluorodeoxyglucose, thyroid, lung, PET/CT, incidental, ultrasonography

Öz

Pulmoner karsinosarkomlar (PCS), epitelyal ve mezenkimal bileşenleri olan ve diğer küçük hücreli dışı akciğer kanserlerinden daha kötü prognoza sahip, nadir görülen ve agresif malign tümörlerdir. Tiroid dışı malignitelerin tiroid metastazları nadirdir. PCS'nin oldukça benzersiz bir izole tiroid metastazı olgusunu bildirdik ve ^{18}F-florodeoksiglikoz (^{18}F-FDG) pozitron emisyon tomografi taramasında tesadüfen bulunan tiroid nodüllerindeki ^{18}F-FDG pozitifliğini tartıştık.

Anahtar kelimeler: ^{18}F-florodeoksiglikoz, tiroid, akciğer, PET/BT, insidental, ultrasonografi

Address for Correspondence: Mehmet Emin Mavi MD, Karaman Training and Research Hospital, Clinic of Nuclear Medicine, Karaman, Türkiye
Phone: +90 543 960 85 80 **E-mail:** mehmeteminmavii@gmail.com ORCID ID: orcid.org/0000-0001-7702-8157
Received: 01.08.2023 **Accepted:** 15.10.2023

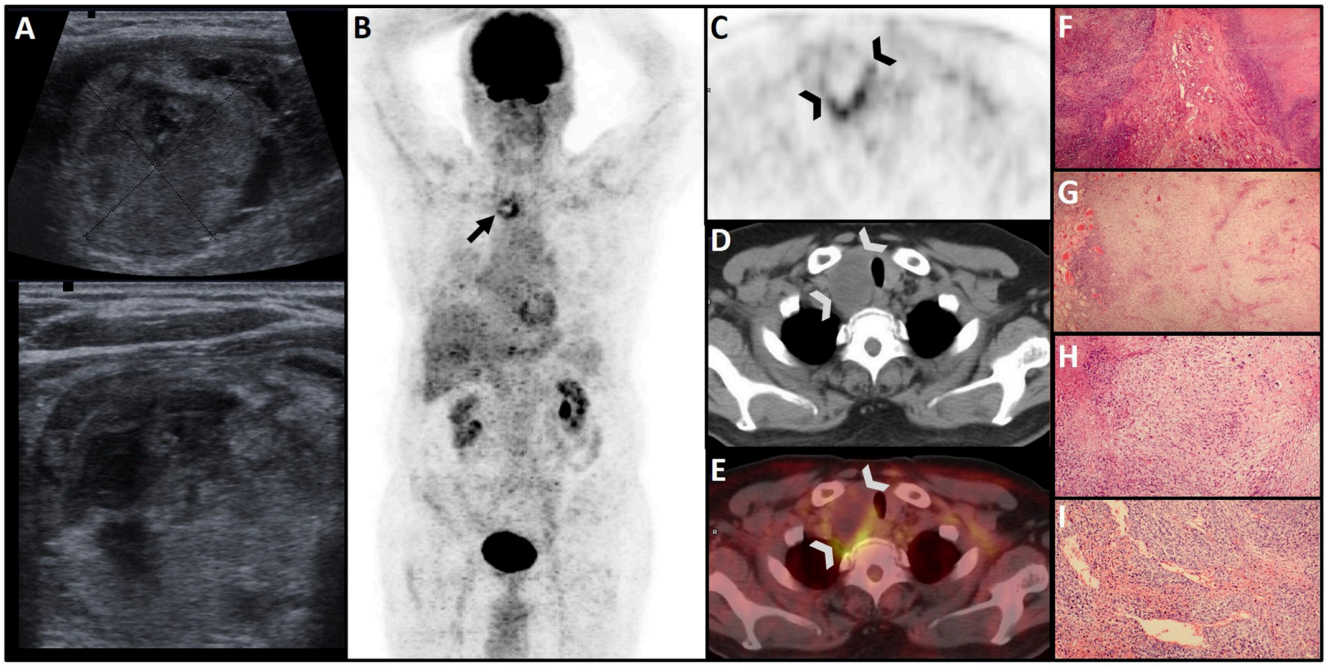

Figure 1. An 81-year-old man underwent right lower lobectomy because of a growing solitary pulmonary mass, and the final histopathology was reported as pulmonary carcinosarcomas (PCS). ^{18}F-fluorodeoxyglucose (^{18}F-FDG) positron emission tomography (PET) scan for primary staging revealed a large thyroid nodule with heterogeneous peripheral ^{18}F-FDG uptake in the right lobe without any sign of regional or distant metastasis in other body parts. Ultrasonography (USG) examination revealed a 44×35 mm, parallel oriented, isoechoic, predominantly solid nodule with scattered cystic areas (A). Although the nodule was deemed to be at low risk of primary thyroid cancer, fine needle aspiration biopsy (FNAB) was performed to exclude malignancy. The cytological samples were hypocellular and mostly comprised cystic components without any sign of atypia, supporting USG findings. Follow-up is recommended instead of repeat biopsy because of age and co-morbidity. One year later, the patient presented with hoarseness and difficulty in swallowing. Follow-up PET scan showed peripheral ^{18}F-FDG uptake [maximum standardized uptake value (SUV_{max}): 4.6] in the thyroid nodule, similar to the previous scan [arrow in (B) maximum intensity projection images and arrowheads in (C) axial PET, (D) CT, and (E) fusion images]. Repeated USG examination showed almost identical USG findings as the previous exam but considerable increase in size (58x38 mm). Thyroid lobectomy was recommended to alleviate local compression symptoms. Direct invasion of the mass into the esophagus and perithyroidal soft tissues discovered during surgery unexpectedly. The final histopathology of the thyroid nodule was concordant with PCS metastasis [(F, G) H&E staining at x4 magnification showing replacement of the normal thyroid parenchyma by malignant cells observed in the lung, (H) heterologous mesenchymal component (chondrosarcoma), (I) diffuse lymphovascular invasion].

PCS, comprising epithelial and mesenchymal components, represents 0.2% of primary lung cancers and has a worse prognosis than other non-small-cell lung cancers (1). Metastases of non-thyroidal malignancies to the thyroid are quite rare (2). There are only a few reports on PCS metastasis (3,4), but to the best of our knowledge, this is the first reported case of thyroidal PCS metastasis.

Incidental ^{18}F-FDG-positive thyroid nodules (IFTNs) are commonly encountered in patients undergoing ^{18}F-FDG PET for non-thyroidal illnesses. It has been demonstrated that the malignancy risk of IFTNs in the low-risk USG category did not show an increase compared with the general population (5). Conversely, IFTNs in the intermediate-high suspicion USG categories showed an increase in malignancy compared with the general population (5). A meta-analysis concluded that there is often considerable overlap in SUV_{max} values between benign and malignant thyroid nodules. Therefore, no SUV_{max} cut-off can be considered safe for benign-malignant differentiation (6). The American Thyroid Association guidelines recommend USG-guided FNAB for thyroid nodules >1 cm with focal ^{18}F-FDG uptake (7). However, this approach potentially may lead to unnecessary FNAB in the majority of patients because two out of three IFTNs will eventually be benign, and tailored decision-making strategies are recommended, considering the USG risk group of nodule and stage of non-thyroidal comorbid illness instead of directly pursuing a potentially co-existent low-risk thyroid carcinoma (8,9). On the other hand, as in the present case, IFTNs in patients with underlying non-thyroidal malignancy and metastasis to the thyroid gland should always be considered. ^{18}F-FDG- positive nodules with low USG risk factors may be of great importance in the clinical context.

Ethics

Informed Consent: Since the information provided is anonymous, obtaining informed consent from the patients was deemed not required.

Authorship Contributions

Analysis or Interpretation: M.E.M., F.A., S.I., Literature Search: M.E.M., F.A., S.I., Writing: M.E.M., F.A., S.I.

Conflict of Interest: No conflicts of interest were declared by the authors.

Financial Disclosure: The authors declare that this study has received no financial support.

References

1. Rossi G, Cavazza A, Sturm N, Migaldi M, Facciolongo N, Longo L, Maiorana A, Brambilla E. Pulmonary carcinomas with pleomorphic, sarcomatoid, or sarcomatous elements: a clinicopathologic and immunohistochemical study of 75 cases. Am J Surg Pathol 2003;27:311-324.
2. Nixon IJ, Coca-Pelaz A, Kaleva AI, Triantafyllou A, Angelos P, Owen RP, Rinaldo A, Shaha AR, Silver CE, Ferlito A. Metastasis to the thyroid gland: a critical review. Ann Surg Oncol 2017;24:1533-1539.
3. Saint-Georges F, Terrier P, Sabourin JC, Bonvalot S, De Montpreville V, Ruffie P. [Pulmonary carcinosarcoma with jejunal metastasis: complete response to chemotherapy]. Rev Pneumol Clin 2002;58:249-252.
4. Arnedillo Muñoz A, Pérez Requena J, Fernández-Berni JJ, León Jiménez A. Carcinosarcoma pulmonar con metástasis cutánea [Pulmonary carcinosarcoma with skin metastasis]. An Med Interna 2002;19:586-568
5. Chung SR, Choi YJ, Suh CH, Kim HJ, Lee JJ, Kim WG, Sung TY, Lee YM, Song DE, Lee JH, Baek JH. Thyroid incidentalomas detected on 18F-fluorodeoxyglucose positron emission tomography with computed tomography: malignant risk stratification and management plan. Thyroid 2018;28:762-768.
6. Bertagna F, Treglia G, Piccardo A, Giubbini R. Diagnostic and clinical significance of F-18-FDG-PET/CT thyroid incidentalomas. J Clin Endocrinol Metab 2012;97:3866-3875.
7. Haugen BR, Alexander EK, Bible KC, Doherty GM, Mandel SJ, Nikiforov YE, Pacini F, Randolph GW, Sawka AM, Schlumberger M, Schuff KG, Sherman SI, Sosa JA, Steward DL, Tuttle RM, Wartofsky L. 2015 American Thyroid Association Management Guidelines for adult patients with thyroid nodules and differentiated thyroid cancer: the American Thyroid Association Guidelines task force on thyroid nodules and differentiated thyroid cancer. Thyroid 2016;26:1-133.
8. Scappaticcio L, Piccardo A, Treglia G, Poller DN, Trimboli P. The dilemma of 18F-FDG PET/CT thyroid incidentaloma: what we should expect from FNA. A systematic review and meta-analysis. Endocrine 2021;73:540-549.
9. Pattison DA, Bozin M, Gorelik A, Hofman MS, Hicks RJ, Skandarajah A. 18F-FDG-avid thyroid incidentalomas: the importance of contextual interpretation. J Nucl Med 2018;59:749-755.

Letter to the Editor
Mol Imaging Radionucl Ther 2024;33:66-67 DOI:10.4274/mirt.galenos.2023.69345

About the Article Titled "A Different Scintigraphic Perspective on the Systolic Function of the Left Ventricle-I"

"Sol Ventrikül Sistolik Fonksiyonuna Sintigrafik Olarak Farklı Bir Bakış Açısı-I" Başlıklı Makale Hakkında

Cengiz Taşçı

İzmir University of Economics Faculty of Medicine, MedicalPoint Hospital, Department of Nuclear Medicine, İzmir, Türkiye

Keywords: Gated myocardial perfusion imaging, systolic volume change, radioactive decay formula, decay constant

Anahtar kelimeler: Kapılı miyokard perfüzyon sintigrafisi, sistolik hacim değişimi, radyoaktif bozunma formülü, bozunma sabiti

Dear Editor,

This article examines whether the decay formula meets the systolic volume change (1), but there is a doubt that it is the correct model to express the systolic ejection dynamics mentioned in the text. The exponential decay formula emphasizes that the activity/substance/volume halves at a certain time and is used to calculate the remaining at a given time. Therefore, the formula expressed here would not be exact to represent the systolic function.

Ejection fraction (EF) shows the ejection volume percentage in each cardiac beat without considering time, which is chronotrophy represented by Heart rate (HR) [EF = (Stroke volume/End diastolic volume (EDV)) x100]. Cardiac output (CO = HR/min × stroke volume) takes time into account with volume. Factors affecting CO, HR, and stroke volume (inoptophy, cardiac muscle power, Frank starling rule) also affect EDV, end systolic volume (ESV), systole, and diastole time. Preload and afterload are the factors that influence all these cardiac functions (2). Some other factors such as partial oxygen pressure and hemoglobin levels do not originate from the heart but affect the cardiac functions at the end (2). This study does not search the remaining volume at a given time, but searches ejection constant (Ec) (k), which might indicate the influences of all structural and functional factors related to cardiac ejection. For this purpose, this study scrutinizes the systolic part of the heartbeat, which is a good idea.

However, this idea needs to be proved clinically and mathematically because the purpose of the decay formula is completely different. The formula needs to be tested particularly on how it responds to situations with different HRs. There areno representative satisfying calculations with volume curves of real patients in the text. Therefore, the clinical value of Ec may be tested with imaginary situations. For example, for EDV: 125 and ESV: 35; EF: 72%. For beat per minute (BPM) =60/min; CO = HR/min × stroke volume: 60x90=5400 mL/min (stroke volume: EDV-ESV: 125-35=90). The normal range for EF is 50-70% and

Address for Correspondence: Cengiz Taşçı, İzmir University of Economics Faculty of Medicine, MedicalPoint Hospital, Department of Nuclear Medicine, İzmir, Türkiye
Phone: +90 232 399 50 50 - 2920 **E-mail:** cengiztasci68@hotmail.com ORCID ID: orcid.org/0000-0003-0962-7515
Received: 22.03.2023 **Accepted:** 18.09.2023

for CO is about 4-8 L/min. Cardiac cycle time: 1000/16 ms, systole time: 5.5 frame x (1000/16) ms =343.75 ms. With the decay formula: ESV = EDV. e^{-kt}; k =0.0037/ms; (Ec) k =3.7/s. In summary, for BPM =60/min, CO =5.4 L/min, EF: 72%, Ec: 3.7 are found, and these results are categorized as normal in the text.

"At a normal heart rate of 72 beats/min, systole comprises approximately 0.4 of the entire cardiac cycle" (2). Considering this statement from Guyton and Hall's Physiology, letus see what happens when the same patient has 72/min HR. Letus take the systole time as 6.4/16 unit time (40% of total cardiac cycle time), and EF =60%, EDV: 100 and ESV: 40, also mentioned as normal in Guyton and Hall's Physiology. Based on these values, Ec (k) is found to be 2.7, which is categorized as "ischemic" in the text. (EF 60%, CO =72x60=4320 mL/min). Despite being within the normal limits (change in BPM: 60 to 72/min), the cardiac HR differences changed Ec (k) dramatically (from normal group into ischemic one). Does this mean that patients can fall into the ischemic category when they are excited? Sympathetic and parasympathetic stimulations influence all parameters (especially the systole time, EDV and ESV), but we know that some compensation mechanisms keep the perfusion constant (2).

As shown in Figures 8a and 8c, different ES and ED volumes in patients with normal EF values might indicate different clinical presentations. For Figure 8a; EDV: 68, ESV: 20, stroke volume: 48 (normal range of stroke volume: 50-100 mL). EF: 70%, Ec (k): 2.5 (normal). For Figure 8c; EDV: 130, ESV: 60, stroke volume: 70. EF: 54%, Ec (k): 1.6 (infarct). Figures 8a and 8c indicate that the infarcted myocardium may have a higher stroke volume than normal. Does the size of the infarct area make a difference? Although Ec (k) does not directly take HR into account, the category of the curve changes. Does this change reflect the myocardial perfusion situation? Robustly, this does not seem very normal logically. On the other hand, the number of patient groups seems similar, and no data are given about the pretest probabilities for each group.

Visual evaluation of the volume curve is a routine part of gated myocardial perfusion imaging interpretation. If there is a constant k value as in the decay constant (λ), it is expected that each heart with the same k value would have a certain systolic volume decrease half-time. Because HR does not take part in the formula, this constant (k) must not change with different HRs. By the way, it is mentioned that all the volume curves were created automatically by QGS software, and it is questionable whether there would be any need to make changes in the drawings.

Although the decay formula does not exactly meet the systolic volume change, it is also exponential. It is not the same but similar. Thus, Ec seems to have a good correlation with EF, EDV, and ESV. EF and Ec that both refer to EDV and ESV are the logically correlated parameters. However, any case with EF and Ec uncorrelated might be an explanatory example.

In fact, visual evaluation seems better than Ec (k) calculation. The visual evaluation of the curve itself can provide more information than this imaginary decay formula. EDV, ESV, stroke volume, systole and diastole time, the slope of the systolic volume curve, and EF can be calculated, and normal and abnormal curves can simply be evaluated visually. The (k) calculation adds nothing more than visual evaluation and may mislead the clinical evaluation.

Ethics

Financial Disclosure: The author declared that this study received no financial support.

References

1. Karaçalıoğlu AÖ, Çınar A. A Different scintigraphic perspective on the systolic function of the left ventricle. Mol Imaging Radionucl Ther 2023;32:206-213.
2. Guyton, Arthur C., Hall, John E. Textbook of Medical Physiology. 14th ed. W B Saunders, 2015; p.118-126.